Aalto University
School of Engineering

Master's Program in Mechanical Engineering

GHULAM HASSAN

Design of Research Oriented Cylinder Head for a Heavy Duty Engine

School of Engineering

Thesis submitted in partial fulfillment of the requirements for the degree of Master of Science (Technology).

Espoo, September 2017

Supervisor: Prof. Martti Larmi

Thesis Advisor: D.Sc. (Tech) Ossi Kaario

Author	GHULAM HASSAN		
Title of thesis	Design of Research Oriented Cylinder Head for a Heavy Duty Engine		
Degree program	Mechanical Engineering		
Major/minor Personal Minor			**Code** MEC-E2010
Thesis supervisor Prof. Martti Larmi			
Thesis advisor D.Sc. (Tech) Ossi Kaario			
Date 01-09-2017	**Number of pages** 89+ 3		**Language** English

Abstract

The swirl flow is considered beneficial to enhance air-fuel mixing in CI engines during compression stroke as the piston reaches TDC, and helps in faster burn during combustion phase. Contrary to that, with the advancement of highly pressurized fuel injection systems and optimized types of IC engines like dual fuel engine demands for low swirl or preferably no swirl intake configuration is prevailing. The swirl structure induces by intake port differs from other flow structures like tumble; swirl not only survives during compression stroke but also throughout the expansion stroke. Therefore, swirl influences spray evolution and evaporation process during combustion and affect heat release due to the crumbling of the large-scale structure into small scale by adding more turbulence.

This thesis work is aimed at designing, performing steady-state CFD analysis, and exercising additive manufacturing technique for a new single-cylinder research-oriented cylinder head with no induced swirl flow. The study also incorporates inclusive evaluation of flow structures produced by existing model of cylinder head through computational fluid analysis by employing Star-CCM+ software and experimental validation; then conjunction with that inquisition a new directed port model is devised. In addition, new ports position is designed, analyzed, and final model is selected based on admissible results. The new exhaust ports, cooling channels, and the main body of the cylinder head with appropriate thickness values are also designed.

Additive manufacturing is a customized fabrication process to produce cost-effective products. AM has completely revolutionized current manufacturing techniques with a diverse selection of methods for different materials. Selective laser sintering is one of the powders based AM techniques with a range of available materials as polymers and metals used to contrive good quality densely structured light parts with flexible, interlocking and functional features. Therefore, SLS technique is adopted for new cylinder head manufacturing for later experimentally check of swirl flow.

Keywords Design, CFD, swirl, dual fuel, cylinder head, Additive Manufacturing

Preface

I would like to thank my supervisor Prof. Martti Larmi for conceding my designing skills and giving me the opportunity to commence this task. Secondly, I would commend my instructor Ossi Kaario for endowing me with useful and pragmatic suggestions at every stage of this thesis work, especially in analysis job. I have learned plentiful new skills in CFD while working with Research group of Thermodynamics and Combustion specifically apposite guidelines gave by Petteri Peltonen regarding Star CCM+ usage. Moreover, during an inquiring study of existing cylinder head model, lab technicians Otto Blomstedt and Olli Ranta imparted useful discussion about effective and tangible designing process based on their experience-based knowledge.

Regarding Additive Manufacturing, I would acknowledge to senior research scientist of 3D printing Mika Salmi for giving me useful conceptions from designing to the manufacturing stage.

In the end, I would like to revere my parents and siblings for consistently supporting me throughout my education career and assisted me to emulate this exertion.

Espoo September 01, 2017

Ghulam Hassan

Table of Contents

Abbreviations and Symbols

Abbreviations

3D	Three-dimensional
AM	Additive Manufacturing
B.C	Boundary Condition
BMEP	Brake Mean Effective Pressure
CAD	Computer Aided Design
CFD	Computational Fluid Dynamics
CGI	Compact Graphite Iron
CM	Conventional Machining
DF	Dual Fuel
EGR	Exhaust Gas Recirculation
FVM	Finite Volume Method
GEB	Global Energy Balance
HPDI	High Pressure Direct Injection
IC	Internal Combustion
ISD	Inner Seat Diameter
MA	Minimum area
NG	Natural Gas
PDE	Partial Differential Equation
PH	Port height
PA	Port angle
PIV	Particle Image velocimetry
RNG	Re-Normalization Group
RANS	Reylonds Average Navier Stokes
RoHT	Rate of Heat Transfer
SA	Swirl Ratio
SLS	Selective Laser Sintering

STL	Stereo Lithography
TA	Tumble angle
TD	Throat Diameter
TDC	Top Dead Centre
VA	Valve angle
GJV	Vermicular Graphite Iron
YAG	Yttrium Aluminium Garnet

Symbols

A_p	Area of Piston
B	Bore of cylinder
^{o}C	Degree Celsius
C_f	Flow coefficient
C_{μ}	Non-constant value for k-epsilon model
D	Inner seat diameter
D_o	Face diameter of valve
D_s	Diameter of the valve stem
D_p	Minimum diameter of the valve seat
E	Non-dimensional valve offset (eccentricity)
kg	Kilograms
m^o	Mass flow rate
l	Stroke length
n	Angular rotation of crankshaft
N	Newtons
P	Pressure
Pa	Pascals
k	Turbulent Kinetic Energy
n_d	Solid body vortex Speed

t	lower deck thickness value
U_i	Component of velocity
$u^/$	Fluctuating velocity Component
$u_i u_i$	Normal Stresses
w_x	Angular velocities for solid body vortex having rotation at x-z planes
w_y	Angular velocities for solid body vortex having rotation at x-z planes
y^+	Non-dimensional wall distance
Y	Valve location offset

Greeks

μ	Dynamics Viscosity
μ_t	Turbulent viscosity
Σ	Summation
θ	Valve face angle
ΔP	Change in pressure
ε	Dissipation
μm	Micro meter

Chemical Symbols

Ar	Argon
CH_4	Methane
CO2	Carbon dioxide
HC	Hydrocarbons
NOx	Nitro Oxides
N_2	Nitrogen
Nd	Neodymium-Doped

1 Introduction

1.1 Motivation

The strict emission regulations in conjunction with new emerging electric vehicle technology having more efficient powered batteries have jeopardized the future of internal combustion engines. In order to encounter growing threats, IC engines should have higher fuel efficiency, and more clean burn conducive to avoid hazardous emissions. Although with overshadowing effects of regulations and emerging futuristic technologies, IC engines usage in heavy-duty vehicles and in marine sector will remain dominant for an unforeseen period in the form of emanating and optimized types like dual fuel engines. Nonetheless, ICE community still not be able to harness the substantial efficiency of IC engines, and lot more to be done in studying the anomalous combustion phenomena.

In dual fuel engine, air passing through intake manifold is mixed with primary gaseous fuel typically NG sprayed through injector nozzle. The mixture of air and NG is then ignited by combustion of a small quantity of pilot diesel fuel injected as the piston reaches the TDC. A large number of flame kernels in the combustion chamber rather than a localized flame result in a wider zone of ignition(enhancing the operating flammability limit), and more regular combustion of charge even for ultra-lean mixtures[1]. The higher octane number of methane (97% of natural gas) makes it ideal to comply with dual fuel strategies without the need to change engine compression ratio and can be employed in compression ignition engines devoid of hardware modifications. The higher knock resistance with low CO_2 emissions due to low carbon content can be achieved from NG, and overall theoretical gains of up to 26% are attainable if methane derives from biogas renewable source [2].

The accurate prediction of the behavior of in-cylinder flow structures is primary step to control turbulence level, air-fuel mixing, and heat loses. During the intake stroke, a large number of complex structures build up and destroy during the compression stroke. On the other hand, the various structures survive during the compression stroke and cause enhanced mixing near top dead center [3]. Swirl is one of the flow structures that not only survives throughout the compression stroke but sustain all the way through the combustion and expansion process. The well-organized rotation of intake flow structure about the cylindrical axis with some initial angular momentum is called swirl [4]. The swirl is known to improve air-fuel mixing and enhance turbulence level in CI engines, but enlarged swirl level during combustion of dual fuel engine decreases thermal efficiency due to heat loss and later ignition [5]. The shape of intake port imparts strong swirl effect, which influences all the sub-sequential processes from the spray evolution to the evaporation process in the combustion chamber [1]. Moreover, during optical research activities relating to combustion, swirl flow creates a mist over premixed air-gas mixture, makes it difficult to study combustion phenomenon ignited by diesel pilot fuel, and creating visualization problems for luminosity study. Therefore, there is need of non-swirl cylinder head for lab research work to study combustion and flame propagation, but production of the cylinder head at customized level is hectic and expensive job through traditional methods. It needs some less-expensive and most demanding manufacturing technique; AM is a growing trend to manufacture such custom level products with higher quality at the smaller scale and less machining work.

1.2 Objective

The specific objectives of this thesis are: to make conceptual CAD model, perform CFD simulations, do additive manufacturing (3D printing) for dual fuel engine cylinder head with no swirl (quiescent combustion systems) and creating modularity for multiple injectors. The existing model of the cylinder head for LEO-I and LEO-II dual fuel engines are based on four valves configuration with two intake ports and exhaust ports in cross flow arrangement. The intake configuration contains one helical port at the upstream position and tangential port on the downstream position. As helical port produces pre-cylinder swirl with imparted angular momentum by moving flow around valve axis at the range of different valve lifts. Therefore, the aim is to remove the current helical port and place the modified tangential port on existing ports location or newly designed position for ports after steady state CFD results verification.

The objectives of this relevant thesis work can be divided into following steps:

1. Literature study relevant to cylinder head designing phase.
2. CFD and experimental validation for swirl ratio calculation for existing cylinder head model with three cases: both ports open, tangential port closed and helical port closed.
3. Evaluation of existing model and designing new model for tangential port.
4. Modeling new ports position and selection of suitable model from two cases (existing ports position/new ports position) after comparison of CFD results for swirl ratio.
5. CAD modeling of complete new cylinder head.
6. Additive manufacturing of newly designed cylinder head by powder based selective laser sintering technique.

This thesis work has wider scope relative to DF combustion research currently carrying out at the Engine Laboratory of Mechanical Engineering Department. In future studies, there is an interest to employ a cylinder head in optical research engine with no-swirl to explore DF combustion in details. The current studies primarily involve optical diagnostics of low temperature diesel/methane dual fuel combustion modes that are mainly characterized by premixed auto-ignition and turbulent flame fronts propagation. In addition, the purpose is to exercise customized manufacturing techniques like AM for cylinder head manufacturing. The format of the thesis is configured as follow: The literature review relevant to the flow structure, theoretical background of dual fuel engine, swirl effect on combustion and heat transfer, cylinder head designing decisions, and additive manufacturing are discussed in 2nd chapter. The espoused designing software, concerned CFD software selection based on finite volume methods with adopted RANS model; a proverbial technique for swirl calculation, and detailed study about existing cylinder head geometry are argued in 3rd chapter. The 4th chapter is encompassed with CFD results and experimental affirmation regarding existing model, based on debated results new port model is created and analyzed with an inquired study on new concept selection phase are presented. In 5th chapter exhaust ports designing phase, cylinder head main body and cooling channels designing process are encapsulated, whereas the 6th chapter is about the selected additive manufacturing process. Finally, discussion, thesis aims review and future perspectives are compiled in 7th chapter and 8th chapter.

2 Background Information

2.1 Intake Flow pattern in IC Engines

The flow pattern during the intake stroke of IC engine is the most important process for air-fuel mixing and combustion process. The flow pattern contains bulk fluid motion and turbulence characteristics of flux; subdivided into large-scale mixing and small-scale mixing modified during compression stroke [6].
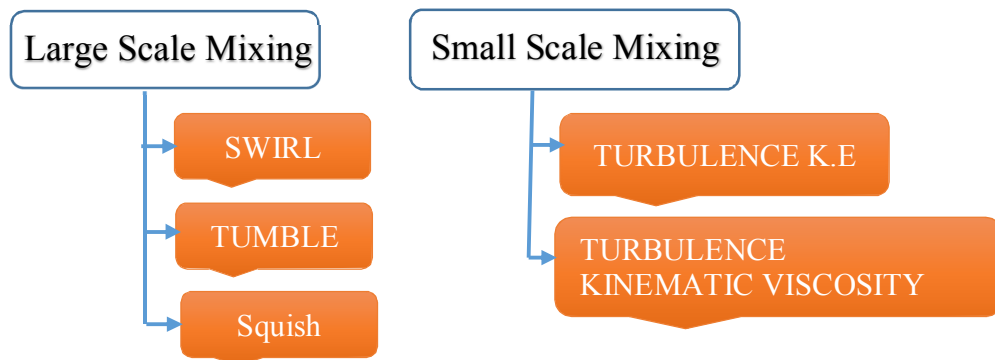

Figure 2.1: Types of large scale and small scale mixing

During induction process, turbulence is generated due to shear strain rate [7]. For large scale coherent structures, turbulence kinematic viscosity is main the indicator of the spatial region that is convenient and inconvenient for their existence, whereas turbulence kinetic energy helps in enhancing small-scale mixing by capturing turbulence creation points[3]. In the course of ignition process: the existence of flame, propagation speed and stability are greatly influenced by the interaction of turbulent flow structures with flame front area [8]. The three mechanisms that contribute to complex flow behavior (turbulent flow) in the cylinder are [3]:

1. Jet-wall Interaction
2. Jet-Jet Interaction
3. Jet-bulk flow Interaction

2.1.1 Large Scale Structures

 a) Swirl

When an intake flow is brought into the cylinder through the pre-defined shape of intake port with initial angular momentum an organized rotation of flow about cylindrical axis occurs, a secondary interaction with walls of piston and jet/cylinder take place. This angular momentum and interaction produce large-scale structure usually known as a swirl. Other flow structures degenerate during intake process, while swirl not only sustains during compression process but also impact throughout the combustion and expansion process [4]. Swirling flows usually have large static pressure deviation at the center of vortex core, in conflict with the non-swirl flow having uniform static pressure at the boundary layer. The

variance of pressure influences vortex core shape. The forced vortex flow also known as solid body rotation is simplest rotational swirling flow [9].

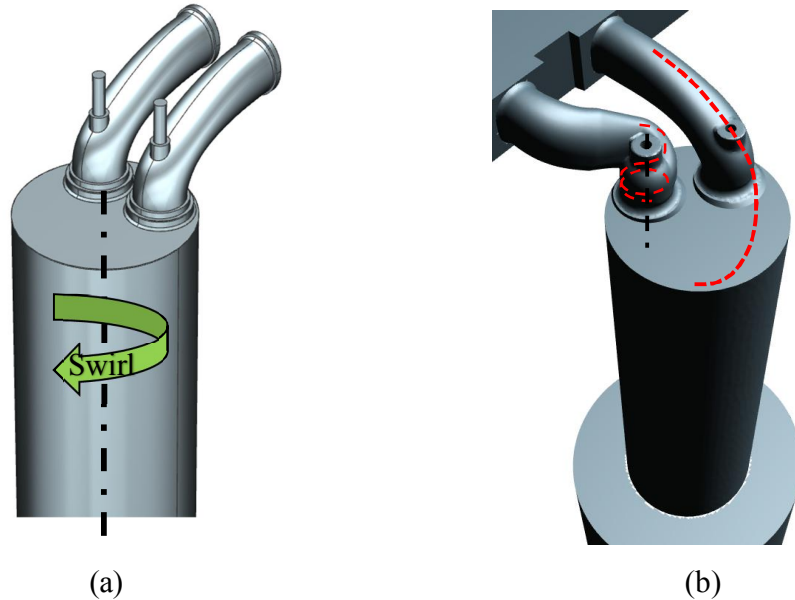(a)   (b)

Figure 2.2: (a) shows swirl flow and (b) exhibits pre-cylinder and in cylinder swirl

The figure 2.2 .b shows forced angular momentum swirl in lower valve and jet-wall interaction swirl on upper valve side indicating two ways of producing swirl either by rotation around valve axis or by directing flow tangent to cylinder wall. Swirl is usually quantify with some non-dimensional parameter like swirl ratio in IC engines. Swirl ratio is defined as angular velocity of solid body vortex normalized by angular rotation of crankshaft [47].

$$\text{Swirl Ratio} = \frac{n_d}{n} = \frac{n_d \rho A_p l}{30 m^o} = \frac{w_s}{2\pi N} \qquad (2.1)$$

where n_d is solid body vortex rotation speed $\left[\frac{1}{\text{sec}}\right]$, ρ is density of air $\left[\frac{\text{kg}}{\text{m}^3}\right]$, A_p is area of piston$[\text{m}^2]$, $l = $ stroke lenght$[\text{m}]$ and m^o is mass flow rate

In IC engine, valve diameter, valve lift, valve seat angle, port eccentricity, port orientation angle, cam dwell, and helix angle in case of helical port are the main parameters, which influence swirl ratio [40].

The mixture preparation always requires some energy; this energy is the combination of injection energy (injection pressure) and air energy (swirl, turbulence) [64]. Swirl has been considered to decrease soot level by diminishing axial fuel penetration and enhancing radial penetration with respect to spray, furthermore, ignition delay could be shorter than non-swirl case. However, swirl originating from higher pumping loses in intake system also increases gas velocity leading to higher heat transfer, and consequently more heat losses [10]. The excessive swirl value results in the reduction of spay penetration, spray overlapping or localization and an increase of in-cylinder heat transfer leading and mean temperature. This

influences soot oxidation by affecting air-fuel mixing during combustion period and consequently higher soot emissions [11].
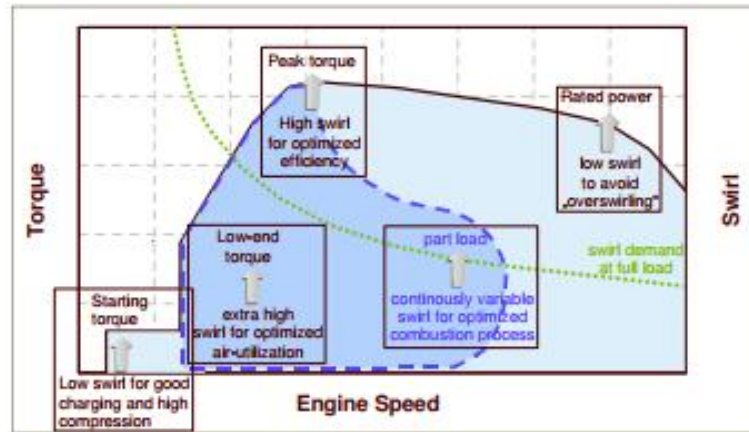

Figure 2.3: Shows demand for swirl (specific to operating point) in engine [12]

Under strict emission regulations, optimum swirl level from charge motion is essential for different modes of combustion under variable loads shown in figure 2.3. The low swirl demand is beneficial at starting torque for good charging and high compression. The engine speed usually governs the swirl demand at full load range [12].

Table 2.1: Factors affecting combustion [64]

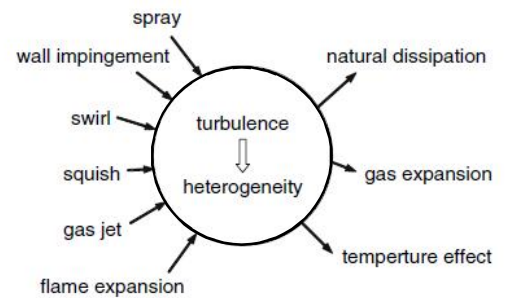| Factors Influencing Combustion			
Number of inlet and exhaust valves	Combustion chamber	Air	Fuel Injection
	Shape	Swirl	location of nozzle
	Compression ratio	Turbulence	Injection Pressure
			Injection Start
			Injection Duration
			No. of Injector Orifices

Figure 2.4: Factors affecting turbulence during combustion [63]

b) Tumble

Tumble plays important role in production of turbulence with substantial advantage in air fuel mixing during rapid combustion period, as it breaks up earlier than swirl during compression stroke [13]. Tumble is usually considered beneficial for pent roof combustion chamber. In order to get best compromise between soot and NOx, moderate tumble is productive at low- load high speed [34]. Just like swirl, tumble is also typically measured

with non-dimensional factor called tumble ratio. The angular momentum and moment of inertia are computed in two orthogonal planes x-z and y-z plane for tumble ratio [4].

$$Tumble\ Ratio_x = \frac{w_x}{2\pi N} \tag{2.2}$$

$$Tumble\ Ratio_y = \frac{w_y}{2\pi N} \tag{2.3}$$

where w_x and w_y are angular velocities for solid body vortex having rotation at y-z and x-z planes, $N\ is\ no.\ of\ rev/min$

$$Total\ Tumble\ Ratio = \sqrt{T_x^2 + T_y^2} \tag{2.4}$$

Tumble breaks down during compression and enhances turbulent kinetic energy with increased combustion rates because of amplified air fuel mixing level at period of injection. This makes tumble unstable structure than swirl that sustain throughout the compression stroke [3].
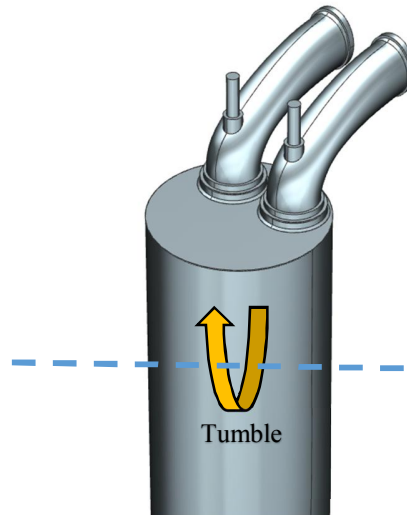
Figure 2.5: In cylinder tumble flow

c) Squish Flow

At the outer radius of piston, a flat area is provided usually known as squish zone and designed to keep small clearance from cylinder head. This accounts for several reasons in diesel engine, the foremost of which is to trap as much air as possible in bowl cavity and contributes to combustion near TDC during fuel injection. The second reason is to get some benefit in terms of compression ratio for improved efficiency, and shrinking the volume at the outer periphery of bowl reduces heat transfer. During end of compression stroke near TDC the squish volume decreases, air trapped in squish volume forces towards cylinder centre and produces a secondary air flow known as squish flow. This squish flow contributes to combustion by affecting fuel injection though enhancing air fuel mixing. The radial distribution of swirl is greatly interrupted by squish flow and alters the convective transport of exhibited turbulence level with generating additional turbulence. The swirl flow influences inward penetration of squish flow immensely, with decrease in swirl flow, the inward penetration increases due to decrease in centrifugal forces. The squish flow contribution

strongly depends on the bowl shape and at different locations within bowl. The swirl/squish interaction imparts angular momentum due to formation of tangential velocity flow structures [27, 63].

2.2 Dual Fuel Study

2.2.1 Natural Gas

Natural gas comprises of large portion (98%) of methane (CH_4) as well as small amount of other alkanes like ethane, propane, and trace impurities like helium, carbon dioxide hydrogen sulphide and water vapor. Matane, the higher percentage of natural gas contains one carbon atom bonded with four hydrogen atoms. In comparison with gasoline having H/C ratio of 1.85, methane has H/C ratio of 4:1 with an advantage of reducing carbon emissions by twenty percent because of higher H_2O formation than carbon dioxide in the end products [14]. The natural gas is considered greener fuel having octane rating of 130 with equal advantage of operating at compression ratio of 16:1 without knock and detonation [15].
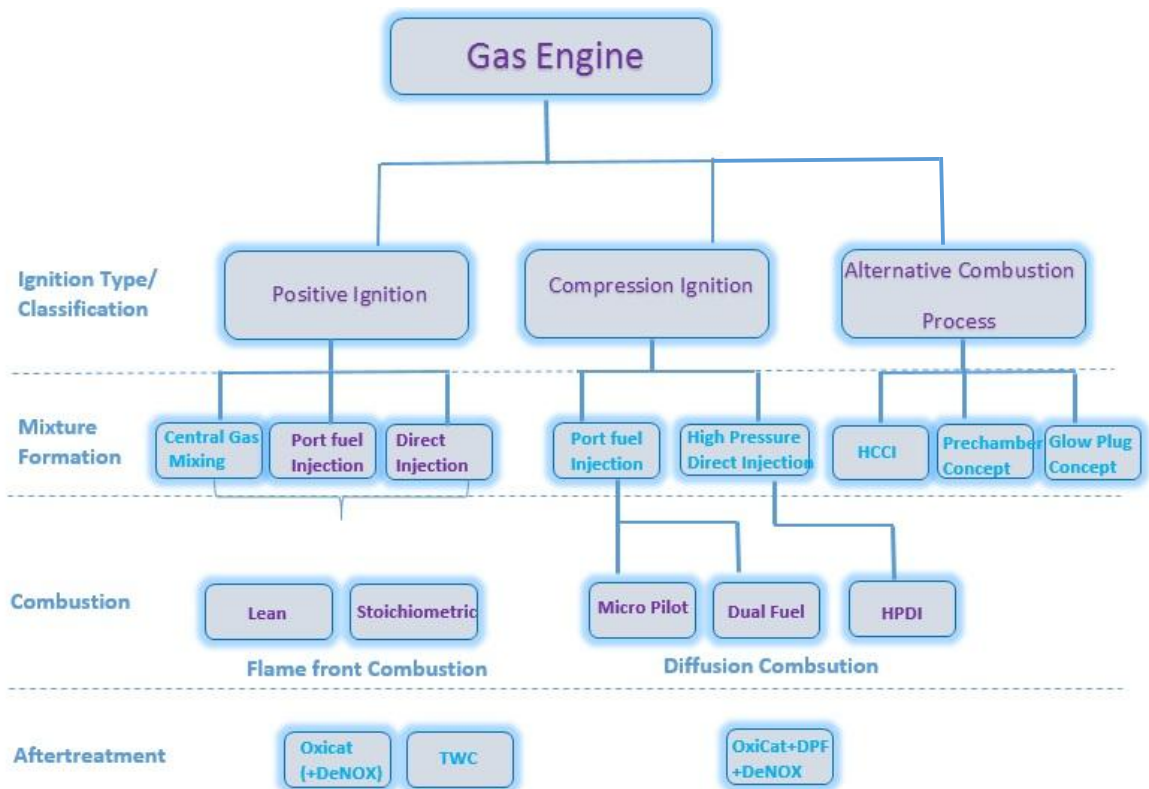

Figure 2.6: Shows gas engine classification according to ignition type, mixture formation, and combustion type and after treatment process [20]

The consideration of methane number (indication of knock resistance) is an important parameter in compression ratio of IC engines, and thermal efficiency increases with compression ratio [20]. The NG offers same compression ratio like conventional diesel

engines, this makes NG ideal candidate fuel to be used in current diesel engines for dual fuel operation [1].

2.2.2 Dual Fuel Engine

Dual fuel engines demonstrate lower emissions and high power density compared to conventional diesel engines [16]. In dual fuel engine, the primary fuel like natural gas is mixed with air in manifold just similar to pre-mixed SI engines, ignited by means of small amount of pilot diesel fuel injected as piston approaches the TDC [2] shown in figure 2.7. High octane number of methane permits dual fuel combustion strategies to be utilized in CI engines without changing compression ratio and reduces cost of engine hardware conversion [2].
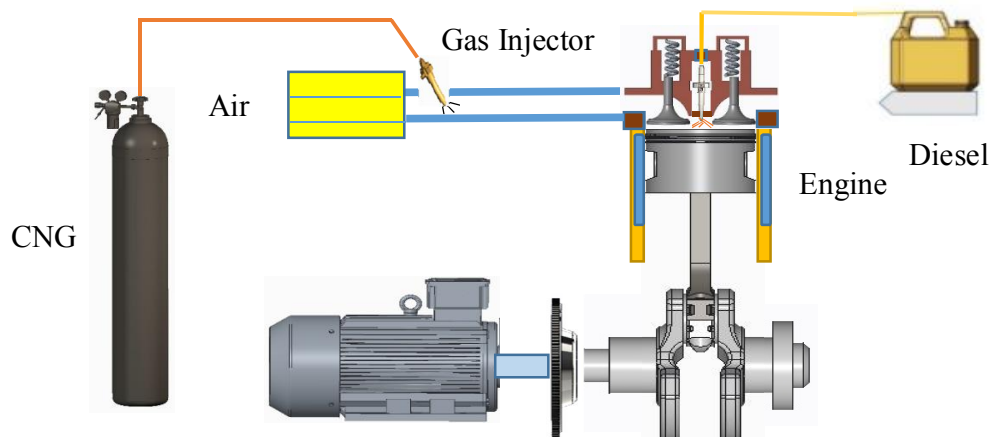
Figure 2.7: Overview of Dual Fuel Engine

In dual fuel, most of energy is obtained from NG having low atomic ratio C/H of methane (larger portion of natural gas) along with good values of fuel specific consumption and combustion of homogeneous charge provides reduced NOx and CO_2 emissions with respect to baseline diesel engine. However, HC and CO emissions from dual fuel engine are higher than conventional diesel engine, especially at part load as charge becomes leaner due to un-throttling and facilitates incomplete combustion [1]. G.A Karim [62] discussed another type of dual fuel strategy for port fuel addition employed with micro pilot injection of diesel for additional improvement in combustion, which utilizes pre-chamber attached to cylinder head for maximum usage of gaseous fuel with respect to liquid fuel(1% only). This arrangement greatly lowers pollutant values, leads to higher efficiency while maintaining engine speed and load ranges similar to base diesel operation. But micro pilot operation assists transient operating conditions or when the gaseous fuel air mixture is very much lean.

2.2.3 Effect of Swirl

The swirl motion is known to change mixture homogeneity and auto ignition delay. The fuel sprays are likely dispersed by strong swirl flows and air cavity is not strongly used due to air fuel mixture blows out of the squish area in DI diesel engines [65]. T. Fuyuto [66] suggested that swirl must be eliminated for optical research engine. Wakisaka [67] investigated diesel spray flames in the optical engine at SR of 2.0 and noticed that sprays were entrapped by

swirl flow with no visualization was available at outside of spray angle; upstream side of the swirl. The strong swirl flow created complexity to visualize the backward flow of the hot-burned gas in optical diesel engine studies. Due to the strong mixing of swirl flow, the profile of mixture became blurred while backward flow cannot be attained from shadowgraph images. A luminous flame with soot incandescence emerged and covered the visualized shadow after ignition. This makes the shadow of hot-burned gas invisible.
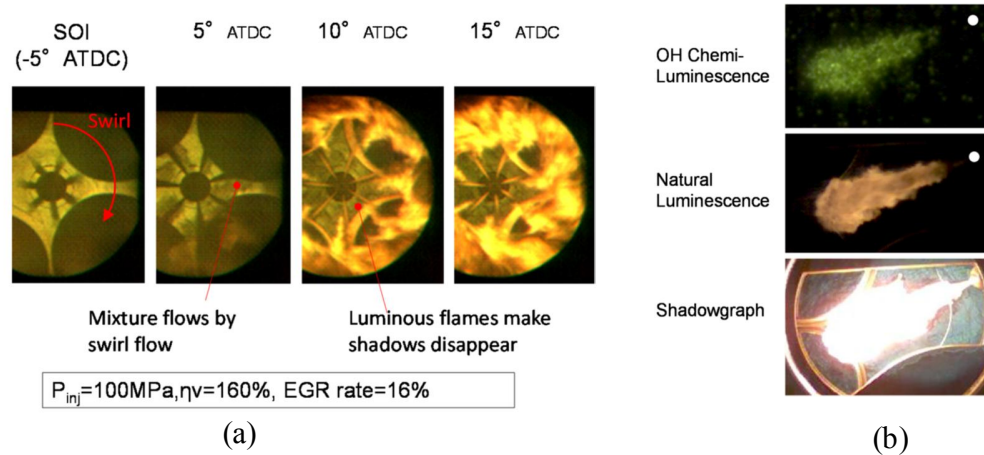

Figure 2.8: (a) Optical Engine with a strong swirl flow (b) Comparison of imaging techniques [67]

P. Olmeda [69] investigated swirl ratio variation with different operating parameters like HT and GEB at speed 2000 rev/min and BMEP of 5 bar and 20 bar. The air velocity increment due to swirl ratio enhances convective HT changes conducive to higher HT loss to chamber walls which in turns increases heat rejection to coolant and oil. The increase in tangential velocity due to increase in swirl ratio from 1.4-3 affects engine efficiency due to changes in RoHR, which results in increase of each 1 % of the fuel energy on piston, cylinder liner and ports with corresponding increase in wall temperatures. The brake and gross indicated efficiency also becomes worse due to higher pumping losses attributed to increase in SR.
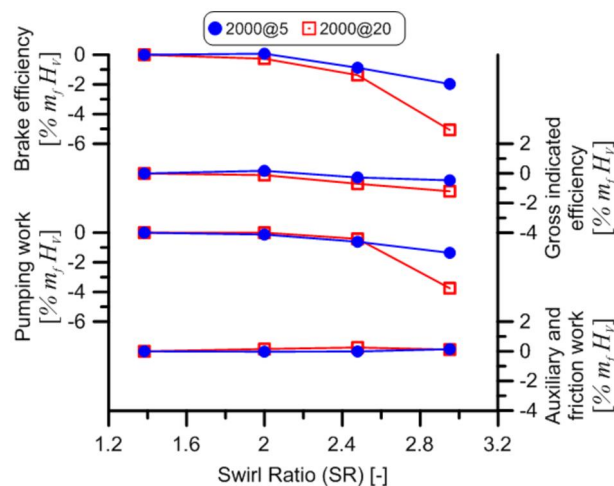

Figure 2.9: Change of brake, indicated efficiency, pumping work and friction losses in $\% \, m_f \, H_v$ with change in swirl ratio from 1.4-3 [69]
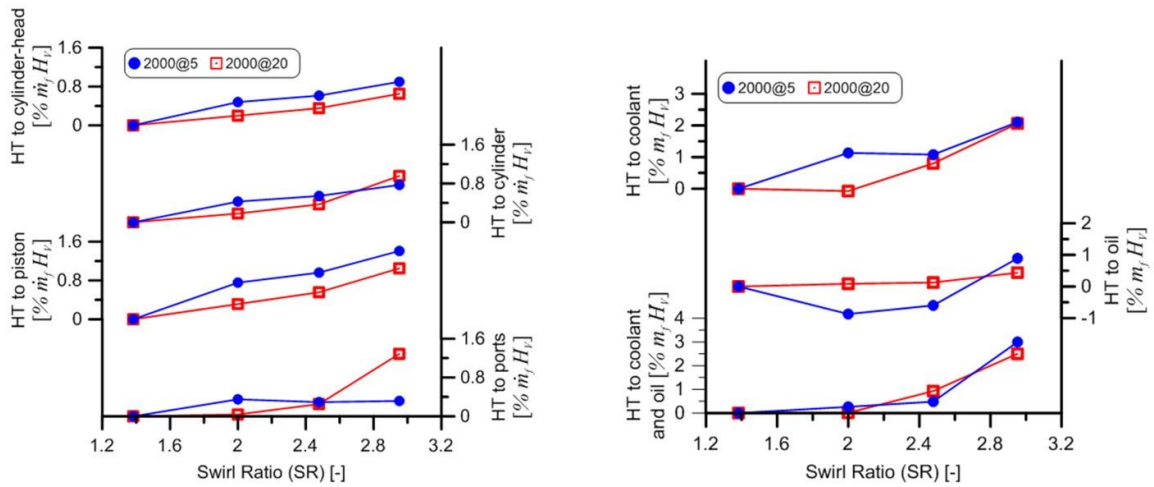
Figure 2.10: Change of modeled heat transfer in chamber and ports with swirl ratio on left side and change of experimental heat transfer to coolant and oil with swirl ratio on right side [69]

The charge mixing of diesel spray and the partial propagation of the turbulent flame fronts in air-methane mixture can be assisted by bulk charge flow driven by intake swirl [68]. However, in dual fuel operation, combustion includes injection of liquid fuel superimposed with premixed gaseous air fuel mixture, which makes it very complex process to study [17]. During experiments in previous work [1], deteriorating combustion quality was detected in dual fuel at light load both on low speed (1250- rpm) and on medium speed (1950 rpm). The quality of combustion process was strongly effected due to swirl flow ascribed to shape of intake port(tangential or helical).This swirl flow effects all subsequent processes initiated from evolution of the spray within the chamber and evaporation shown in figure 2.11. The distortion from spray direction by flow field contributes to the formation of regions where most of diesel vapor (n-heptane) is localized shown in figure 2.12. By controlling the turbulence level inside the combustion chamber before ignition can effectively promote lean air methane combustion [18].
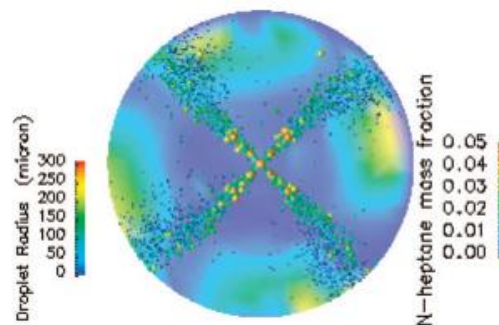

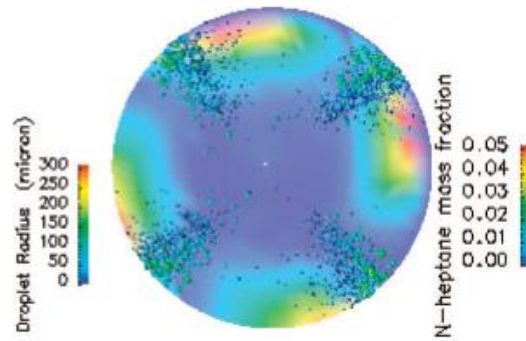Figure 2.11: Effect of swirl motion on the spray evolution CAD 360° [1]

Figure 2.12: Effect of swirl motion on the spray evolution CAD 362° [1]

One other study[18] relating to the impact of intake port on combustion performance, also found that higher swirl level in dual fuel engine due to configuration of inlet ports causes higher heat release generation from intense flame intensity and distribution in combustion chamber. This results in prior cessation of oxidation process during expansion stroke due to intense and sudden heat release. Another reason is that to reach the same level of power as that of diesel engine, intake boost pressure demands rise in dual fuel but this eventually increases knock inside combustion chamber. This situation serves to decrease pressure and temperature by increasing the swirl flow and turbulence level that subsequently results in enhancing heat loss to walls. The swirl level decreases thermal efficiency primarily due to heat loss and later ignition, thus value of initial intake swirl ratio should be optimized to obtain higher thermal efficiency and lower NOx emissions along with reduction of knock [19]. The increase in heat loss can be observed with increase in swirl ratio in figure 2.13.
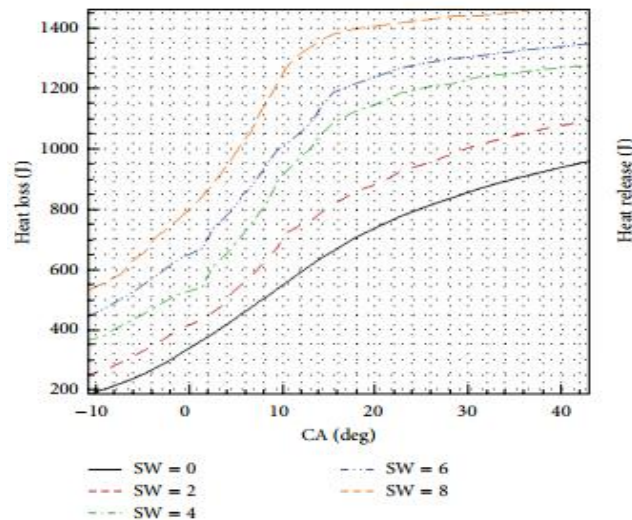

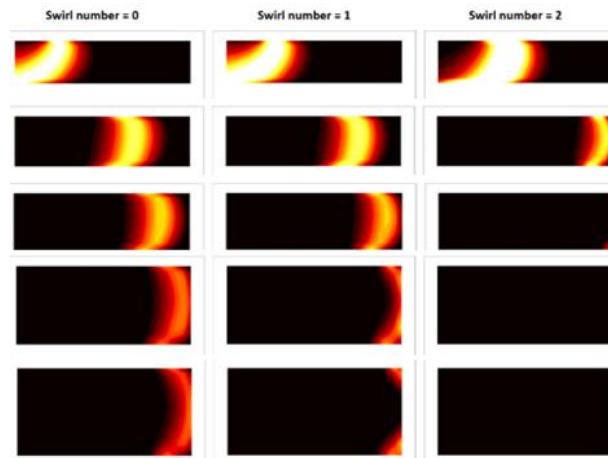Figure 2.13: Effect of initial swirl ratio on Heat loss through walls [19]

Figure 2.14: shows premixed gas combustion with progression of crank angle at three cases of swirl levels for S=0, S=1 and S=2 [32]

A premixed gas combustion phenomenon is shown in figure 2.14 at non-swirl, low swirl, and high swirl cases simulated by O. Kaario [32]. The swirl has impact on flame shape, stability and size. At low swirl level, the flame produced by premixed mixture is less wide and slower than higher swirl case. It shows less radial penetration length when S= 1 than the higher-swirl case for S= 2.The oxidation process during high swirl case extinguishes prior during the expansion stroke. There is more axial penetration of flame length in the non-swirl case and sustains over wider crank angle but could have smaller high-temperature area. The swirl number S indicates the intensity of swirl, which is the ratio between axial flux of angular momentum to the axial flux of axial momentum [33]. The combustion simulation was performed between crank angles of 330°- 400° with ignition at 345°, λ= 1.3, and at speed of 1500 rpm.

2.2.4   Direct Injection

The injection of gas in the intake manifold causes considerable reduction of volumetric efficiency attributed to fuel quality and needed to be adjusted with higher boost pressure by charging the system. The reduction of volumetric efficiency can make worse engine performance during dual fuel operation. In addition, during manifold injection of gas, the displacement effect of gas (the post-injector expansion of gaseous fuel) could create reduction in cylinder charge, which leads to power reduction up to 10% [20]. The spontaneous self-ignition, poor flame propagation, incomplete combustion at part loads, higher tip temperature of diesel injector nozzle, incompetent with future emission regulations and methane slip are some of the major issues related to port injection [20, 21]. On the other hand, high-pressure direction injection of gas using special diesel/gas injector [22], produces diffusion combustion similar to diesel process by injecting high-pressure gas just after injection of pilot diesel fuel. This process enables substitution rates of above 90% by keeping transient behavior, BMEP, and power density similar to base diesel design. The lean burn combustion, un-throttled part load operation, and higher compression ratio similar to diesel engine can be retained [20]. The HPDI handles injection pressure for gaseous fuel up to 600 bars, this process helps to eliminate auto-

ignition knock problem due to non-premixed air gaseous mixture , and higher pressures contribute to faster combustion rate[59].The HPDI helps to improve thermal efficiency of a diesel engine by 5%, and reduction in NOx emissions up to 40%. S. Dumitrescu [23] also reported that engine load carrying capacity could be increased up to 25% relative to normal diesel operation by converting conventional engine into HPDI configuration. However, HPDI system has drawback of high combustion noise due to higher injection pressures of gas, higher heat release due to bitter combustion and increased NOx emissions [20, 59]. The high rate of EGR in consistent with high injection pressures can be employed to keep NOx emissions at constant level [59].

2.3 Cylinder Head

2.3.1 Introduction

Cylinder Head is one of the most critical components and holds complicated configuration of the entire engine assembly. The cylinder head of IC engine has to perform multiple functions like bringing charge air through intake ports, taking exhaust gas out from the cylinder with minimum pumping losses, maintaining coolant flow across critical points with retained thermal loads, and holding the integrity of the structure under compression and tensioning of bolts on account of varying loads. The principal dimensions and construction of cylinder head depend on intake and exhaust port layout, an actuation system, bolt pattern, fuel injector positioning, coolant flow, and more rigorously on the shape of combustion chamber [28, 24]. The prime job of a cylinder head is to [24]:

1. Withstand high thermal and mechanical stresses
2. Support actuation system for valves opening and closing
3. Holds integrity of entire engine unit by means of bolted joints
4. Contain injectors, spark plug, intake and exhaust ports along with valves, valve seats, and valves guiding tubes
5. Routing air/exhaust gases in and out from main engine body with minimum pumping loses and optimized flux motion.
6. Maintain cooling of components as it contains complicated cooling passages
7. Maintain combustion and peak firing pressure
8. Path for fluids (oil, coolant, and delivering fuel to injectors)

2.3.2 Loads acting on cylinder head

There are generally three types of loads act on cylinder head [29]:

1. Assembly loads due to pre-tensioning of bolts, and frictional contact between rough surfaces of cylinder head, gasket, block and intake manifold.
2. Injection, air/fuel mixture and combustion pressure which increases operating forces as product of peak firing pressure and combustion chamber projected area [30].
3. Thermal loads rely on conduction and convection phenomenon acts periodically with engine operation.
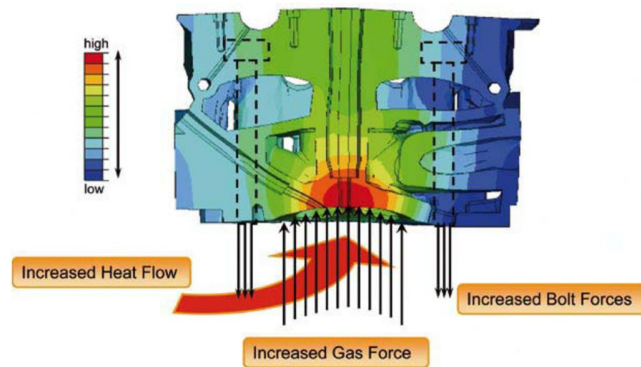
Figure 2.15: Cylinder head loads due to increased peak pressures [30]

2.3.3 Cylinder Head Design Decisions

Cylinder head design decisions are most critical in engine designing process, whether to model a new cylinder head or optimizing the existing one. There are many paired, interconnected technological disciplines like heat transfer, structural fatigue strength, material selection, intake flow, and combustion loads that have to be considered in process of design decisions [31].The starting point for any cylinder head design is the selection of two-valve arrangement or four valve arrangement interconnected with required/determined functions. The multi-valve normally four valves layout is often considered to provide increase valve area having an advantage of centrally located injector hole for improving air-fuel mixing with reduced swirl level [34]. After deciding two or four valves arrangement, the next step is the selection of shape for the combustion chamber, and location of spark plug/injector position. The rate of heat release strongly depends on the speed at which flame front travels is critical in determining engine efficiency, power output, and emission control. There are many other factors like selection of valve layout angle, in diesel engines, to reduce combustion chamber volume for increasing static compression ratio; a narrow valve angle is preferred [24]. The port selection mostly relies on type of flow through specific arrangement of intake system in cylinder head. The tangential port is suitable for moderate swirl level, while a helical port is known for higher swirl flow arrangement and produces uniform response throughout valve lifts. Moreover, the type of orientation and port profile arrangement plays a significant role in flow structures production rate [34]. To summarize the selection procedure, the design decisions relating to cylinder head can be divided into three main categories shown in table 2.2, the table is constructed after going through several theoretical studies [35, 34, 24].The three main designing decision categories are:

1. Global Design Decisions
2. Port Design Decisions
3. Valve Design Decisions

The three main decision elements are largely influenced by constrained factors show in table 2.2. The number of cylinder head bolts depends on peak cylinder pressure and bore size, as bore size and peak firing pressure increases, the number of bolts increases from four to six even up to seven for heavy duty engines. The accurate number of bolts are indispensable for

even distribution of clamping load, and for diminishing cylinder bore distortion. The number of clamping bolts have influence on decision concerning valve layout and space available for ports [34].

Table 2.2 represent necessary design decisions and constraint factors for cylinder head modeling [35, 34, and 24]

Design Decisions	Description	Detail
1. **Global Design Decisions**	Cylinder Capacity Compression Ratio Rated Speed Valve Actuation System Material Selection Frame thickness Combustion Chamber Shape Cooling flow Two valve/four valve configuration Location of the spark plug/Injector Deck chamfer angle	Bore, piston, stroke length Cam/Hydraulics Bottom Deck Thickness Value Pent roof /Flat type Uni/cross/Parallel Effect heat release rate Effect on flow coefficient
2. **Port Design Decisions**	Directed Port ⎤ Cross flow/ Helical Port ⎦ Uni-flow	Swirl/Non swirl/Tumble/ Port angle/ Port cross-section/ Port configuration/Ratio of port dia. to port length/Discharge flow coefficient
3. **Valve Design Decisions**	Valve stem Valve guide Valve size Valve pattern Valve axis angle Valve seat Valve Bridge thickness Valve head Valve cross section	Diameter Distance from valve seat Inner seat diameter Angular location (skew, deg.) Main angle (deg., 30 or 45) 11-12% of Bore Diameter Smallest for high torque Engines
4. **Constraint factors**	Injector/injector boss Cylinder head bolt bosses Coolant jacket features	 Assembly/Thermal/ Combustion loads

2.4.4 Valve and Seat Designing

The intake and exhaust valve are imperative integral of any cylinder head, use to control intake and exhaust flows. The valve face is used to seal combustion chamber and usually made with alloyed steal nickel and chromium. The material choice depends on consideration of high/low temperature and strength observations. Another important unit of valve is valve stem, which can be constructed as one or two pieces welded together. The stem for exhaust valve is usually made thicker with respect to intake to cope with higher temperature levels but the target should be to have thinner stem [24].
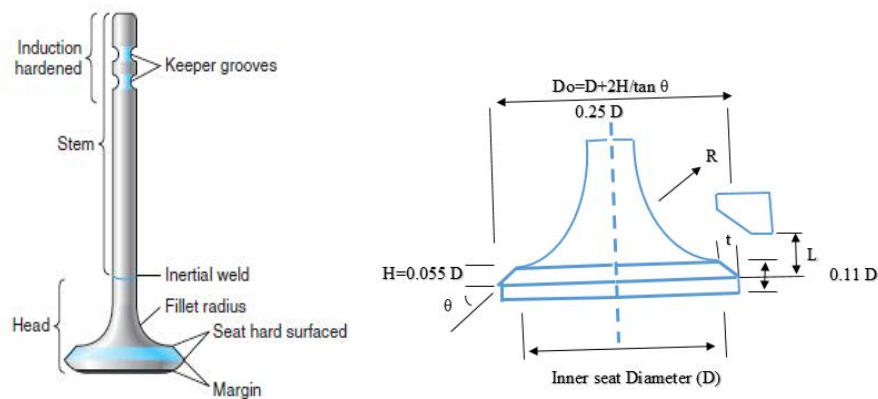

Figure 2.16: Shows most relevant dimensions for valve designing [34]

The valve cone angle affects the flow separation, higher cone angle suppresses the flow separation from valve seat at low lift of valve and improves the flow behavior. In case of higher valve lift, radial flow is encouraged by smaller cone angle and flow separation from cylinder head seat face could be repressed. The valve seat angle of 45º in combination with larger fillet radius improves low lift flow [24].

Some important parameters for valve designing [34]

Non-dimensional inlet valve size $= \frac{D}{B}$ (2.5)

Non-dimensional valve offset (eccentricity), $E = \frac{Y}{B - D_O}$ (2.6)

There are many parameters which do have/do not have influence on swirl ratio coupled with port type like directed port [42] are listed below:

Table 2.3: Shows swirl effect with different parameters change relating to valve and valve seat

Effect of valve seat width	Insignificant
Decrease of valve diameter	Increase in swirl ratio
Increase of valve seat angle (deg.)	Decrease in swirl ratio
Increase of valve lift	Increases then decreases after certain value
Boss height of intake valve	Min effect on swirl ratio

Some important relations that needed to be considered for valve and valve guide designing process [24] are:

$$\frac{Valve\ guide\ length}{Valve\ guide\ diameter} \approx 6.7 \tag{2.7}$$

$$\frac{Int.valve\ head\ diameter}{Int.valve\ stem\ diameter} \approx 5.8 - 7.0 \tag{2.8}$$

$$\frac{Exh.valve\ head\ diameter}{Exh.valve\ stem\ diameter} \approx 5.3 - 5.6 \tag{2.9}$$

$$\frac{Total\ intake\ valve\ area}{Total\ exhaust\ valve\ area} \approx 1.2 - 1.3 \tag{2.10}$$

Valve head diameter as a function of piston diameter

$$\frac{Intake\ valve\ head\ diameter}{Dia\ of\ piston} \approx 0.35 - 0.42 \tag{2.11}$$

$$\frac{Exhaust\ valve\ head\ diameter}{Dia\ of\ piston} \approx 0.28 - 0.37 \tag{2.12}$$

$$\frac{Max.\ intake\ valve\ lift}{Intake\ valve\ head\ diameter} \approx 0.25 - 0.31 \tag{2.13}$$

$$\frac{Max.\ exhaust\ valve\ lift}{Exhaust\ valve\ head\ diameter} \approx 0.30 - 0.36 \tag{2.14}$$

The geometric port area in relation with valve inner seat and valve stem diameter is

$$Geometric\ port\ area = \frac{\pi}{4}(Dp^2 - Ds^2) \tag{2.15}$$

Ds= Diameter of the valve stem
Dp= Minimum diameter of the valve seat

The basic values for seat angle ranges from 15 to 45°. The seat angle plays an important role for effective flow, which increases more rapidly at shallower seat angle for initial lift of valve from seat. The shallower seat angle also plays crucial role for reducing wear at impact load. However, increased flow separation, and sealing problems could be occurred at shallower seat angle. For proper sealing, 0.5–2.0° difference between valve and seat angle is applied. The increase in flow coefficient and reduction in flow separation are usually achieved by marking two-three valve seat angles but this process makes difficult to control valve seat width [24]

2.4.5 Intake Port Designing

Intake port geometry plays a crucial role in nature and intensity of charge motion. Nonetheless, a decisive factor in controlling combustion cycle as combustion efficiency strongly depends on turbulent characteristic of charge flow. Intake Port layout influences other parameters of engine like torque, fuel consumption and emission behavior [12]. The swirl formation together with coupling of intake air inertia is strongly effected by eccentricity of intake port [36].

a) Helical Port
In helical ports, helical shape forces the flow to move around valve axis to produce swirl motion. Helical port usually has slightly better discharge coefficient at medium and low valve lifts [13]. Helical port produces uniform flow and rotational component of velocity about valve axis [37]. The spiral shape of helical port produces pre-swirl around valve axis and angular momentum flux is provided as air flows to cylinder through valve curtain area. The ramp shape and port orientation are geometrical parameters in helical port [38]. At wider speed range, helical port generates higher ordered motion, and higher discharge coefficient in cylinder throughout the intake; at cross ponding swirl level with equally good performance [39].

b) Directed Port
The filling of cylinder is usually high in case of directed port flow. The directed Port plays a decisive role in governing the intake swirl. This port imparts a significant amount of momentum with no substantial vortical structure, and directs the flow to cylindrical line to generate a swirl structure on the scale of cylinder bore [41]. At small valve lift, helical port induced higher swirl ratio with maximum being generated at 60% of maximum valve lift up to intermediated lift level as predicted by J. Kawashima [42]. At time of max valve lift, tangential and helical ports showed same trend but mean swirl ratio inducted by tangential port was at shallow level as shown in graph. This attributed to fact that airflow through helical port was concentrated at certain range, while in case of tangential it was dispersed uniformly across entire tangential port throat [42].

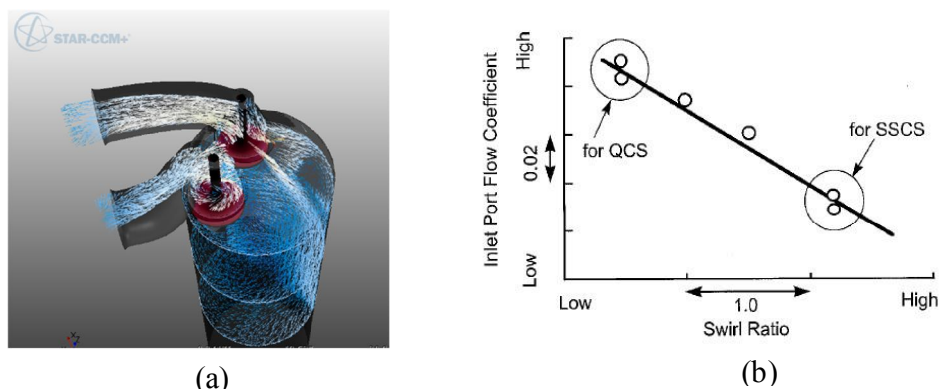| (a) | (b) |

Figure 2.17: Shows shape effect on flow through helical and tangential port (b) quiescent combustion system demands port with high flow coefficient and smaller swirl ratio, while swirl supported combustion system demands ports with higher swirl that will result in low flow coefficient [70]
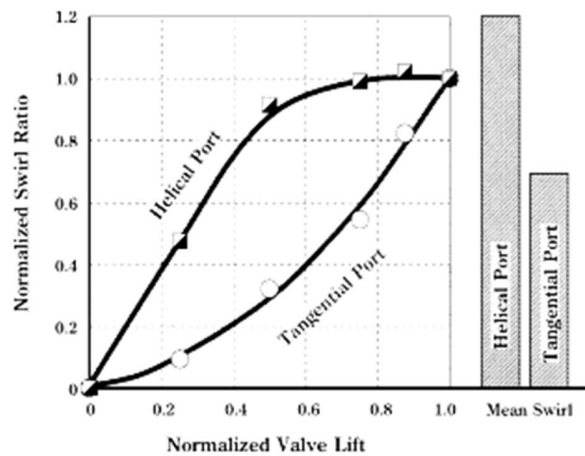
Figure 2.18: shows swirl ratio comparison between directed and helical ports for range of valve lifts [42]

The design parameters for directed intake port are shown in table 2.4:

Table 2.4: Shows design parameters for directed port [45]

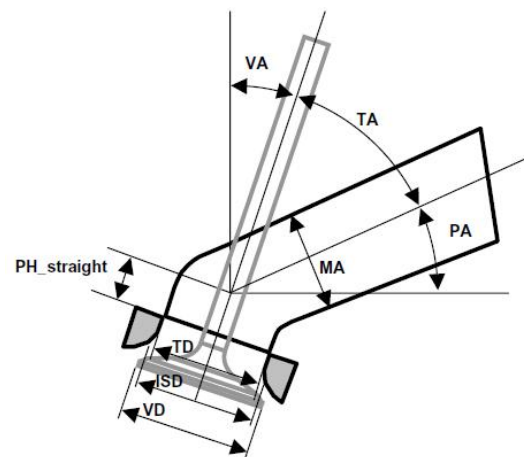| Abbreviation	Description
VA	Valve Angle
PA	Port Angle
TA	Tumble Angle
PH_Straight	Port Height Straight
MA	Minimum Cross Sectional Area
ISD	Inner Seat Diameter
TD	Throat Diameter
VD	Valve Head Diameter

Figure 2.19: Shows designing parameters for directed intake port [45]

c) Intake Port Modeling Requirements:

The designing of intake port has always been challenging to maintain balance between aimed in cylinder motion and pressure loss [37].

Andreatta [25] and Zhen Lu [26] presents necessary design restriction parameters to consider, while designing intake port:
1. Housing for valve guide
2. Bolt bores designed for Cylinder head
3. Housing for injection nozzle

4. Raw material Min. thickness consideration for valve seat top to withstand combustion loads
5. Diameter of valve seat
6. Interface of intake manifold
7. Ref. face machining
8. Positioning and diameter of valve
9. Fixation for injector nozzle
10. Circulation of fluid flow on cylinder head bottom face and injector nozzle
11. High combustion pressure relevance to guarantee sealing of cylinder head gasket by means of bolt load distribution.
12. Consideration of water jackets thickness aimed for coolant flow

2.4.6   Design of Cooling Channels

During high load conditions under abnormal combustion in IC engines, peak temperature could reach around 2200ºC. Therefore, effective heat transfer is crucial for fatigue life of the cylinder head as well as for entire unit [26].

The cylinder head thermal load management is critical factor in cylinder head design. Like too much cooling can also diminish fatigue life of cylinder head because of stern temperature gradients [book]. The motivation of effective cooling jacket design is to limit wall temperatures within adequate range and to keep thermal stresses as low as possible to hinder power loss. Due to complex shape of jacket design, there is possibility of stagnant and high velocity zones because of uneven distribution of flow. This problem should be avoid because this can create hot spots as well as higher pressure zones. In the regime of high heat flux, coolant boiling is another problem near the walls of exhaust port and especially near fire deck that may have adverse effect on job of cooling jackets [27]. Kevin Hoag [24] has recommended some critical issues relating to temperature control that needed to be consider while optimizing cooling jackets design shown in figure 2.20.

Critical Issues in Temperature Control

Component fatigue
Gasket performance
Knock margin
Oil life
Deposit Formation
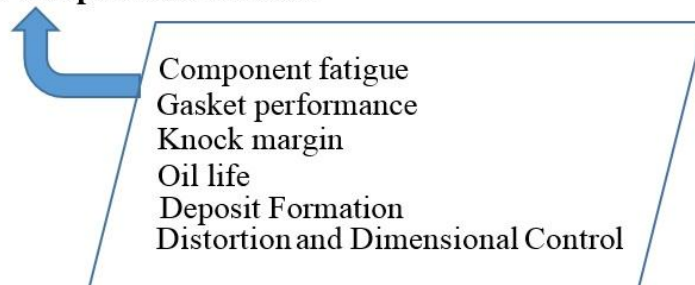Distortion and Dimensional Control

Figure 2.20: Critical issues relating to temperature control [24]

In automobile engines, there are normally three types of coolant flow: series parallel and cross-cooling flow. In series flow arrangement shown in figure 2.21, coolant flows from foremost of block to the rear side and then moves up towards cylinder head where it transfers to front side. The rise of temperature occurs as coolant flow from block to cylinder head, so cylinder head experiences higher temperature at front side than at backside. In this type of flow, coolant jacket possess simple design but cooling imbalance can appear between forward and backward side of cylinder head but problem can be prevented by progressively increasing the cooling channels dimension. In parallel flow design arrangement shown in fig. 2.22, coolant enters from front side and instantly transfers to cylinder head, a distribution of flow occurs between cylinder head and block. The coolant holds two paths, one for cylinder head and other for main block with advantage of lower coolant temperature variation in cylinder head maintaining balance level between two components. Another type of coolant flow arrangement is shown in figure 2.23; the most popular in truck engines or heavy-duty vehicles is cross flow coolant flow having property of reduced temperature variation but at expense of more expansive casting. A high-pressure coolant header is casted along the length of cylinder block, whereas coolant is supplied by means of pump to individual cylinders and collected at upstream low-pressure water manifold [24].
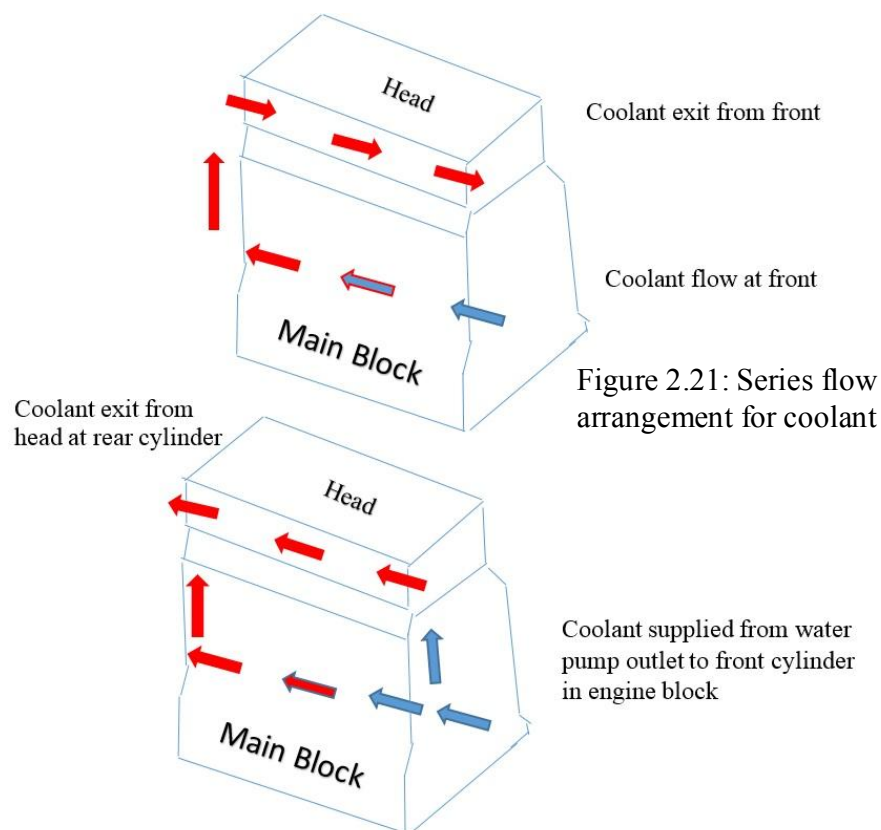

Figure 2.21: Series flow arrangement for coolant
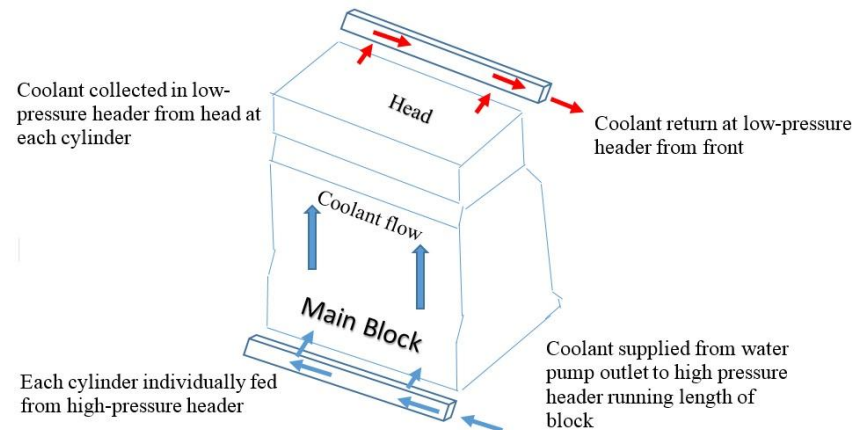
Figure 2.22: Parallel flow arrangement for coolant

Figure 2.23: Cross flow arrangement for coolant

a) Coolant jacket design for Cylinder Head

In cylinder head, there are many critical regions containing high heat flux due to enormous exhaust temperature that needed to be control, consequently an effective cooling jacket is indispensable. The main objective of any effective coolant jacket design is to avoid temperature imbalance, stagnation points and high velocity areas [24]. The imbalance of temperature can be avoided by varying flow areas and adding restrictions for critical passages as shown in figure 2.24.
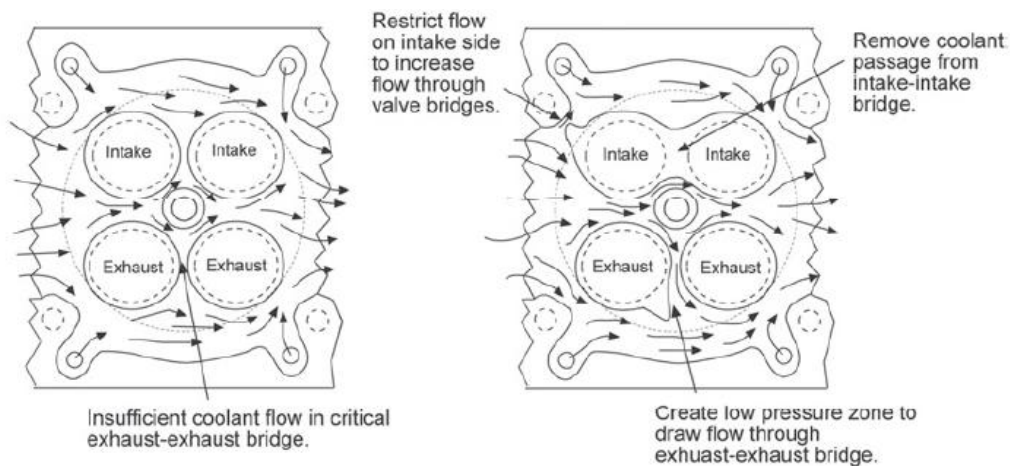

Figure 24: Shows cylinder head cooling jacket modification on right side for flow improvement in critical regions [24]

Advanced engine cooling system prefer to use high temperature cooling technique to achieve high temperature cooling effect through nucleate boiling. Therefore, greatly reduce volume of coolant by increasing the operational temperature and lessen warm up time from cold start condition. This condition proportionally effects the power performance and fuel economy [44].

2.5   Advanced Optical Engine Configuration

The advanced optical research engine configuration is shown in figure 2.25, which includes 2-color pyrometry probe and an infrared (IR) absorption probe (La Vision ICOS) for temperature and optical thickness evaluation of particulate matter clouds and local fuel concentration measurements [71].
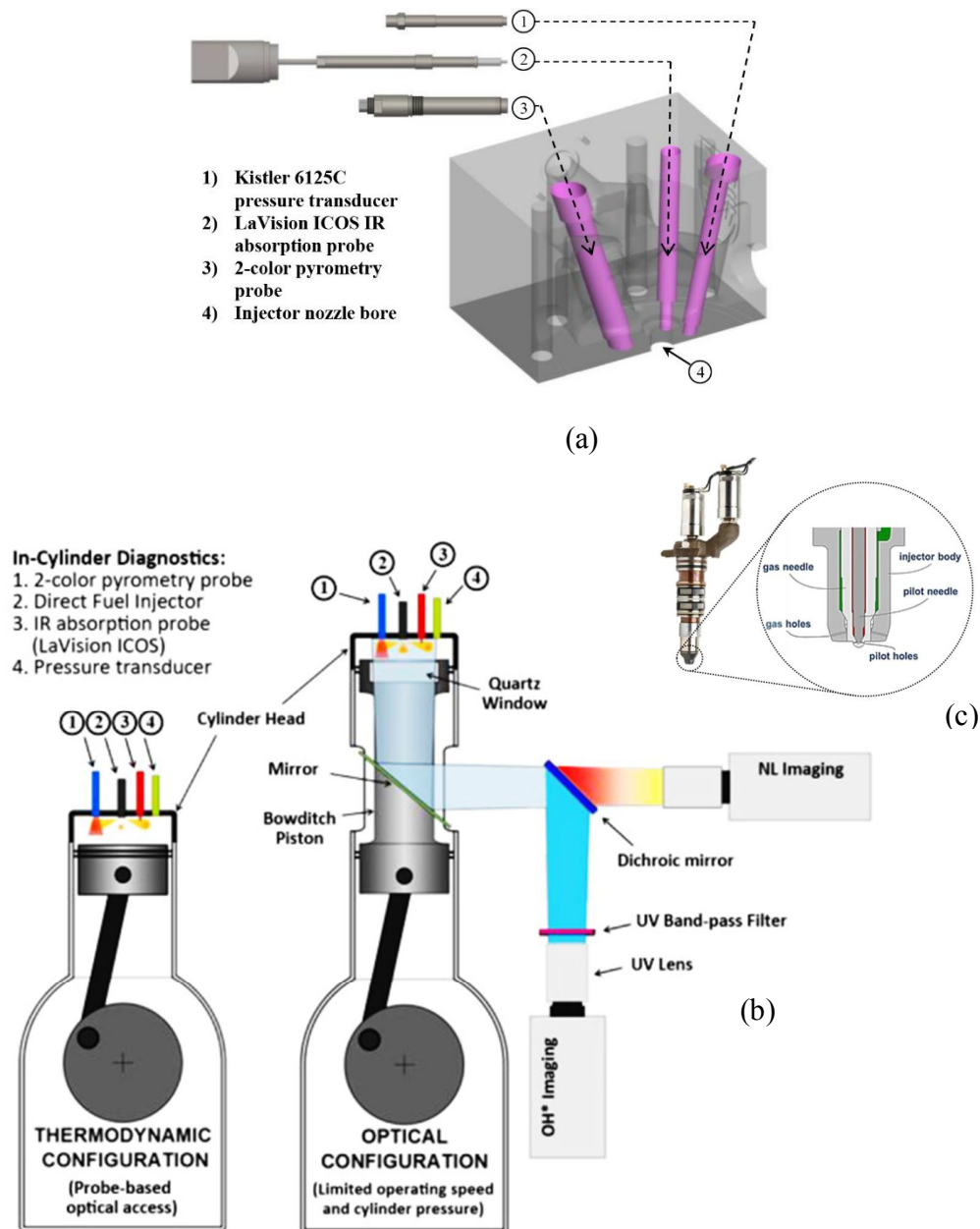

(a)

(b)

(c)

Figure 2.25: (a) Cut-view section of cylinder head (b) Advanced measurements configuration on modern cylinder head with direct fuel injectors both for optical and for common engine (c) Direct Dual Fuel Injector type for HPDI system [71]

2.6 Additive Manufacturing

Additive Manufacturing, well known as 3D printing has achieved its recognition for customized products in automotive, biological, and aerospace industries. This layer wise manufacturing technique can be used to build any kind of complicated shapes by selecting tailored materials. The lowering cost of CAD software and 3d printers with increasing competition has created space for individuals to make their own custom made products and extemporize this technology. Instead of these features, there is still long way head for this technology to capture batch production market and replace existing conventional manufacturing techniques because of its moderate fabrication process. Still AM is influencing traditional methods in terms of mass production e.g. big industrial giants like General Electric is investing heavily on metal based techniques to improve efficiency of their products like engines and get self-reliance from third party suppliers. They have intended to produce beyond 100,000 additive parts for its LEAP and GE9X engines by 2020 [43, 44]. Brett P. Conner [44] has presented different regions in comparison with conventional manufacturing process to highlight the significance of AM: (1) AM has complexity advantage because CM requires multiple parts fabrication to make complex part. AM can exhibit complexity to part in terms of features, geometries, part and fabrication step consolidation (2) Mass complexity improvement in AM (3) AM has also dominance in individual part customization (4) mass customization is difficult job with CM (5) Artesian products manufacturing is another fascination that can be achieved with AM. (6) Complete manufacturing freedom (7) Mass manufacturing of AM is no doubt still less than conventional method (8) AM has edge over traditional methods in manufacturing of few.
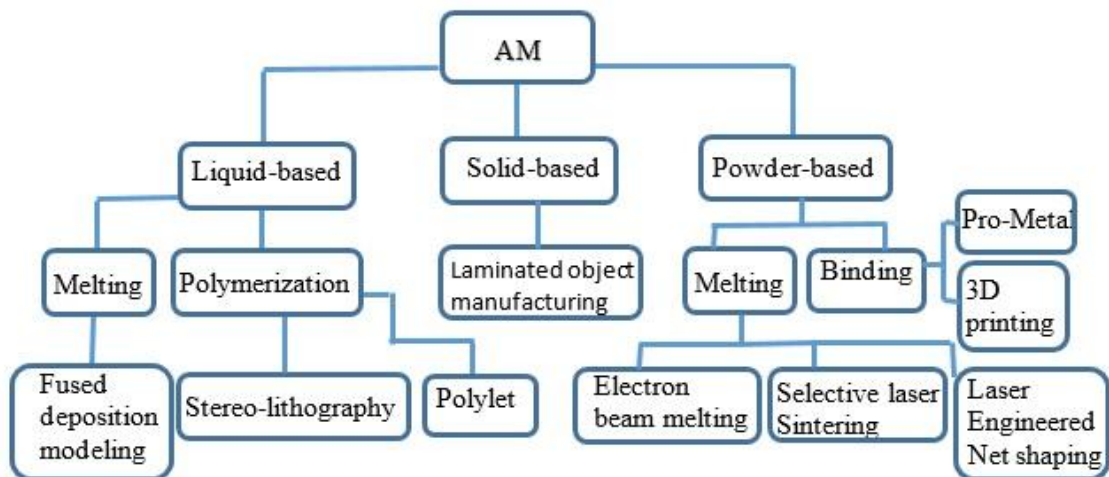

Figure 2.26: Pictorial overview of AM processes [58]

Table 2.5: Shows Different categories of AM, their selection of materials, power source, strength and downsizes [60, 61]

CATAGORIES	TECHNOLOGIES	PRINTED INK	POWER SOURCE	STRENGHTS/ DOWNSIDES
Material Extrusion	Fused Deposition Modeling (FDM) Contour Crafting	Thermoplastics, Ceramic slurries, Metal Pastes	Thermal Energy	• Inexpensive extrusion machine • Multi-material Printing • Limited Part Resolution • Poor surface finish
Power Based Fusion	Selective laser sintering(SLS) Direct Metal Laser Sintering(DMLS) Selective Laser Melting(SLM) Electron Beam Melting(EBM)	Polyamides/Polymer Atomized metal powder, stainless steel, cobalt chromium, titanium Ti6Al-4V), Ceramic Powder	High Power laser Beam Electron Beam	• High accuracy and Details • Fully Dense Parts • High specific Strength/stiffness • Powder handling and Recycling • Support and anchor structure
Vat Photo polymerization	Stereo lithography (SLS)	Photopolymer, Ceramics	Ultraviolet laser	• High Building speed • Good part resolution • Over curing, scanned line shape • High cost for supplies and materials
Material Jetting	Polyjet/Inkjet Printing	Photopolymer wax	Thermal Energy Photocuring	• Multilateral Printing • High surface finish • Low strength material
Binder Jetting	Indirect inkjet Printing(Binder 3DP)	Polymer Powder Sand, metallic Powder	Thermal Energy	• Full color objects Printing • wide material Selection • High Porosities on finished Part
Direct Energy Deposition	Laser Engineering Net shaping(LENS) Electron Beam Welding(EBW)	Molten Metal Powder	Laser Beam	• Repair of damaged/worn Parts • Require- Post Processing machine

2.6.1 Selective laser Sintering

The parts with intricate details and exhibit complex features can be manufactured with SLS technique. Selective laser sintering is a process in which laser beam is applied to fuse or sintered the powder-based material (nylon or any other polymer, metals) and joined together by each layer specified by design. A piston driven bed contains powered material and lowers according to specified thickness of each layer [55]. The commercially available machines are classified according to deposited powder, the maintained atmosphere (Ar or N_2), and type of laser usage (Nd:YAG laser,CO_2 laser) [56]. The discrete intervals (approximately 100 – 200 μm) are used to slice CAD file, a build file is employed to store resulting cross-sections successively, and then scanning algorithms guide the route of laser for each sliced cross section. The wide variety of products like ceramics, metals and polymers can be deployed in SLS process [57].

2.6.2 Binder Jetting Process

AM is also contesting in foundry industry, as internal combustion engines house excessive number of sand core casted parts like main block, cylinder head, cooling jackets and crankshaft as well. The sand core fabrication through AM has eradicated the usage of hand tooling, grants design freedom, and significantly lessens lead time over traditional pattern building process. The well-known process is binder jetting powder based process which can knob sand, powder based polymer and metals. The binder jetting process involves printing, curing, cleaning, sintering and finishing [45].The process involves spreading of binder on each layer of activated sand through appropriate printer head, and the operation of printer head is controlled through designated CAD file. The polymerization reaction takes place when binder reacts with activated sand and binds the particles of sand together. The used curing process depends on binder usage, and can be done in air or by some external heat source [58].
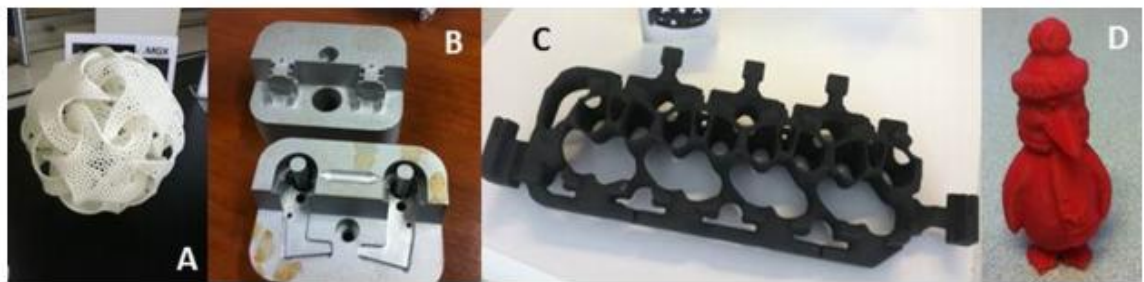

Figure 2.27: Shows examples of AM products. (A) An intricate ornamental piece printed from nylon-11 material using selective laser sintering. (B) Laser based powder bed fusion 3D printing process for injection molding dies made of stainless steel. (C) Binder jetting process for 3D printed automotive cylinder head water jacket sand core. (D) A logo printed using a desktop material extrusion printer [44].

3 Methods

3.1 Requirements for New Cylinder Head

Before going into outline of approach adopted for designing and CFD analysis, it is imperative to discuss the set requirements for new cylinder head design and configuration under constrained features already present in existing model.

1. Aim to have less swirl or no swirl flow in cylinder. As with advancement of injection system to achieve quiescent combustion (which do not depends on air motion but more rely on momentum of fuel spray), and to better visualize combustion phenomenon during dual fuel operation requires less swirl or no swirl.

2. No major modifications relating to bolts layout position for clamping of new cylinder head with main block.

3. Intake port designing under constraints of using existing valves, valve guides and bolts location.

4. Exhaust port designing according to former bolt positions.

5. Material optimization.

6. Additional space for injector sleeve for pursuit of direct gas injection , which requires more space because of additional sized dual fuel injector.

7. Cooling channels study and optimization.

8. Suitability of CAD model for 3D printing to test model for later swirl check experimentally.

9. Aptness of CAD model for 3D printing of core for casting in later stage.

3.2 Method overview

The procedure implemented and steps followed in this thesis work are illustrated in form of block diagram shown below in figure 3.1.
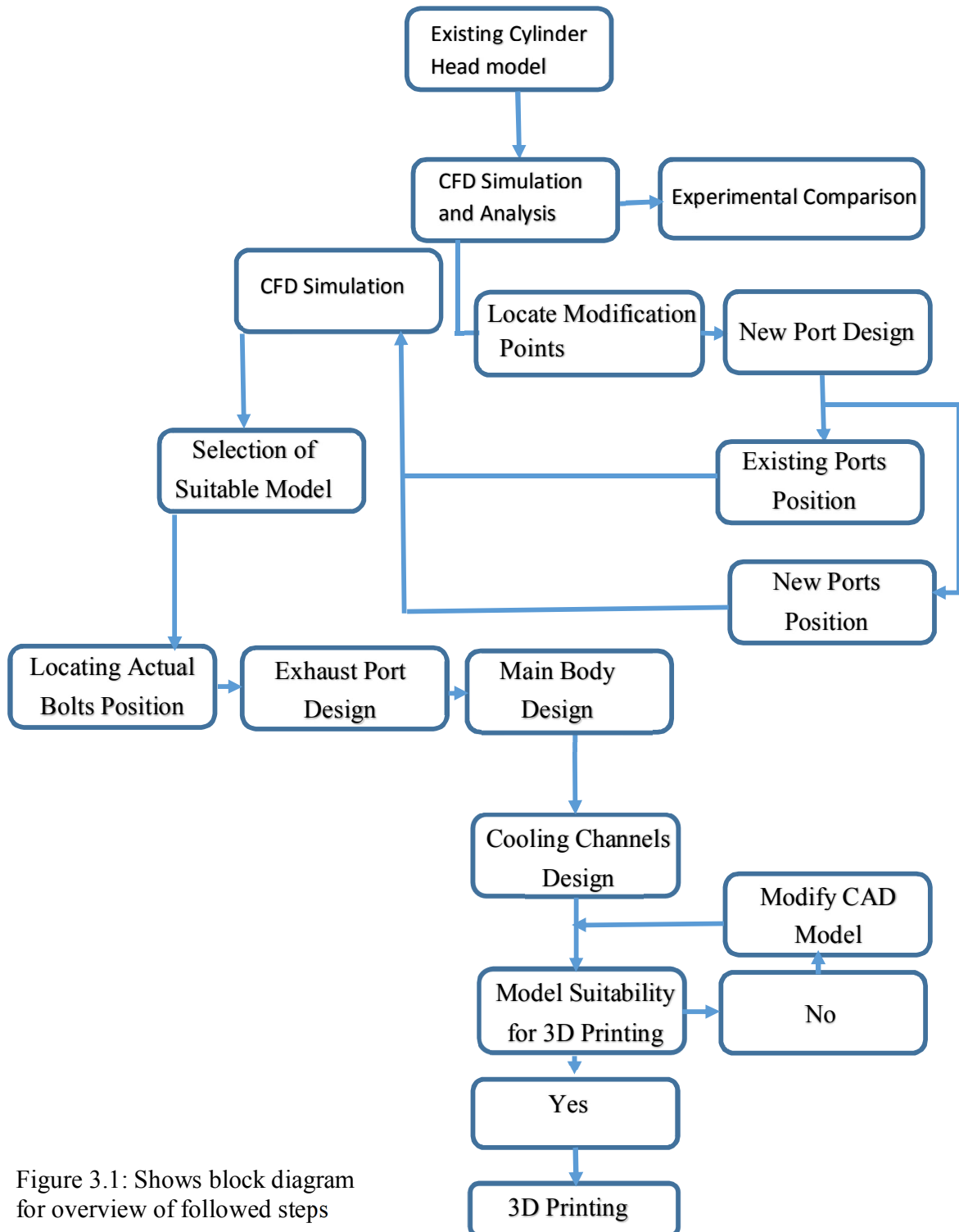

Figure 3.1: Shows block diagram for overview of followed steps

3.3 CAD MODELING

The CAD modeling was done by utilization of PTC Creo Parametric software (University Edition). The CAD modeling was performed for new intake ports, exhaust ports, valves, valve seats, valve guides, springs, main body, bolts and for cooling channels. The designing process was employed by using appropriate relations already described above in theoretical study of section 2.4, and some supplementary relations are discussed in Results and Analysis section. The CAD models for the valve, valve seat and valve guides are shown in figure 3.2.The duplicates of these components for new and existing cylinder head were created due to unavailability of their CAD models. The CAD modeling of other components is described separately in accordance with CFD results in Results and Analysis part.

Table 3.1: Shows Dimensions for valve seat

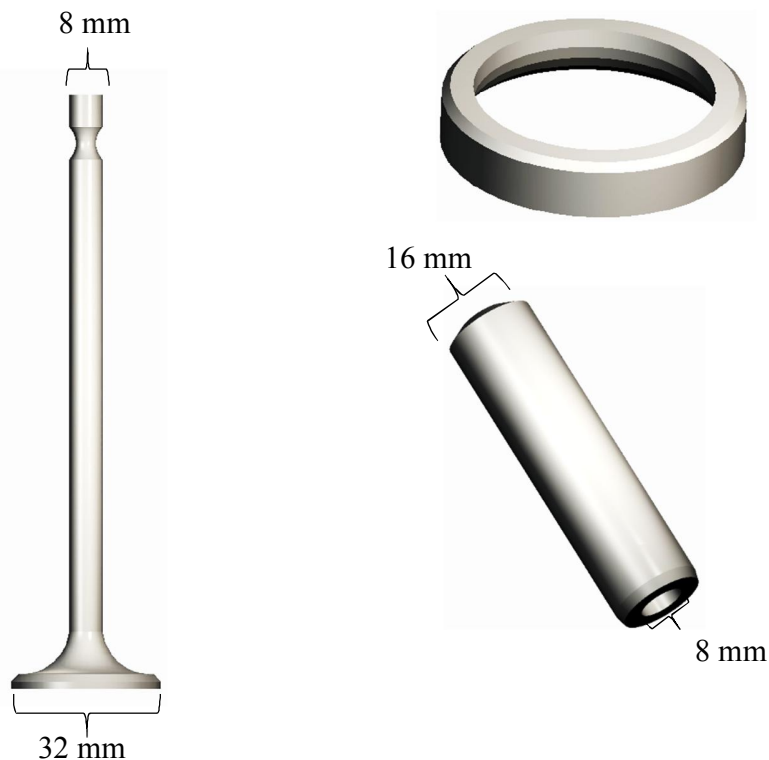| Dimensions Valve Seat	Intake side	Exhaust Side
Inner Diameter	16 ± 1.5 mm	14.25± 1.25 mm
Outer Diameter	20.5 ± 1.5 mm	18 mm ± 1.5 mm

Figure 3.2: Shows newly designed model for intake valve on left side, valve seat and valve guide on upward and downward of right side respectively (The main dimensions were measured, and appropriate relations were used to calculate unmeasured values)

3.4 Existing Cylinder Head Geometry

The current model of cylinder head for LEO-1 and LEO-11 engine is based on four valves configuration, containing two intake ports and exhaust ports. The intake and exhaust ports are positioned opposed to each other in cross flow layout. The intake side has one helical and directed port shown in figure 3.3 to take advantage of generating pre-swirl and after swirl air flow inside the combustion chamber. The purpose of helical port is to produce optimum swirl at low valve lift, and avoid sudden pressure drop at range of valve lift. Because when the valve lift is small, the impact of shape of port on flow pattern reduces and flow is mainly hindered by valve. The helical port was placed upstream at off centered position because of which it is not possible to produce concentric swirl in the cylinder. By considering that point in mind tangential port was placed tangentially towards cylinder liner to produce secondary rotational momentum, and merging of two flows (flow from helical and directed port) produces a concentric swirl motion. By placing helical port in upstream direction and small flow interference near valves reduces sensitivity of swirl ratio on orientation of helical port [46], and dominant swirl flow from tangential port at higher valve lift.
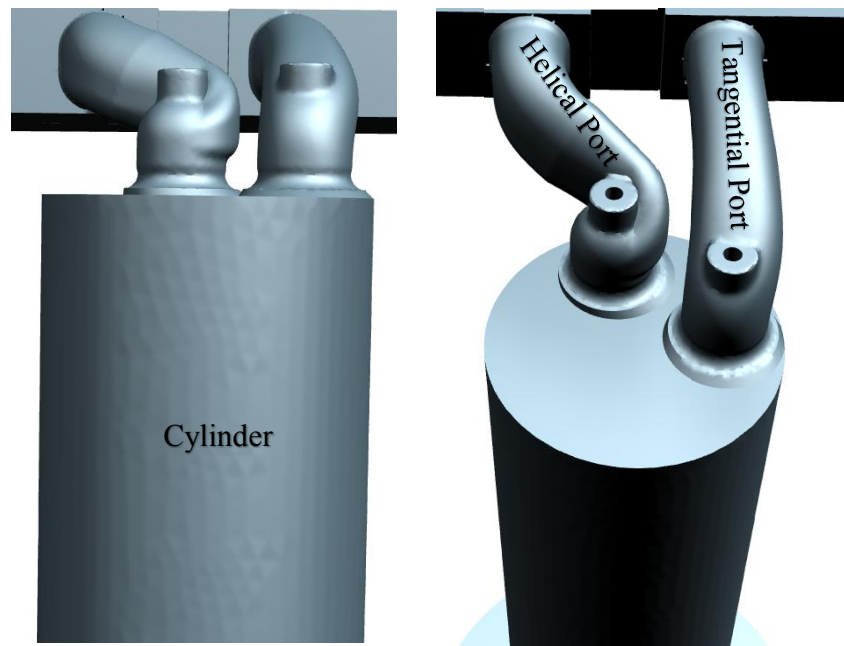

Figure 3.3: Front view on left and isometric view on right side shows tangential and helical ports in existing model of cylinder head

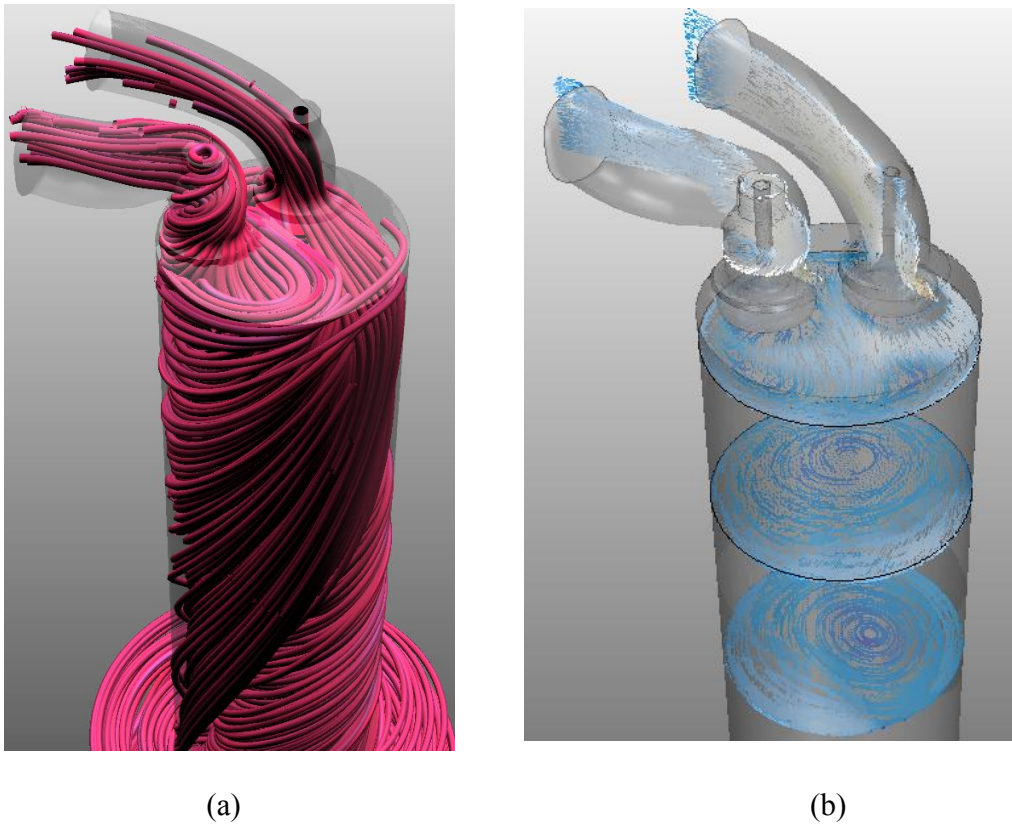(a)   (b)

Figure 3.4: Shows dominant swirl flow from tangential port at higher valve lift in (a) depicted by means of tube streamlines, (b) shows concentric swirl at mid and lower plane due to emerging of flow from two ports

3.5 Specifications of Engine

The laboratory research engine is an AGCO 84AWI 6-cylinder common rail diesel engine having dual fuel capacity, revamped into single-cylinder engine for research-oriented applications named as LEO configuration.

Table 3.2: Major specifications of engine

Engine Specifications	
Cylinder Bore	111 mm
Compression ratio	16.5
Displacement total	8.42 liter
Stroke	145 mm

3.6 Experimental Procedure of Swirl Testing for Existing Cylinder Head Model

The PIV is based on instantaneous whole field measurement technique, where several pictures for charged tracer particle of flow passing from laser sheet are taken with short time delays. The two dimensional in plane velocity components of local flow structures are calculated through displacement of particles [65]. The experimental results for current model of cylinder head are copied from previous study performed by O. Kaario [47]. The steady state flow rig was utilized for both PIV (particle image velocimetry) and paddle wheel measurements. The pressure difference of 2500 Pa was maintained among cylinder head at upstream and balancing reservoir at downstream ahead of measurements plane. The measurements were made at valve lift height of 1, 2, 4, 6, 9, and 11mm. The planes selected for measurements were 9 mm and 194 mm (1.75B) from cylinder head.
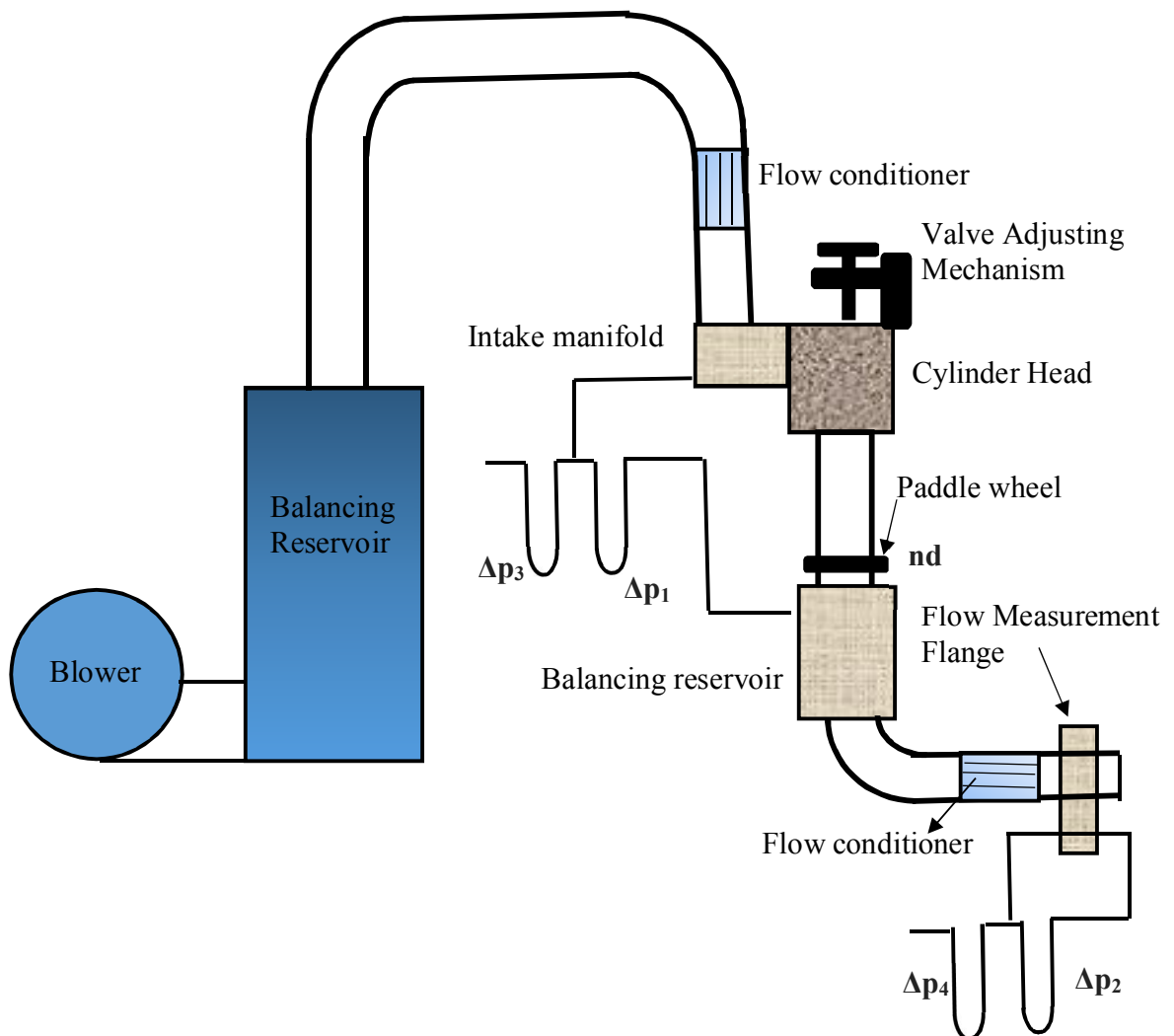
Figure 3.5: Shows Experimental Setup for PIV

3.7 CFD Simulations

CFD simulations are performed by considering steady state incompressible flow based on RANS turbulence modeling approach as solver. Star CCM+ [48], a commercially available software is used for CFD analysis.

Star CCM+ relies on Finite Volume Methods and configured with numerical algorithm to solve fluid and heat transfer problems. It contains:

i.   preprocessor (changing geometrical parameters, defining geometrical domain and fluid properties, grid generation),

ii.   numerical solver (discretization, iteration)

iii.   Post-processer (vector and scalar scenes, plots, grid display)

3.7.1 Finite Volume Method

Finite Volume method is a numerical approach of converting partial differential equations exhibiting conservation laws into discrete algebraic equations over finite cell volumes. The solution process involves discretization of geometric domain into non-overlapping elements or grid nodes. The subsequent step is converting PDE's into algebraic equations by integrating upon individual elements, and values of dependent variable for each element or point are computed through solving system of algebraic equations. The distinct property of FVM is being conservative, and can be devised in to unstructured polygon meshes [49].
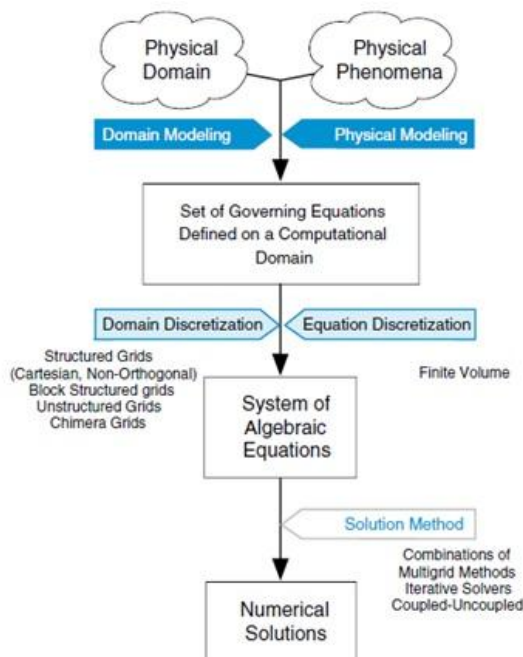

Figure 3.6: Shows the discretization process in FVM [49]

3.7.2 RANS (Reynolds-averaged Navier-Stokes)

To extract large-scale dynamics of flow averaging is utilized over small-scale fluctuations. RANS is based on same ensemble averaged approach, uses to solve effects of large-scale flow motion by means of taking averages of small scales of turbulence, and modeling the nonlinear small scales that change large-scale motion.

The steady state Reynolds averaged Naiver–Stokes continuity and momentum equations can be written as

$$\frac{\partial (\mathrm{U}_i)}{\partial x_i} = 0 \tag{3.1}$$

$$\rho \frac{\partial}{\partial x_j}\left(\mathrm{U}_i \mathrm{U}_j\right) = \frac{\partial P}{\partial x_i} + \frac{\partial}{\partial x_j}\left[\mu\left(\frac{\partial (\mathrm{U}_i)}{\partial x_i} - \rho \overline{u_i \acute{u}_j}\right)\right] \tag{3.2}$$

Where P is pressure, ρ is fluid density, U_i component of velocity in x_i the direction, μ is dynamics viscosity, and $\acute{u}$ is fluctuating component of velocity, $-\rho \overline{u_i \acute{u}_j}$ are called Reylonds stresses, which are additional terms introduced in Navier stokes equations because of Reylonds averaging, and must be solved. The Boussinesq hypothesis is used to relate Reylonds stresses to mean velocity gradients.

$$\rho \overline{u_i \acute{u}_j} = \mu_t\left(\frac{\partial \mathrm{U}_i}{\partial x_i} + \frac{\partial \mathrm{U}_j}{\partial x_i}\right) - \frac{2}{3}\left(\rho k + \mu_t \frac{\partial \mathrm{U}_i}{\partial x_i}\right)\delta_{ij} \tag{3.3}$$

$k = \frac{1}{2}\rho \overline{u_i \acute{u}_j}$ is turbulent kinetic energy

A disadvantage of Boussinesq hypothesis is that it consider μ_t as isotropic scalar quantity, which is not true [50].

3.7.3 Turbulence Model and Solver

There are small scale and high frequency fluctuations in turbulent flows characterized by erratic velocity fields. The governing equations can be manipulated to eliminate small-scale high frequency fluctuations with an outcome of set of equations that are computationally less expensive to solve. The modified equations contain extra-unknown variables, hence turbulence model will be required to solve these values. Turbulence model is a way of closing mean flow equations (modified Navier–Stokes equations), without first solving full time dependent flow field [51].
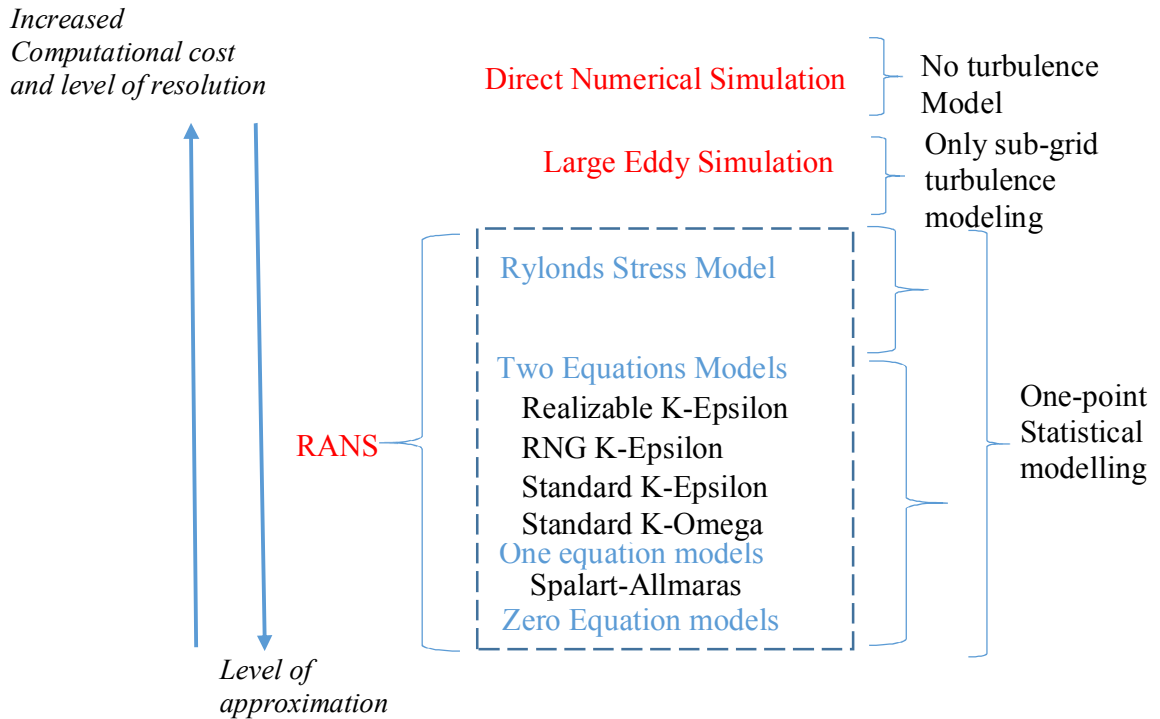
*Increased
Computational cost
and level of resolution*

Direct Numerical Simulation

No turbulence
Model

Large Eddy Simulation

Only sub-grid
turbulence
modeling

Rylonds Stress Model

Two Equations Models
    Realizable K-Epsilon
    RNG K-Epsilon
    Standard K-Epsilon
    Standard K-Omega
One equation models
    Spalart-Allmaras
Zero Equation models

RANS

One-point
Statistical
modelling

*Level of
approximation*

Figure 3.7: Shows schematics of turbulence modeling [51]

i) Two equation Realizable *k*-epsilon

The standard *k*-Epsilon displays better performance for boundary layer flows, however does not exhibit good behavior under strong separation due to over predicting the eddy viscosity term. To overcome this problem, T.H Shih [53] developed a new k-epsilon model called realizable *k*-epsilon. The term realizable defines that it fulfils certain mathematical constraints for Reynolds stresses through maintaining consistency with turbulent flows physics. The realizable *k*-epsilon model makes certain that normal stresses are positive for flows with large mean strain, as in case of standard k-ε it becomes negative. The normal components of Reynolds stress tensor:

$$(u_i u_{i)} = \sum_i (u_i^2) = \frac{2}{3}k - 2v_T \frac{\partial (U_i)}{\partial x_j} \qquad 3.4$$

By definition, normal stress $(u_i u_{i)}$ should be larger than zero due to sum of squares but equation (3.4) implies that normal stress turns into negative value when strain is sufficiently large. The realizable k-ε introduces a variable C_μ (non-constant value) to avoid the negative term for normal stresses, and under any type of flow conditions, it ensures positive value being function of local state of the flow. This process of keeping positive value for normal stresses is known as realizability. The realizable *k*- ε model also involves modification for dissipation equation, a production term for dissipation of turbulent energy [51, 53].

- **Advantages**

Perform better for boundary layers under adverse pressure gradients
Good to simulate flows involving high mean shear rate or separation
Predict round jet spreading accurately
Equivalent benefits as RNG along with advantage of resolving round jet anomaly
Better simulate flows containing swirling, rotation, recirculation, and robust streamline curvature [52].

- **Weakness**

Limitation in relation to assumption of eddy viscosity
Under the considerations of above-mentioned advantages, realizable k-Epsilon is selected to simulate swirl flows [52]

3.7.4 Solver, Boundary Conditions and Geometry Preparation

By using segregated flow solver, a nexus between the momentum and continuity equations is performed with predictor corrector approach as it solves flow equations in uncoupled way. This solver is most suitable for constant density flows with advantage of using less memory with faster convergence rate [48].

The suitable use of boundary conditions play a dominant role in numeric stability of CFD results. There were three kinds of boundaries being used: inlet, wall and outlet boundary. The inlet and outlet boundary conditions used are same as in experimental process [47], a pressure difference of 2500 Pa over cylinder head is created by applying inlet and outlet pressure. The pressure B.C's are chosen to simulate real engine conditions. The cylinder liner was extruded in normal direction to avoid reverse flow, and the fast convergence demanded to have extruded inlet and outlet boundaries away from cylinder head region in CFD computation domain.

3.7.5 Wall Treatment and Meshing

The suitable capturing of near wall effects are extremely important relating to internal combustion engine flows because of nature of highly disorder Reynolds number variation and chaotic behavior of separated flows. Near wall treatment approach should be correctly evaluate for boundary layer behavior i.e. anisotropy of shear stresses aimed at accurate assessment of flow separation [31].

The flow details within boundary layer especially in turbulent flows are of great importance in CFD simulation. In order to get acceptable boundary layer results, two layer of prismatic cells were generated adjacent to wall for maintaining $30<y^+<150$ in logarithmic region using all y+ hybrid wall treatment.

To better capture swirl and re-circulating flow behavior, polyhedral mesh was selected. Polyhedral mesh offers equal benefits of automatic meshing as tetrahedral mesh with overcoming the problems of limited stretching and poor gradient approximation as exhibit by tetrahedral meshes. A polyhedron with 12 faces and large number of neighboring cells causes lower cell count with better solution and convergence [48].
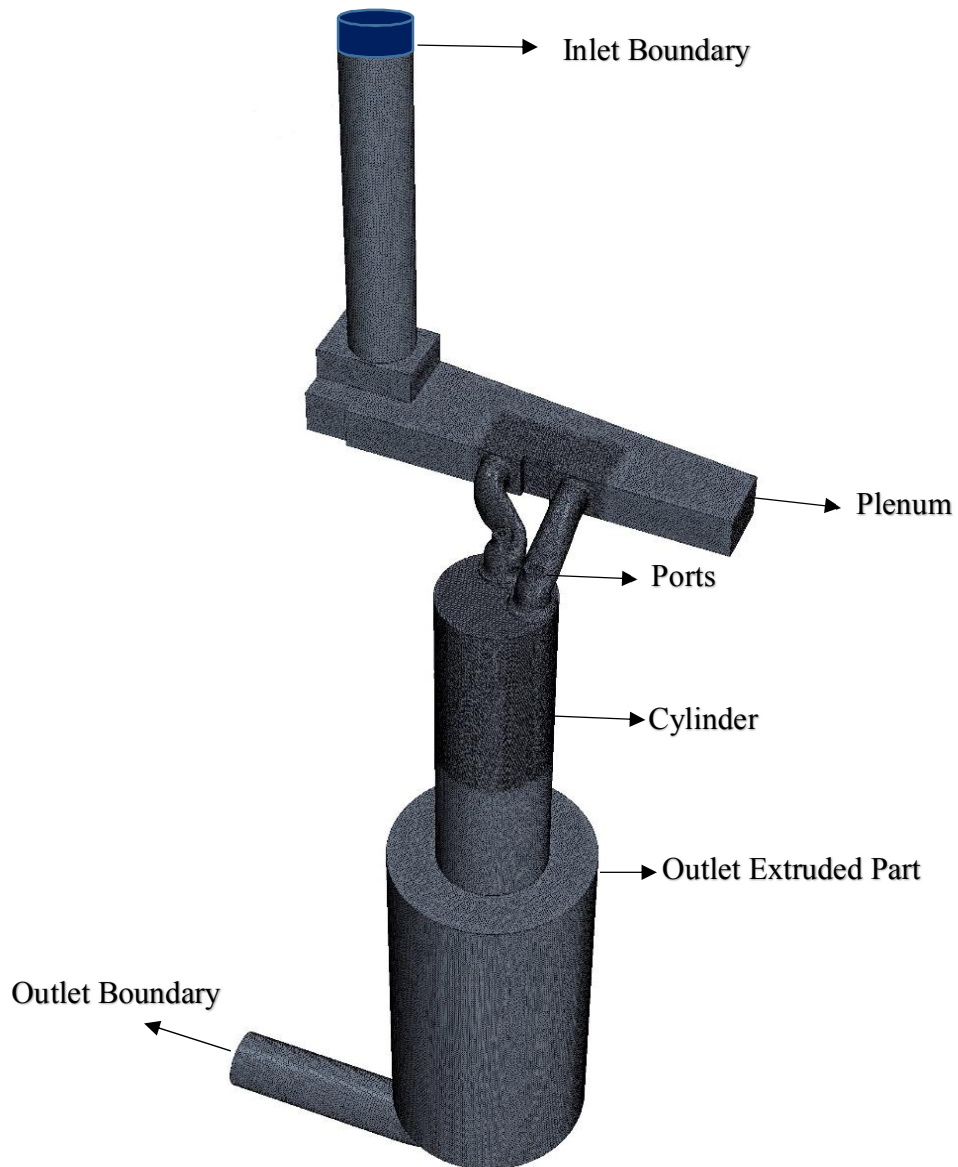

Figure 3.8: Depiction of computational domain for flow

4 Results and Analysis

As already described in previous chapter 3, the steady state incompressible simulations were performed because of air density was considered constant. The simulations were made at three valve lifts, to check the behavior and swirl of the air flow with variation in valve lifts. The valve lifts of 3.7, 7.7 and 12.7 mm were selected being one lowest, medium and highest respectively. The turbulence intensity was kept at default value of Star CCM+, and turbulence length scale was typically about 5% of the characteristic dimension of the inflow. The solution was initially run with first order upwind scheme for couple of iteration and then second order upwind scheme was employed for better convergence. The mesh independence study was devised for existing model of cylinder head at three different grid densities, then selection of most suitable number of cells was made at which solution is independence of grid. The grid dependence study has significance in good predictive solution of CFD, especially in intake flow analysis of internal combustion engine.

Table 4.1: Adopted mesh density

Classification of Mesh Density	No of Cells	Mesh Size in Valve Lift Region
Coarse mesh	1,500,000 Cells	3 mm
Medium mesh	3,800,000-4,000,000 Cells	1 - 0.8 mm
Refined mesh	6,000,000 Cells	0.6-0.4 mm

During mesh independence, the variation in value of rotational speed (1/sec) of solid body vortex was checked by using appropriate relation from which swirl ratio was calculated. The rotational speed was calculated by taking average of tangential velocity in measured plane divided by average distance of each cell center form cylindrical axis. The medium mesh size was chosen because solution was almost independent at higher refined grid size. The swirl plane was selected at 1.75B as it in experimental procedure [47], where B represents bore of cylinder. The same relation described in equation 2.1 was used to calculate the swirl ratio in CFD numerical solutions.
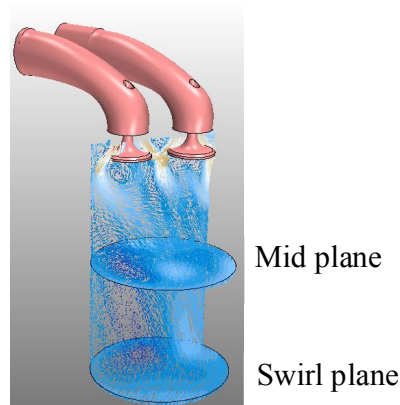

Mid plane

Swirl plane

Figure 4.1: Shows swirl measured plane at 1.75B length

4.1 Results from Existing Cylinder Head Geometry

The mass flow rate and pressure difference value graphs for current geometry containing helical and tangential port are shown in figures 4.3 and 4.4 respectively. The mass flow and pressure difference values are very much proximate to experimental [47] results for defined range of valve lifts. The swirl ratio vs valve lift graph is also depicted in figure 4.6. The tube streamlines illustrate that dominant clockwise swirl flow is from tangential port at maximum valve lift. A detail discussion has been made in proceeding section 4.4.4 regarding flow field by means of planner streamlines imposed on vector scenes.
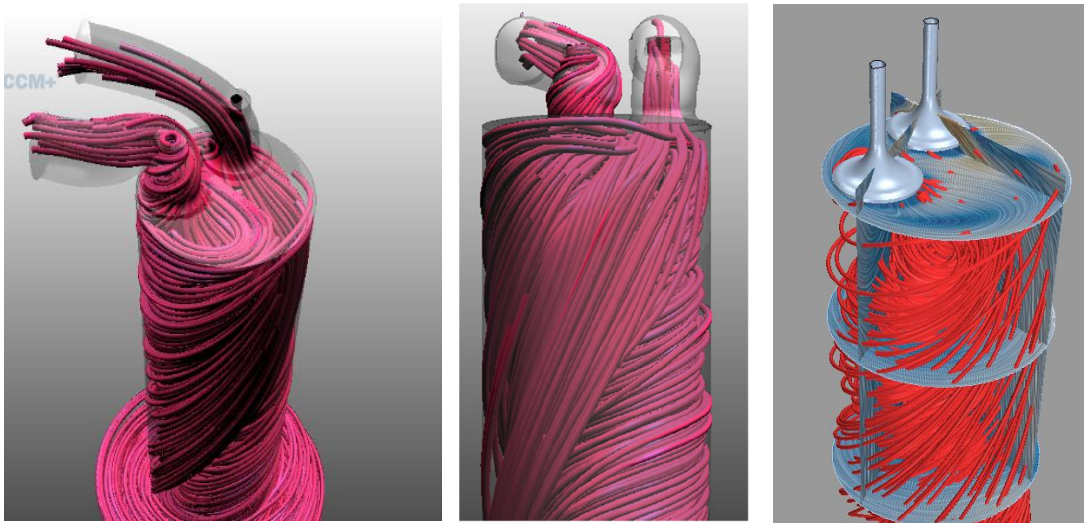

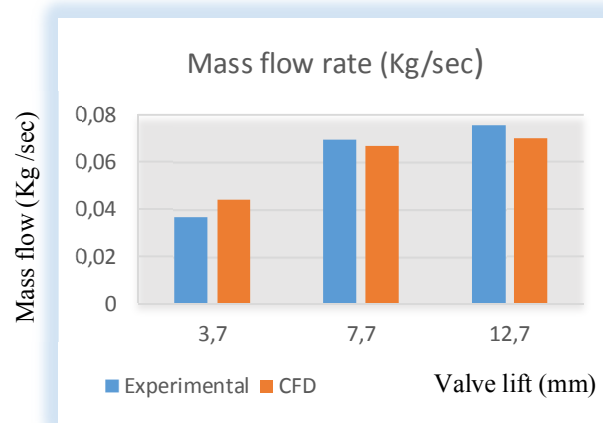Figure 4.2: Shows streamlines inside cylinder

Figure 4.3: Shows mass flow at defined valve lifts for existing model of cylinder head
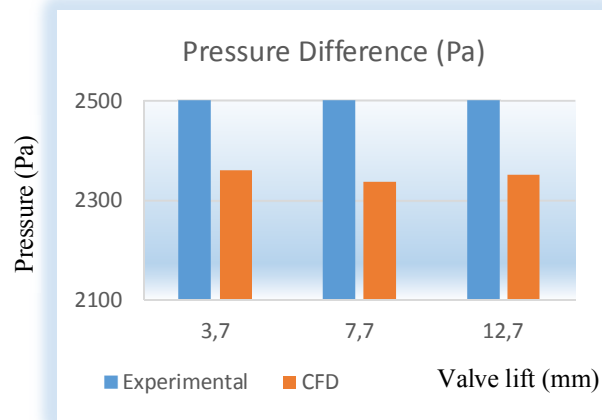
Figure 4.4: Shows mass flow at defined valve lifts for existing model of cylinder head
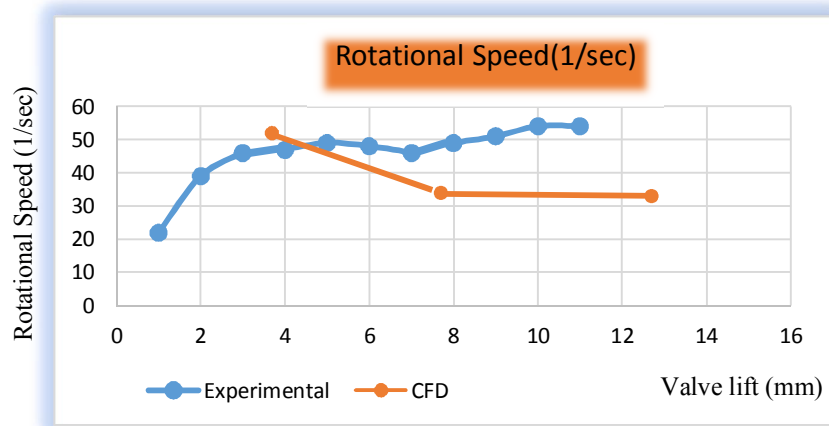

Figure 4.5: Shows graph for rotational speed at defined valve lifts for existing model
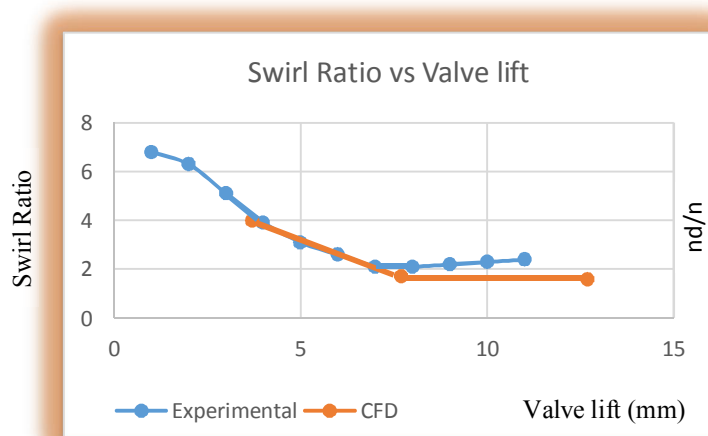

Figure 4.6: Shows graph for rotational speed at defined valve lifts for existing model

The swirl ratio is higher at lower valve lift and decreasing with valve lift as mass flow rate from tangential port is increasing, the impact of tangential port is larger as valve lift surges.

Before going to new conceptual models, two more elemental studies were performed by means of closing the helical and tangential port. The swirl levels were checked to validate prior to moving towards exclusively new cylinder head design, whether the existing cylinder head could be modified or not. In this study, throttling the individual port was totally rejected after going through literate review. Retiz [34] studied that throttling the helical port enhances the swirl ratio with diminishing effect on mass flow entitled to strangled pressure drop. Although, throttling the tangential port curtails the swirl ratio by means of redirecting the flow through helical in which swirl is more localized and do not contribute much in relation to overall swirl level. However, restricting the flow through tangential port, one would make flow structure more complex at expense of reduction in total momentum.

4.2 Closed Tangential Port Case

The Closure of tangential port results in forcing the flow to pass through helical port that would keep the overall swirl level above average value due to spiral shape of helical port as show in figure 4.10. The experimental results show that rotational speed increases with increase of valve lift, whereas at lower valve lift annular jet strikes with cylindrical walls/valve body and reduces total angular momentum.

Table 4.2: Shows mass flow and pressure drop for closed tangential port

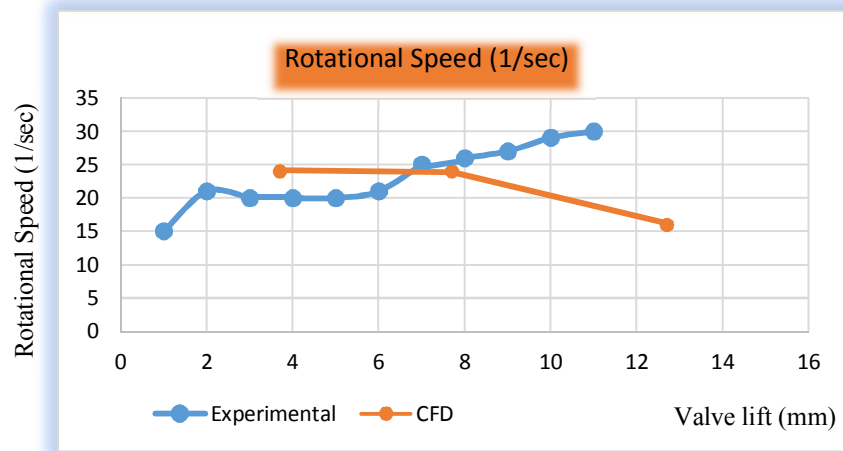| Valve Lift	Mass flow (kg/sec)	Pressure Difference (Pa)
3.7 mm	0.023	2462
7.7 mm	0.028	2452
12.7 mm	0.03	2456

Figure 4.7: Shows graph for rotational speed at defined valve lifts for closed tangential port case

4.3 Closed Helical Port Case

The directed mode of swirl is owing to irregular flow structures near valve seat. As valve lift increase, the directed mode of swirl increase and uneven or large variation in rotational speed values can be seen at all valve lifts.

Table 4.3: Shows mass flow and pressure drop for closed helical port case

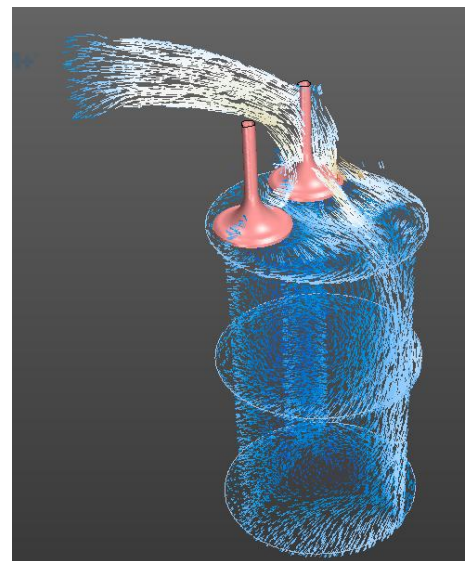| Valve Lift	Mass flow (kg/sec)	Pressure Difference (Pa)
3.7 mm	0.029	2448
7.7 mm	0.043	2397
12.7 mm	0.0473	2370

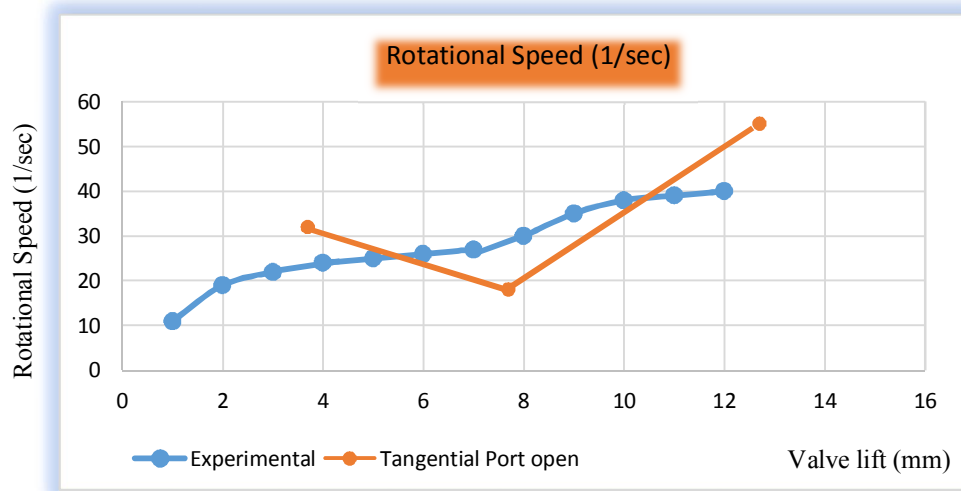Figure 4.8: Shows flow on directed side of tangential port

Figure 4.9: Shows graph for rotational speed at defined valve lifts for closed helical case
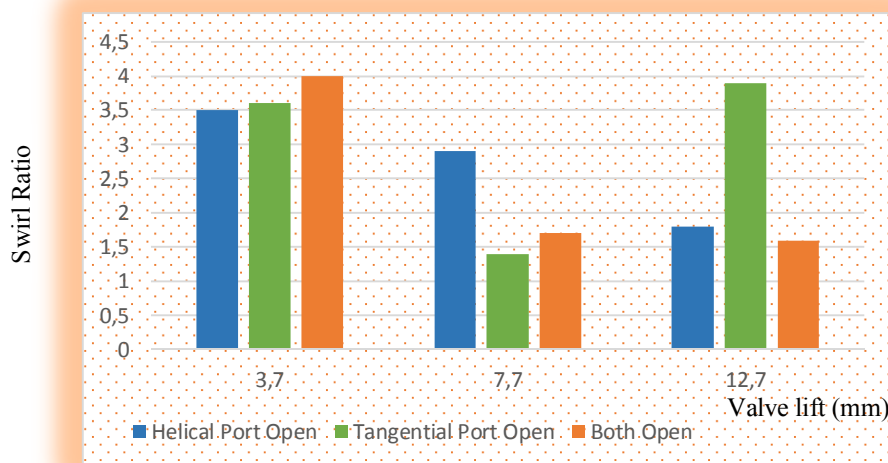

Figure 4.10: Shows comparison of swirl ratio for all three cases (both ports open, helical port open and both ports open for existing cylinder head model

The graph shows the limitations involve in all study cases of existing cylinder head model for producing low swirl ratio at each valve lift, and indicates the necessity of completely new cylinder head with modified ports. The tangential port produces low swirl at middle or intermediate valve lift than helical port case. At higher valve lift of 12.7 mm, the dominant angular momentum arising from flow striking with cylinder liner has produced a strong swirl flow in case of open tangential port. At low valve lift case, the flow structure rely less on shape of port but rather depends on valve flow interaction mainly in case of tangential port case. The helical port is dropped from initial concept selection phase because it is generating higher swirl ratio at lower and middle valve lift, which is difficult to control.

4.4 New Concepts Development Phase

Designing the new non-swirl intake ports was a daunting task under the constraint of keeping same bolt positions and cooling channels location specifically overhead of intake ports, depicting in 2D and 3D models respectively. The two-dimensional figure 4.11.a shows placement of bolts in the vicinity of helical port, directed intake port and exhaust port in existing-cylinder head. Moreover, the 3D-diagram 4.11.b depicts clearly the limitation involved in designing the new directed intake ports.
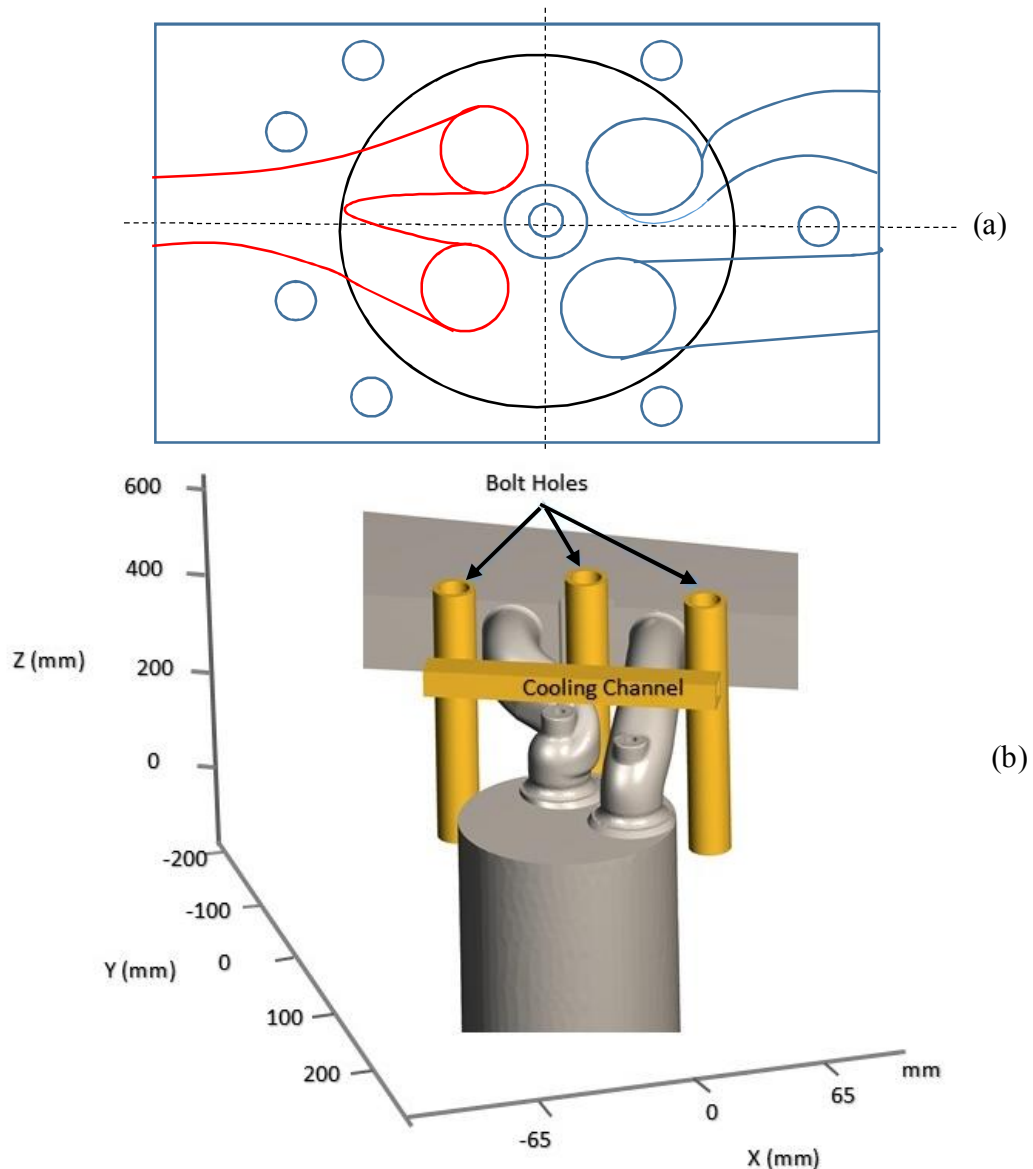

Figure 4.11: 2D drawing (a) shows location of bolts around intake and exhaust side, and 3D model depicted in (b); demonstrates cooling channel with bolts location around intake side

4.4.1 Directed Port in Existing Model Configuration

In current model of cylinder head, the directed port was modeled to produce the swirl rotation by pointing the flow velocity at a tangent to the wall of cylinder. There is no neck choking at lower side of port, while on the upper side of port (upstream of port) air flow followed diagonal path with respect to cylindrical axis. The charge separation occurs at the lower neck side results in considerable reduction of flow velocity; nonetheless on directed (upper) side the velocity increases with proportionally enhanced swirl in cylinder as flow moves towards outward in circumferential direction. Higher swirl ratio could be gained when directed port is positioned towards cylinder line [41].
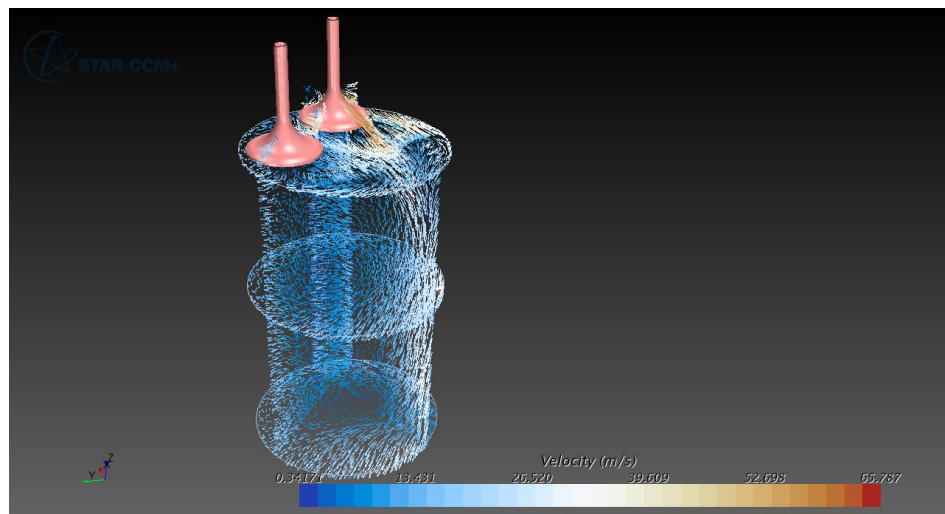

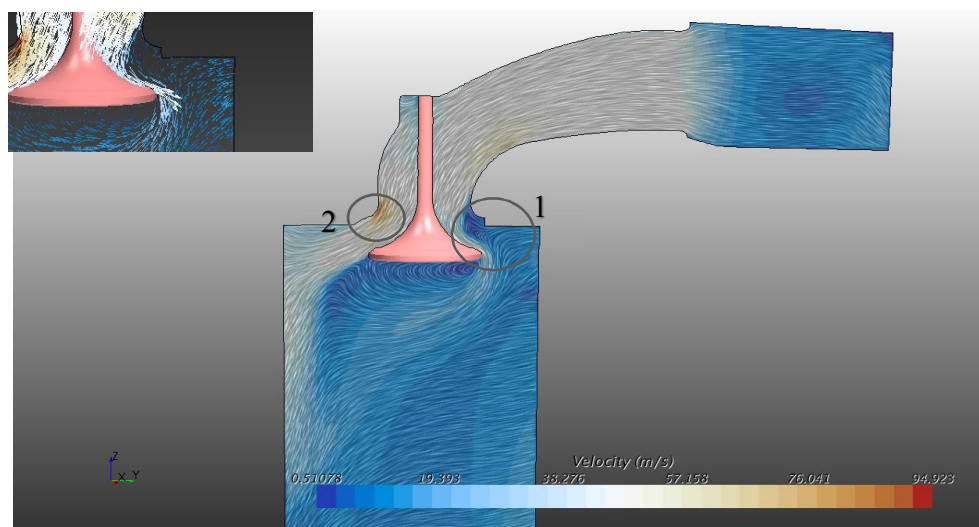Figure 4.12: Shows directed port flow towards cylinder liner

Figure 4.13: Shows velocity profile at 12.7mm valve lift

1. Flow separation at bend (lower neck) due presence of an adverse pressure gradient.

2. Upper neck forces the flow diagonally and increase velocity of flux.

The minimum velocity and loss of momentum at boundary layer causes the flow separation under adverse pressure gradient. Because if fluid unceasingly drives opposite to that of adverse pressure gradient, the obstruction will create zero velocity and detach from wall. A convex curvature like bend of fluid domain is detrimental for pressure gradient [60, 61]. The boundary layer suffering from adverse pressure, flow separation and steep gradients near walls can be accurately predicted by realizable k-ε model turbulence model [53], which also justify the precise usage of turbulence model. The separated boundary layer moves along the fillet face of the valve creates an unstable free shear layer and forms a roll vortex while disengaging itself from surface as can be seen in figure 4.13.

After careful examination of above velocity profile, the available option under mentioned constraints already discussed above was to eliminate directed component on upstream side by making throat opening straight, which would force the flow downward direction not towards the liner of cylinder. In addition, at downstream side the port neck is made little chocked by changing dimensional value of MA discussed in theoretical study of section 2.4.5 for directed port to acquire equal distribution of flow in either direction of valve stem to avoid sudden flow separation near the fillet face of intake valve. The modification points are depicted in following figure 4.14.
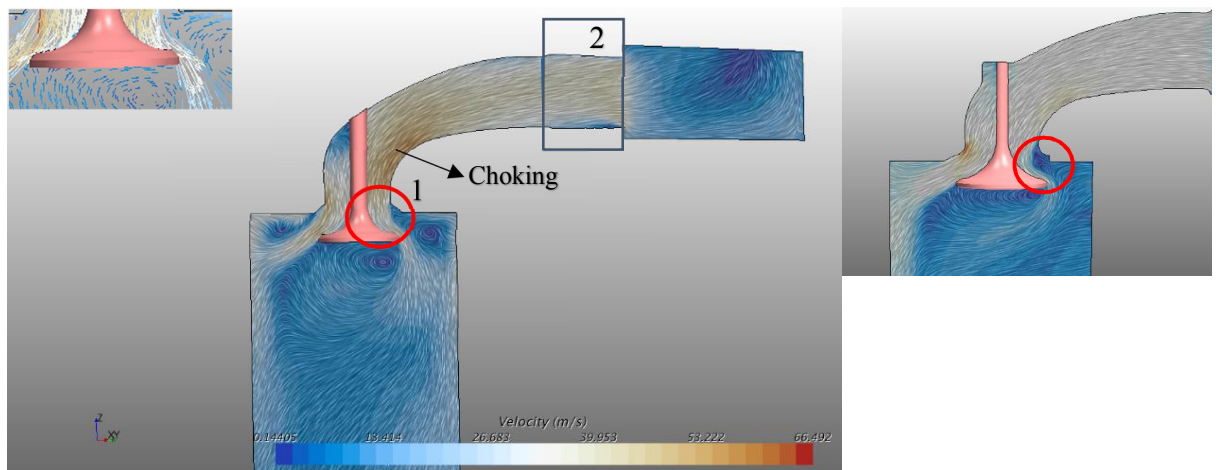

Figure 4.14: Shows new (on left) and actual port profile (on right) (Ref: Table 4.4 for dimensions of port).The perceived dimensional difference of valves in two models is due to capturing scene. The valve dimensions are same in both cases with stem diameter of 8 mm

1. Less separation
2. Joint to adjust port length with plenum box

Table 4.4: Comparison of Dimensions

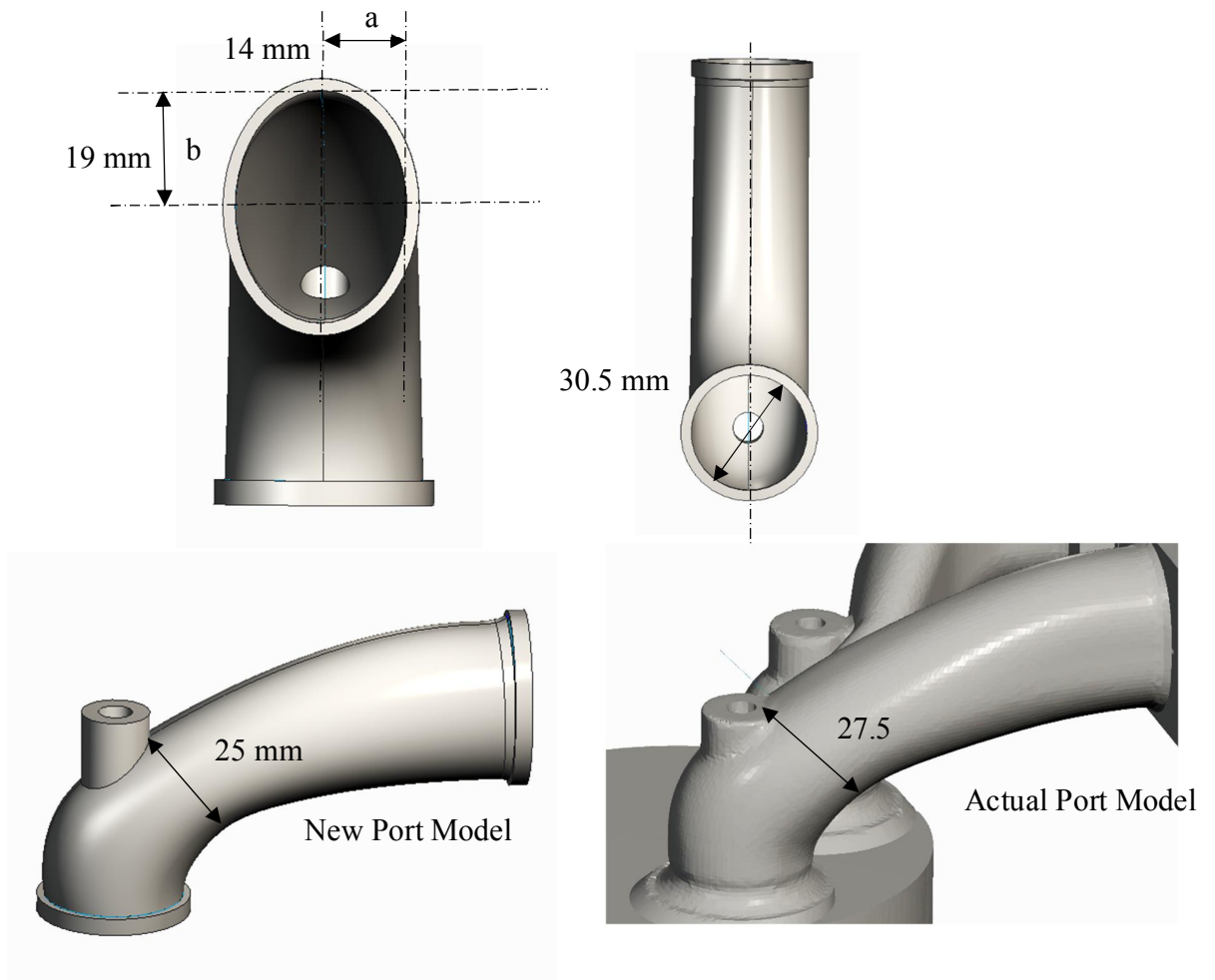| Dimensions	Actual model of Directed Port		New Directed Port	
Inlet Throat Dimensions	a 14 mm	b 19 mm	a 14 mm	b 19 mm
Outlet Throat Diameter	30.5 mm		30.5 mm	
Area of Inlet throat ($\pi.a.b$)	835.66 mm^2		835.66 mm^2	
Minimum Neck Dimension	27.5 mm		25 mm	

Figure 4.10: Comparison of main dimension

4.4.2 First Concept (Existing ports position)

After finalizing the directed intake port shape, the first concept is based on utilizing existing cylinder head orientation for intake ports (Ref: Appendix A for dimensions). As the target was to produce non-swirl cylinder head, so helical port was dropped during initial concept selection phase. The reason behind dropping helical port is already discussed in section 4.3, since it produces pre-cylinder swirl around valve axis that is difficult to control. This concept employs actual ports position with modified intake ports, where the both intake ports were newly designed directed ports of same dimensional profile described in detail during section 4.4.1.
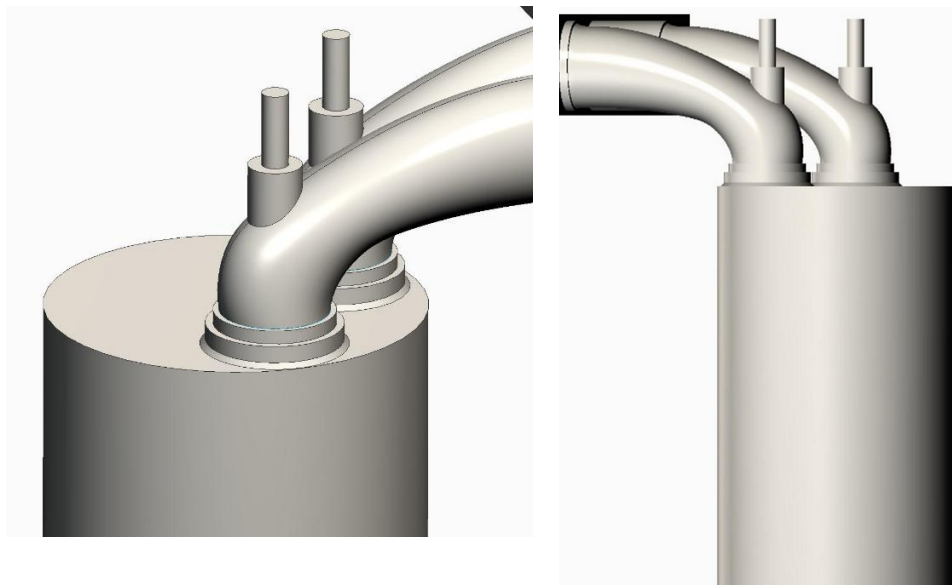

Figure 4.15: Shows actual ports position with modified directed port

Table 4.5: Shows CFD results of mass flow and pressure difference for actual ports position with modified directed port concept

Valve Lift	Mass flow (kg/sec)	Pressure Difference (Pa)
3.7 mm	0.0416	2402
7.7 mm	0.0627	2280
12.7 mm	0.0676	2248

4.4.3 New Ports location

To create extensive flow interaction for reducing swirl value, a new cross flow location for ports is made at off center position of 45º from cylinder center as shown in figure 4.16 by means of which the interference between two valves will be significantly high. The ports would have symmetric air flow because of positioned alongside transverse axis of cylinder. This concept also employs newly designed directed ports of same dimensional profile described in detail during section 4.4.1 on symmetrical ports position.
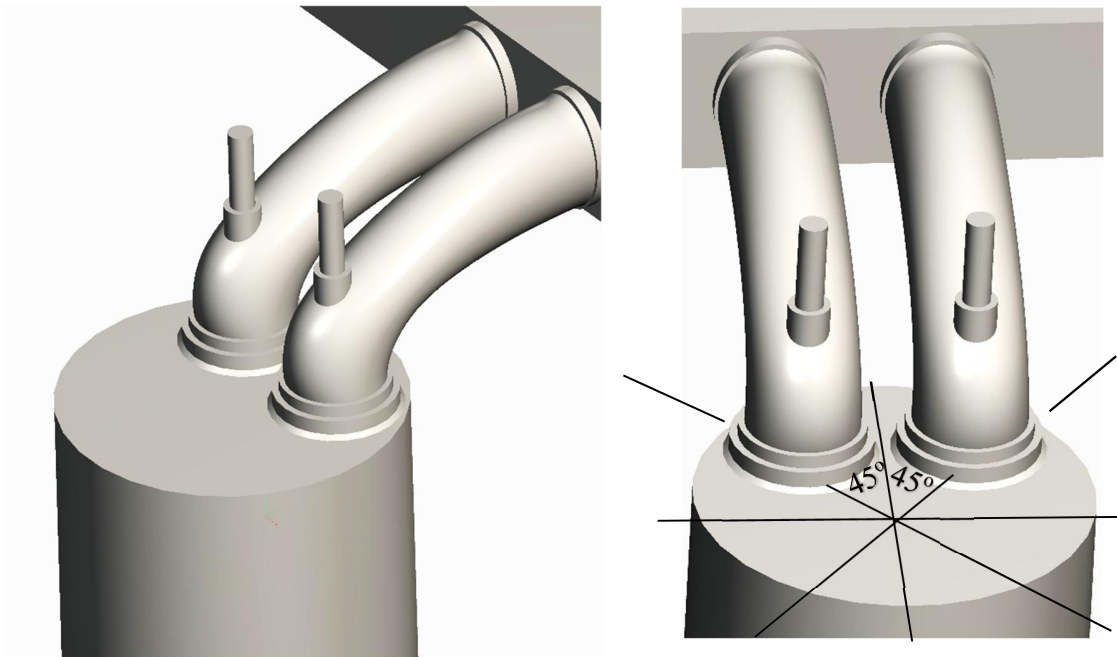
Figure 4.16: Shows new ports position with modified directed port

Table 4.6: Shows CFD results of pressure difference for new ports position with modified directed port concept, and mass flow comparison with existing layout of cylinder head (with helical/tangential ports)

Valve Lift	Mass flow (kg/sec)	Pressure Difference (Pa)	Mass flow (kg/sec) (Existing model)
3.7 mm	0.0416	2401	0.044
7.7 mm	0.0640	2273	.0670
12.7 mm	0.0675	2352	.070

Figure 4.17: Shows graph for comparison of swirl ratios between new ports position (with modified ports) and actual ports position (with modified ports) cylinder head model

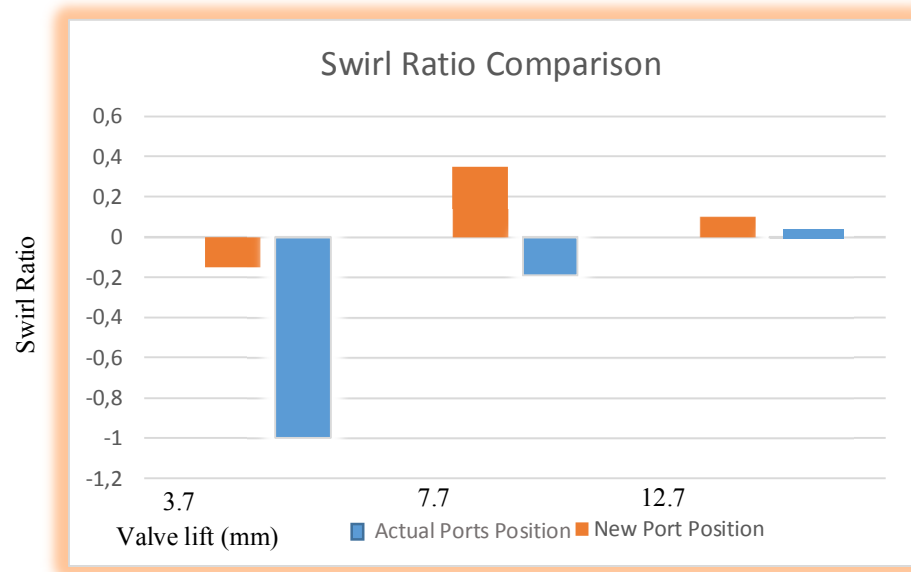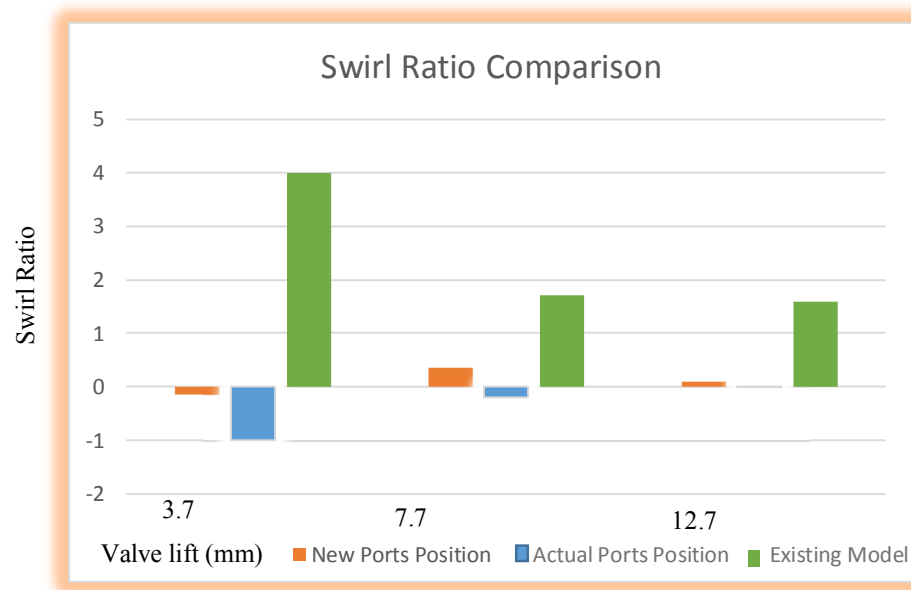Figure 4.18: Shows graph for comparison of swirl ratios between new ports position (with modified ports), actual ports position (with modified ports) and existing model of cylinder head(helical/tangential combination)

4.4.4 Detail Analysis of Three Cases

As already discussed, the existing model of cylinder head is producing high swirl ratio at range of all valve lifts, whereas, in case of actual position model (with modified ports) the average value of swirl ratio is negative due to influence off axis location of upstream port. The downstream port produces clockwise swirl (positive value of swirl in the cylinder) but the dominant bulk momentum flow is from upstream side makes overall swirl ratio a negative one. On the other hand, new ports position model (with modified ports) is producing almost no swirl at all valve lifts except at middle one; the value is around 0.36 shown in the graph of figure 4.18.

For actual position (with modified ports) model titled as a first concept in section 4.4.2; at valve lift of 12.7 mm, the two rotating vortices are formed at first stage below valves and merges together further downstream direction in the cylinder through mixing of substantial portion of their core vorticity. This is clearly visible in tumble plane of figure 4.19 with line convolution scene on right side. The line integral convolution is a best technique to visualize complex flow behavior. It creates steady state two dimensional vector field images similar to oil flow visualization. The two rotating vortices were produced due to interaction of flow with cylindrical walls, and due to less flow interaction between two ports no vortex formation can be seen in between two valves. A wobbling swirl motion is evident at plane of 0.875B due to conservation of angular momentum and form single vortex core as can be seen in figure 4.20.b for first conceptual model. This non-concentric swirl motion represents a weaker swirl flow and not fully developed even at 1.75B plane.

There are two pairs of rotating vortices are formed near the face of valves in case of new position (modified ports) model; called as second concept in section 4.4.3. The two pairs of vortices are depicted in convolution scene on left side of figure 4.19. One pair of vortices is formed due to flow interaction with wall of cylinder, while the other two vortices under valves are due to strong mixing, which are not evident in actual position model with modified ports concept. This strong mixing produces high velocity distribution because of flow interaction. The central region between the valves indicated with marked circle in left side of figure 4.19 (glyph scene) has high velocity distribution, which does not contribute much to the swirl generation mechanism. The cancellation of swirl velocities under valves produces no visible swirl even at 1.75B plane.

The main purpose of selecting 12.7mm valve lift is to clearly show the impact of ports profile on flow behavior, which could be less evident in lower lift case.
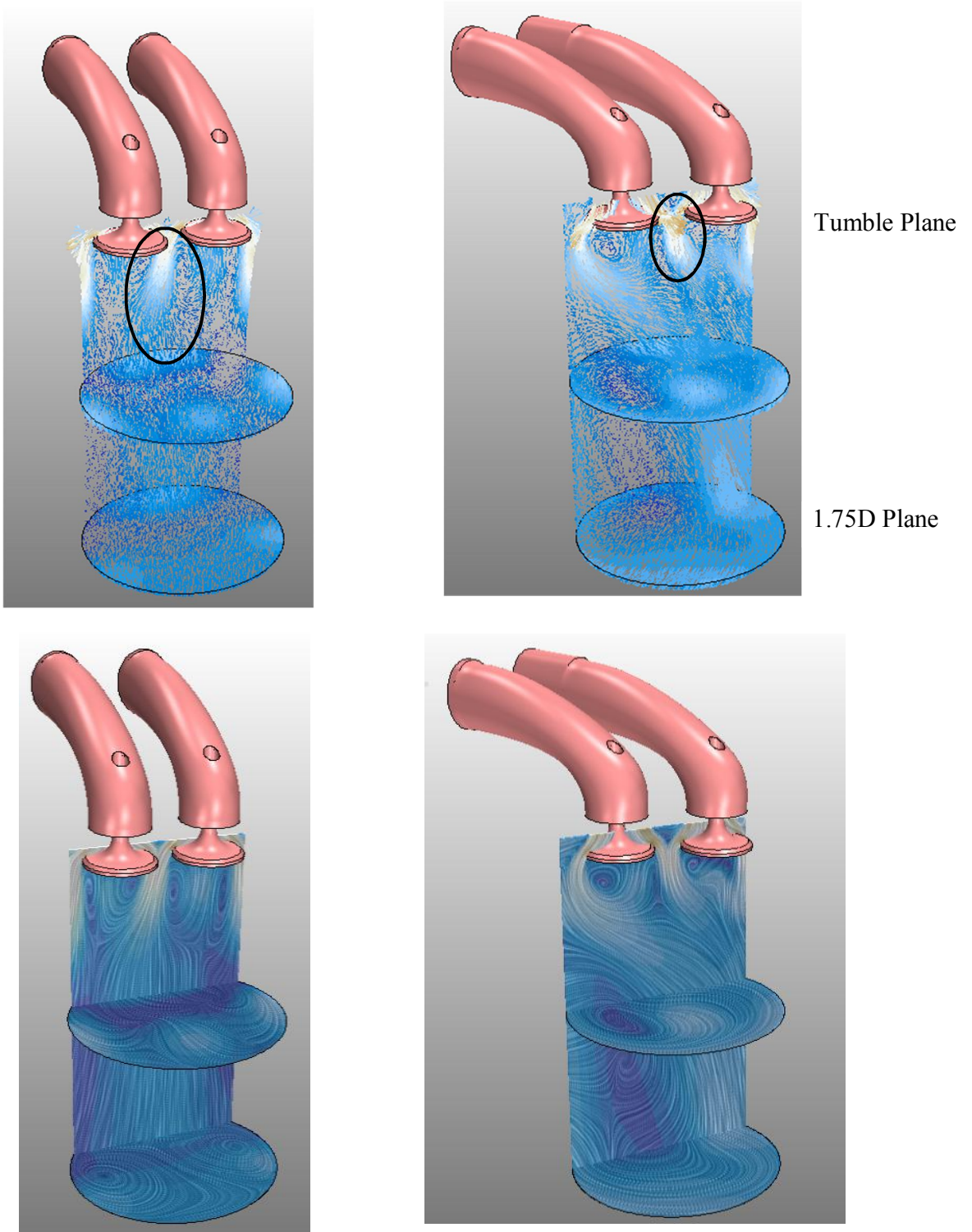
Tumble Plane

1.75D Plane

Figure 4.19: Comparison of flow interaction between two new conceptual models (on left side new ports position and right side actual ports position models)
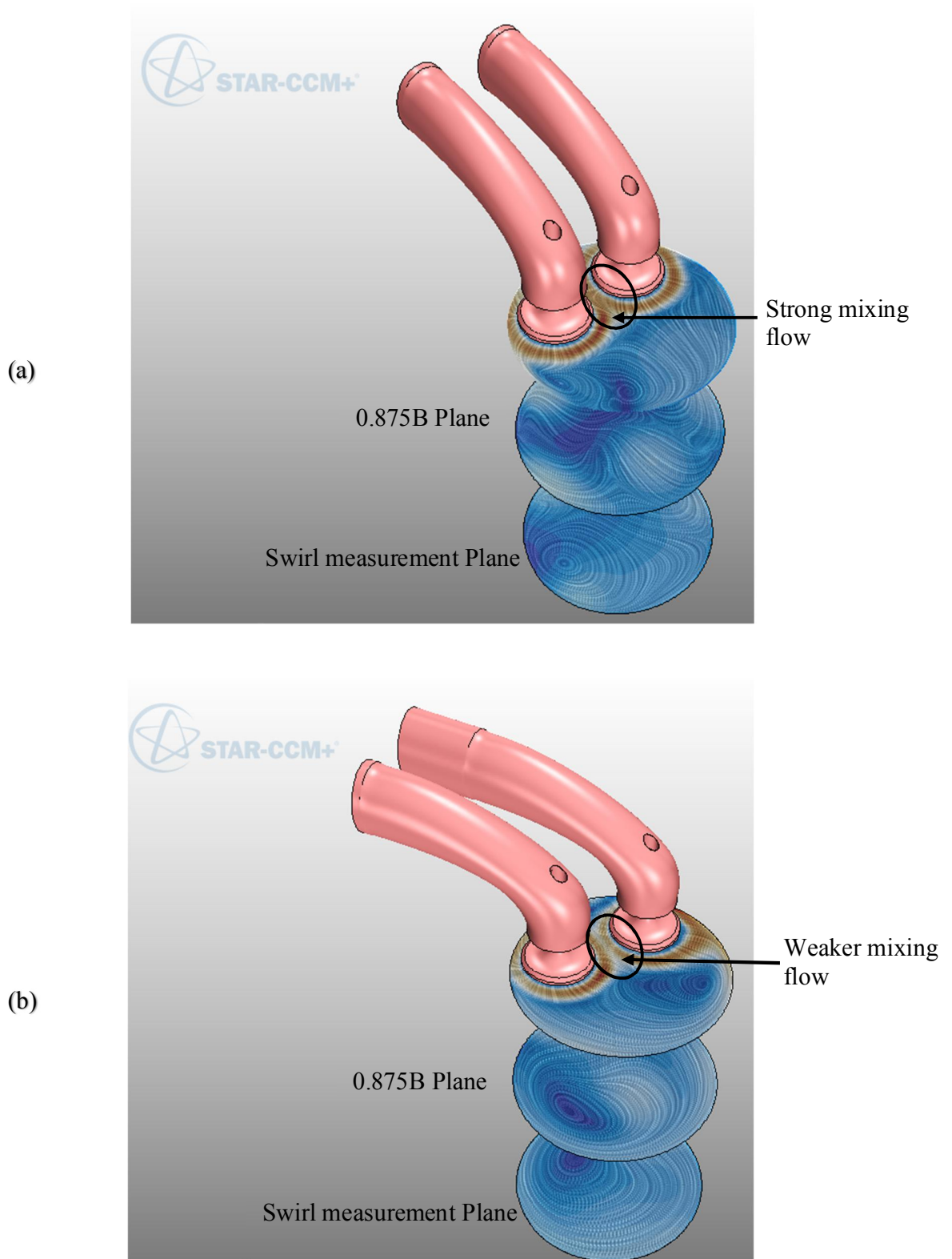
Figure 4.20: (a) shows stronger mixing flow in new ports position model (b) weaker mixing in actual ports position model (with modified directed ports)

The planar streamlines and in plane velocity component are shown in figure 4.21 and 4.22 at 1.75B plane from cylinder head for all three models. At 3.7 mm valve lift case for existing model of cylinder head; only one vortex is formed at the center location of cylinder as shown by planar streamline imposed with tangential velocity component in figure 4.21.a. The adequate swirl level has produced a recirculation zone for existing cylinder head model having helical and tangential ports configuration. The helical port is playing dominant role in swirl generation at low valve lift for case a; due to imparted pre-valve angular momentum. However, at low valve lift, the valves-flow interaction is very much evident in figures 4.21.b and 4.21.c for actual position (with modified ports) and new position (with modified ports) models respectively. This interaction has made multiple counter rotating vortices and generates negative component of swirl ratio at 3.7 mm valve lift shown in the graph of figure 4.18.
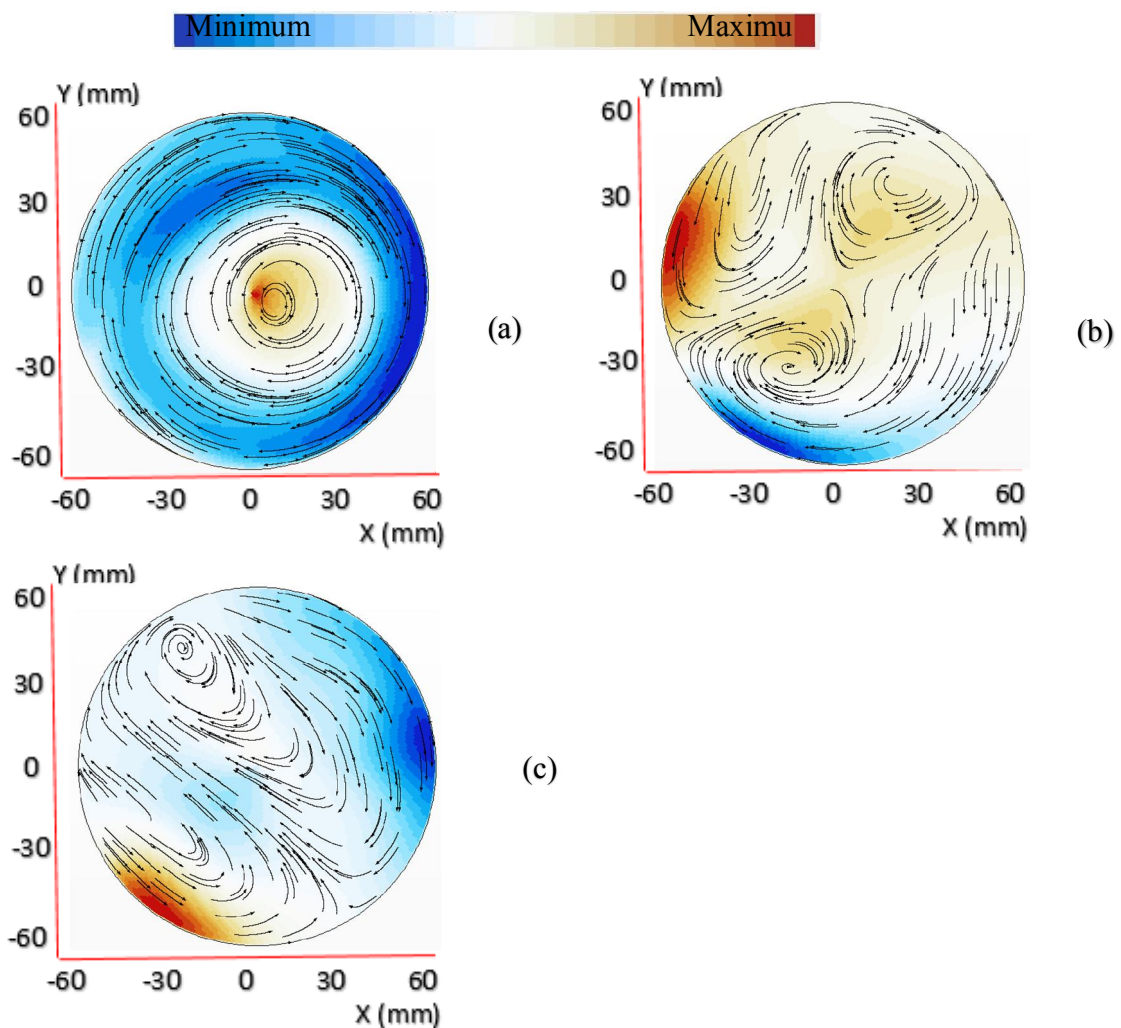

Figure 4.21: Shows tangential vector scenes imposed with planar streamlines at 3.7 mm valve lift: (a) Existing model (b) Actual position model and (c) New position model
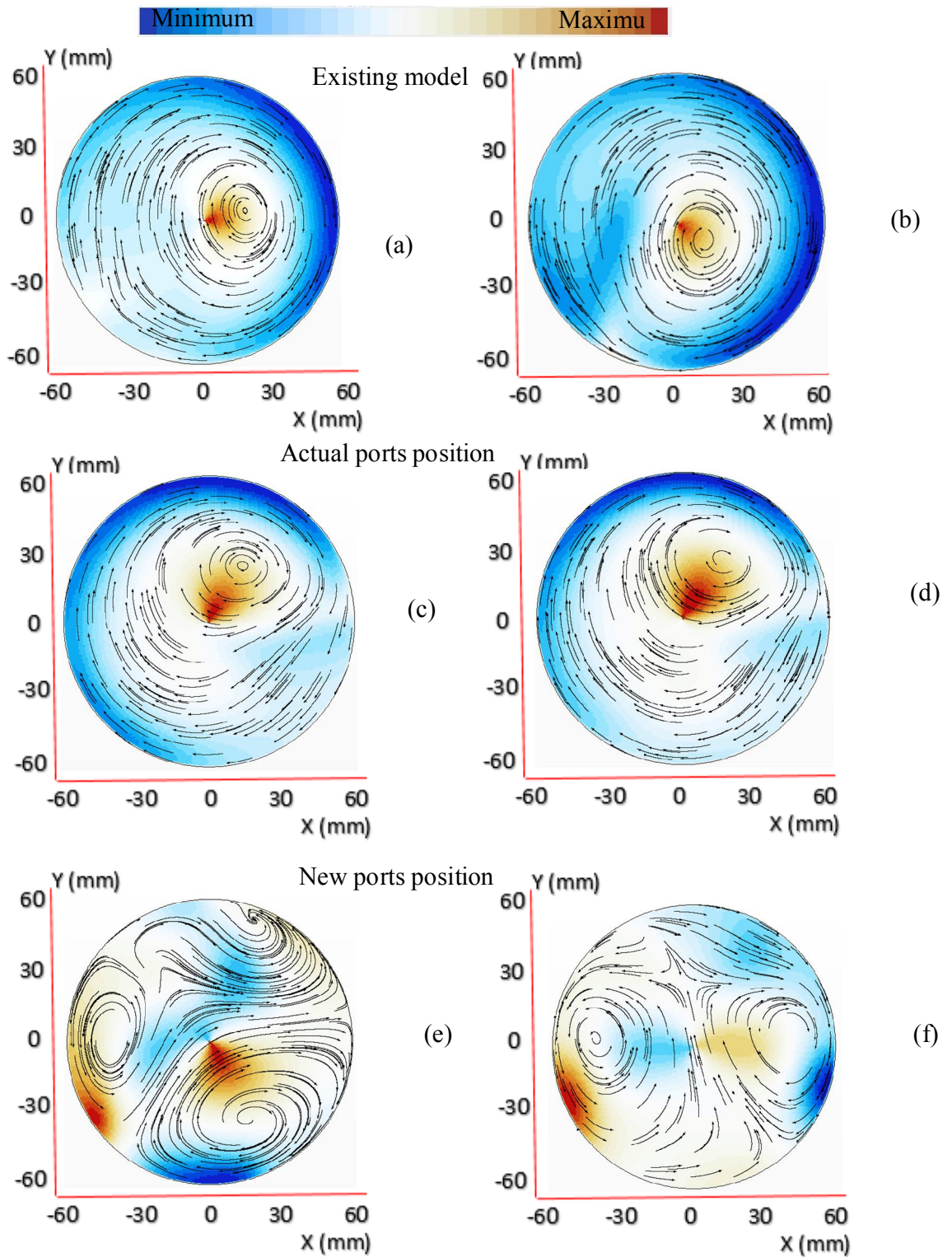
Figure 4.22: Vector scenes with imposed planar streamlines at 7.7 and 12.7 mm lift for all three cases. Left side shows 7.7 mm case and on right side is 12.7 mm lift case
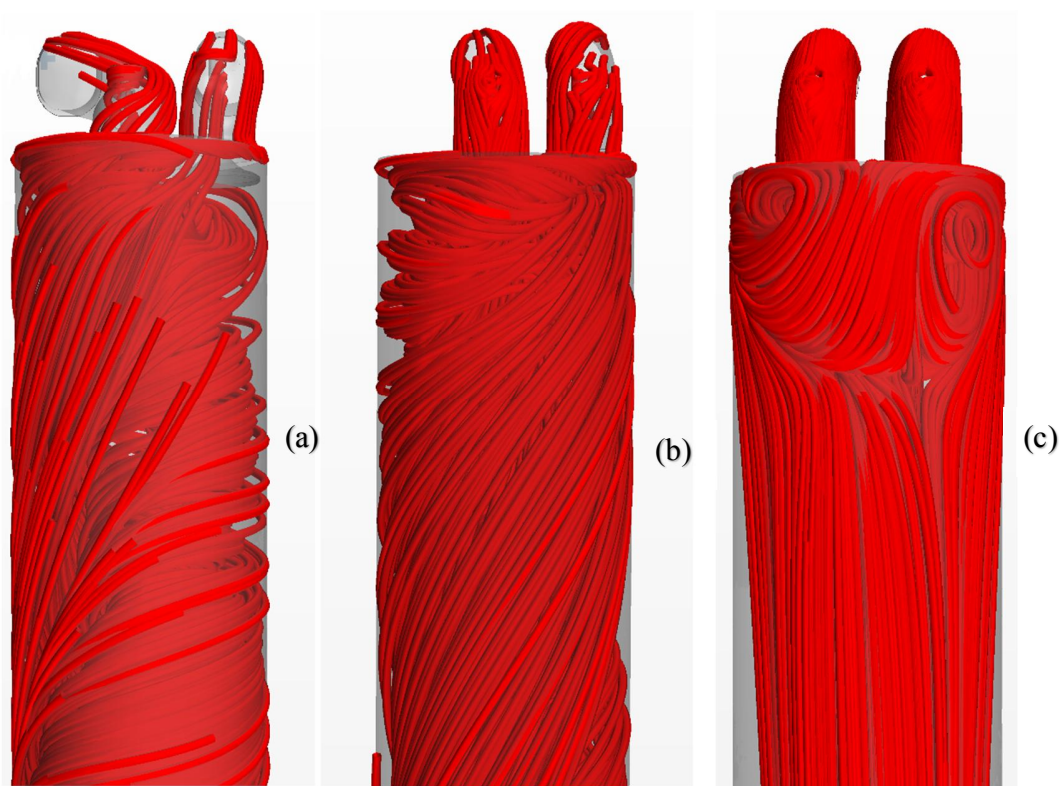
Figure 4.23: Streamlines flow pattern in (a) existing model configuration (b) actual position (modified ports) model (c) new position (modified ports) model

The order of flow vector in the cylinder with port and valves geometries greatly defines flow structure (swirl or tumble) and turbulence level. At medium and higher valve lifts of 7.7 mm and 12.7 mm in case of existing model shown in figures 4.22.a and 4.22.b, the core of clock-wise swirl (solid body vortex) is almost coincident with centre of cylinder. This shows vortex is located rigidly in the cylinder center by exhibiting uniform swirl behavior. A weak swirl (non-centric) is also very much evident in case of actual position (modified ports) model at range of medium and higher valve lifts shown in figures 4.22.c and 4.22.d. However, in the case of new position (modified ports) model, two vortices flow are apparent at 1.75B plane, which generates dual swirl flow and weakens overall swirl momentum. The net angular momentum of swirl flow is greatly influenced by excessive vortices. This is due to effect of local compression/expansion of global swirling flow and local vortices [35].

Another way to demonstrate swirl behavior is by means tube streamlines. The streamlines demonstrate substantial swirl flow in case of existing cylinder head and actual position (with modified ports) models shown in figures 4.23.a and 4.23.b respectively. At the same time, the new position of ports clearly exhibits two counter rotating tumble vortices, and at further downstream clearly demonstrate non-swirl flow. This makes new ports configuration an ideal position to be selected for zero swirl cylinder head, and the graphical results in figure 4.18 validate this decision.

4.4.5 Comparison of flow Coefficient

To check the resistance posed by valve/port geometry to air flow, flow coefficient is calculated from CFD results for existing model of cylinder head and newly selected model.

$$Cf = \frac{m_{actual}}{m_{theoratical}} = \frac{m^o}{A\sqrt{2\rho\Delta P}} \tag{4.1}$$

Where C_f is flow coefficient, m_{actual} is mass flow calculated through CFD computational domain for specific pressure drop at inlet and outlet of intake ports. "ΔP" is pressure drop across selected points, "A" is valve opening area of valve by considering valve inner seat diameter and "ρ" is density of air taking to be a constant value for incompressible flow. $m_{theoratical}$ is theoretical rate of mass flow. The port flow coefficient generally increases with increase of valve lift.
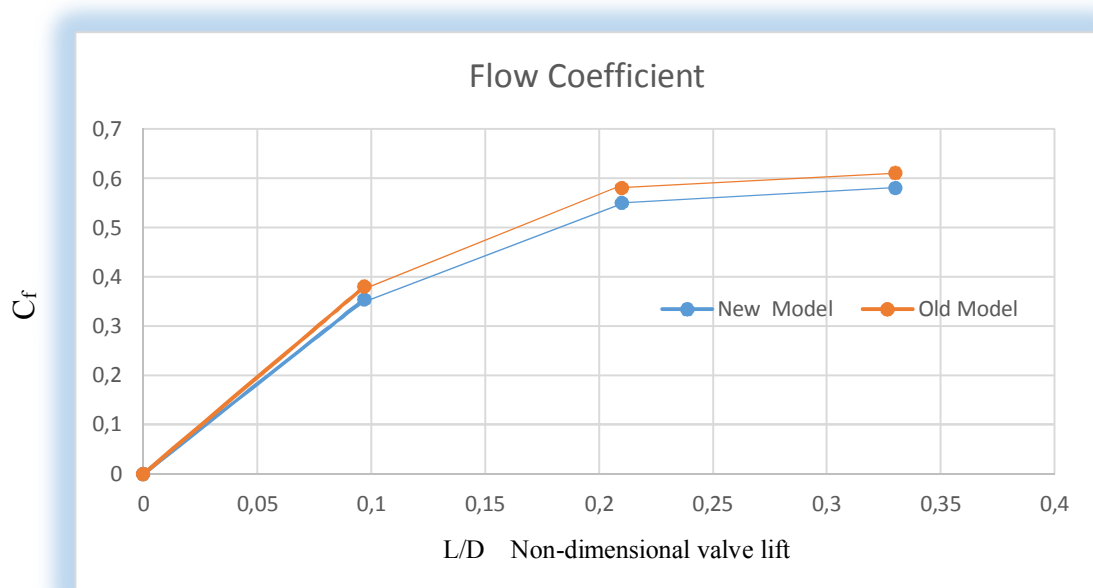
Figure 4.24: Shows graph of flow coefficient plotted from CFD results from new and existing models of cylinder head

5 Designing of Additional Components

5.1 Exhaust Port Design

The restriction in designing the identical exhaust port present in previous existing model was owed to the presence of bolt holes for clamping the cylinder head with main block. The change in intake ports orientation from original position to new position also forced to alter the configuration of exhaust port. A comparison has been made with highlighted section in figure 5.1 b, which represents new cylinder head design possessing same exhaust port.

(a)

(b)

Figure 5.1: (a) shows existing model of cylinder head and in (b) highlighted section shows position of upper end bolt position too close to exhaust port in new cylinder head model by retaining the same existing model of exhaust port

The heat rejection from exhaust port imparts appreciable impact on overall cooling load. The surrounding metal temperature of exhaust port is typically higher than anywhere else in cylinder head, and impacts greatly on engine overall performance. As temperature increases, the th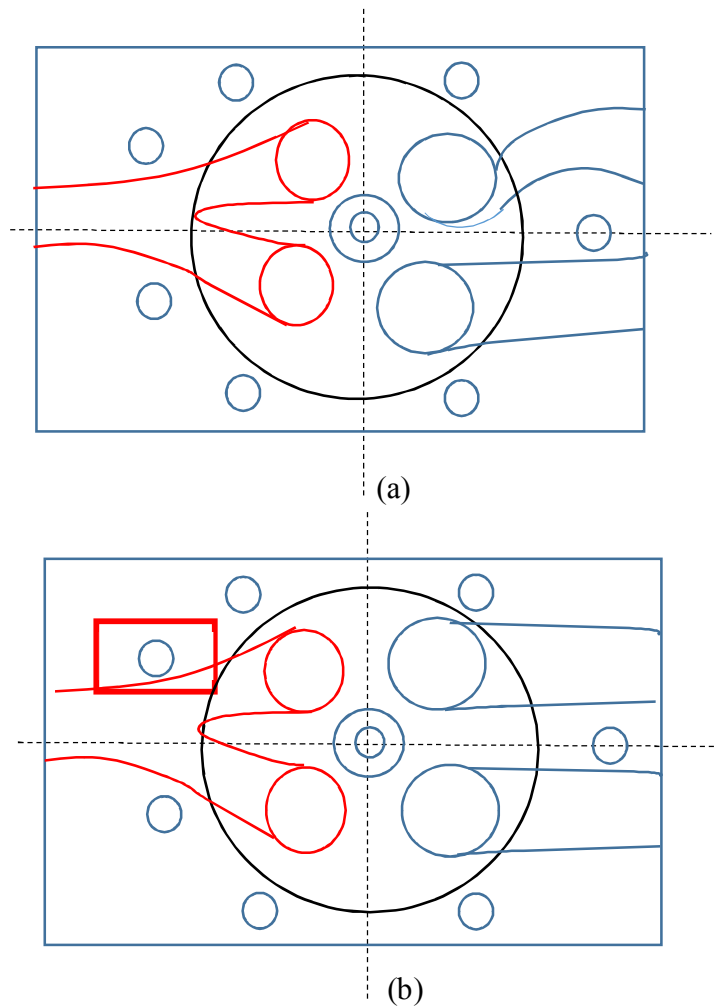ermal expansion of bolt could increase clamping load beyond the compressive strength of material and eventually failure of bolt head [27]. The highlighted bolt figure 5.1 b in new cylinder head configuration is very close to exhaust port, which could result in creep due to high thermal stresses and eventually loss of tightness as bolt fails. The problem emerged at expense of maintaining the equivalent discharge coefficient by keeping same inlet and outlet throat dimensions of port. Under the consideration of above-mentioned problems, there were two options 1. Designing the two-exhaust ports layout as shown in figure 5.2.a, 2. Changing the dimensional value of port near the bolt face but it would chocked that throat section of port as depicted in figure 5.2.b.

(a)

(b)
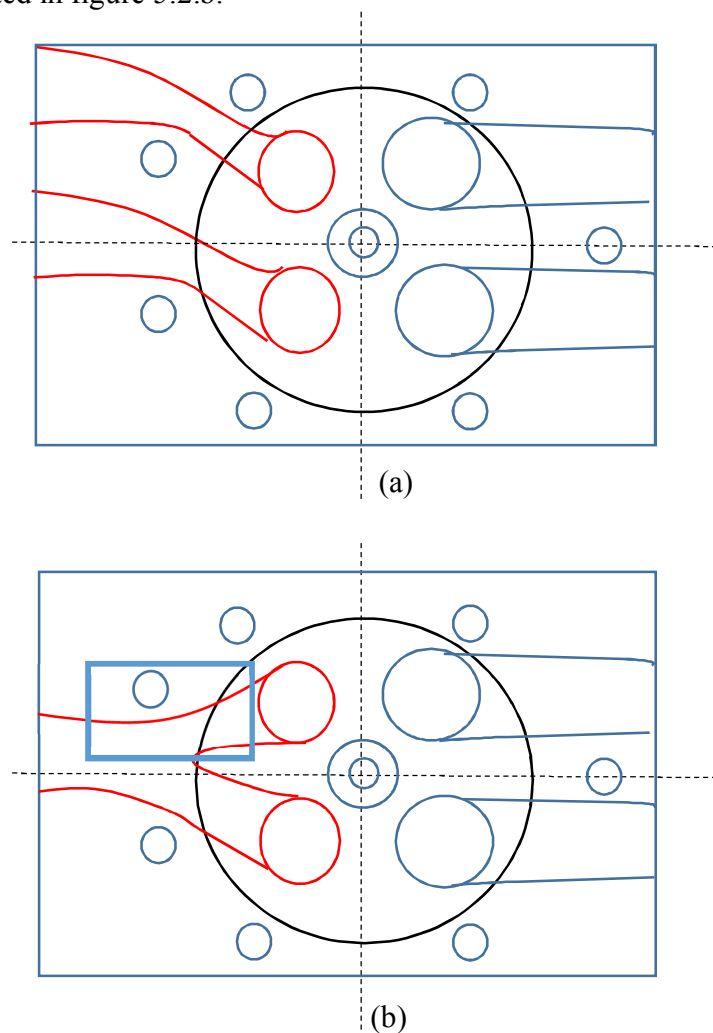
Figure 5.2: (a) shows two exhaust port configuration for new cylinder head and (b) twin exhaust port concept

(a)

(b)

Figure 5.3: (a) shows two-exhaust ports model and (b) shows twin ports with single outlet model for new cylinder head configuration

As analysis of exhaust port is beyond the scope of this thesis work, so both of the above designs are recommended unless or until some CFD analysis would be performed to check flow and discharge coefficient.

5.2 Cylinder Head Body Design

Before going to detail of complete body design, it is worthwhile to mention the suitable material for new cylinder head. The existing material of cylinder head is grey cast iron, which is not suitable for high in cylinder combustion pressure of up to 220 bars because of existing bottom deck thickness value of 8 mm. The usage of existing cylinder head material would require more material and eventually will add more weight in terms of increasing the deck thickness. Compact Graphite Iron is another advance material making its space in automobile especially engine manufacturing industry. The study[28] has acclaimed that wall thickness could be lessened to 3-4 mm by using CGI because of high fatigue strength instead of 6 mm for cast iron. The fatigue limit of CGI is almost twice to that of grey cast iron and aluminum alloys, and improves dimensional stability of cylinder head due to strength and stiffness. Nonetheless, also helps to decrease the wall thicknesses at many locations inside the head, the reason is that there is a strong bond between iron matrix and complex coral like structure (rough surfaces) of graphite. The nodular (spheroidal) particles in graphite enlarge stiffness and strength of any material and smaller change in as-cast properties reduces safety factors [54].The reason for dropping aluminum alloys from the list of selected material is that mechanical strength decreases sharply beyond 150 ℃ with increase in temperature [28].
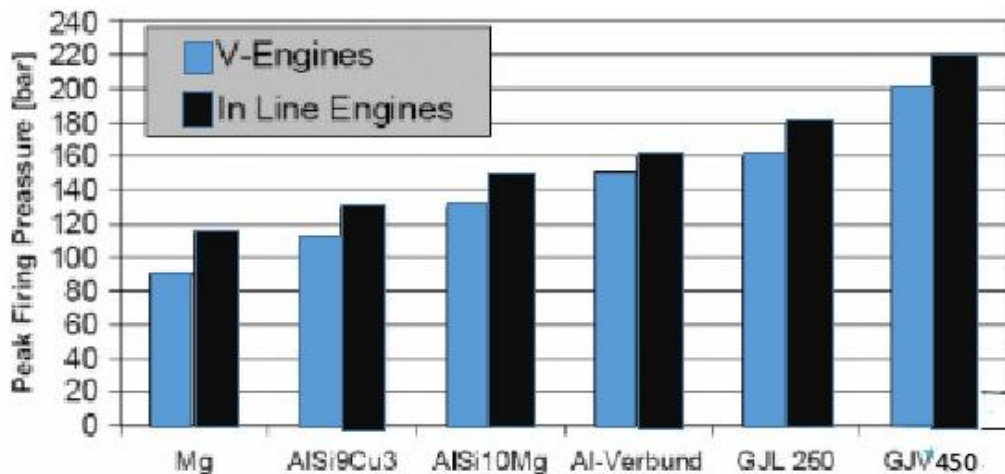
Figure 5.4: Shows the superiority of CGI (vermicular graphite GJV 450) on other materials in terms of peak firing pressure [30]

5.2.1 Valve Bridge Thickness

In between inlet and exhaust valve seats, an appropriate valve bridge thickness is essential to deter cracks at intense firing temperature and pressure. A minimum of 11-12% of bore is suggested for valve bridge thickness [36]. The large temperature differential at liner interface produces stresses that may result in cracks devoid of proper thickness level. The cracks are usually produce due to compressive/tensile nature of heating and cooling of bottom deck under huge thermal gradients of combustion gas, therefore appropriate value of valve bridge thickness is essential to withstand loads and avoid cracks with proper cooling passage near that region.

5.2.2 Bottom Deck Thickness and Chamfer Angle

The bottom deck thickness can be measured by following relation [28]:

$$t = \frac{B\sqrt{cp}}{s}$$ 5.1

$t = lower\ deck\ thickness\ of\ cylinder\ head(mm)$
$p = pressure(bar)$
$c = constant\ 0.1$
$s = allowable\ stress\ 5000\ to\ 8000\ N/mm^2$
$B = 111\ mm\ bore\ of\ cylinder$

A more precise relation is
$$t = 1.5 + B \times .09 + 3$$ 5.2

A thickness value of 12 mm is most suitable for 220 bar injection pressure with material usage of CGI. This study is performed for future usage of direct injection of gas, whereas in current designing process a value of 8mm is maintained to sustain conformity with present value.
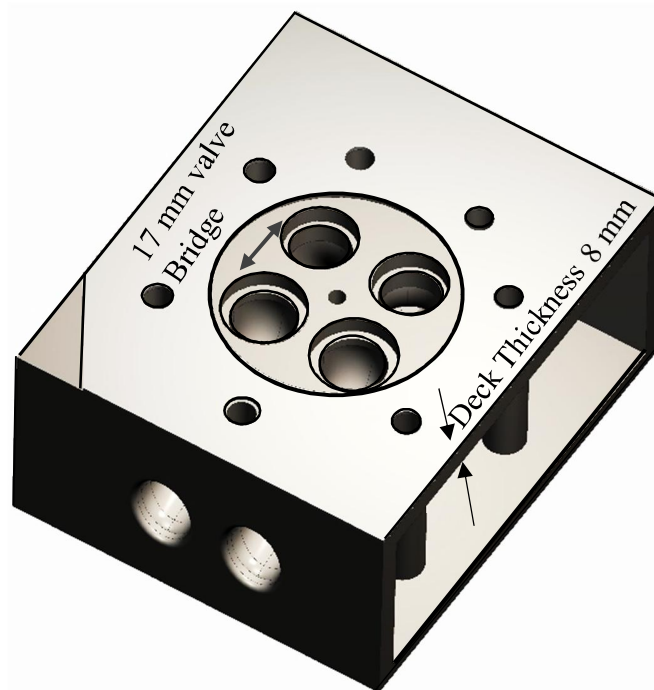

Figure 5.5: Shows valve bridge thickness and deck thickness values

The sidewall thickness value of 12 mm was retained in compliance with existing head values. The chamfer angle was not provided for straitening the flow towards intake side in new selected model, although chamfer angle has some benefit on discharge coefficient. Along

with shape of port, the chamfer angle also imparts little directed component to flow direction for getting little more swirl which is not beneficial in this study.

5.2.3 Bolts Layout

The bolts layout is same as in existing model of cylinder head; there are total seven number of bolts per cylinder for tight sealing between cylinder head, gasket and main block. The valve skew angle (line parallel to crankshaft to the line through valve centers) of 0º is maintained, therefore, keeping same configuration of bolts layout was not a big issue. As the probability of escaping gas is exceedingly high due to weak spots between gasket, cylinder head and block under low contact pressure. The bolts have to sustain assembly loads, thermal loads and gas pressure thus tight sealing is essential to maintain desired combustion pressure and equal load transfer across entire structure.
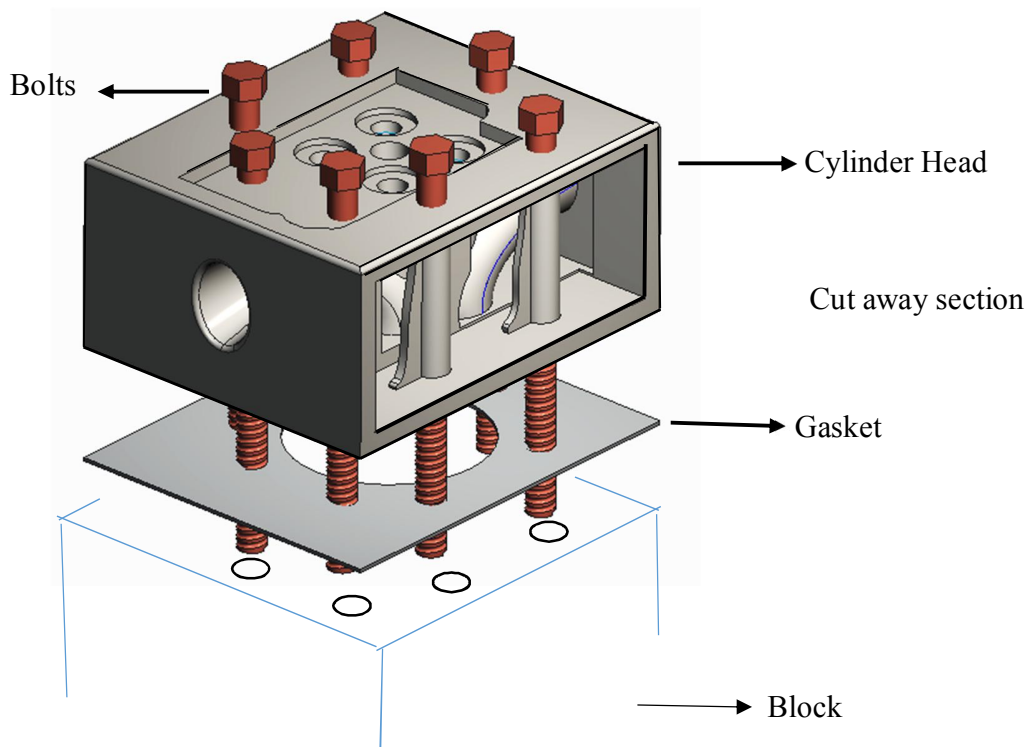
Figure 5.6: Shows exploded view for bolts layout on new cylinder head model, gasket and block. The radius of hole for each bolt is 6.5 mm

The holes for bolts inside cylinder have been providing with 5-7 mm wall thickness to avoid failure under clamping and thermal loads, whereas each hole has inner diameter of 13 mm to embrace bolt. The pressure oil holes were not considered due to usage of hydraulic actuation system in the research engine.

5.2.4 Cooling Channels Design

As already described in theoretical study of cylinder head cooling section (2.4.6), there are three types of coolant flows in automobile engines:
1. Series flow or uni-flow
2. Parallel flow
3. Cross coolant flow system

The available research engines: LEO-1 engine has uni-flow (longitudinal flow) arrangement; this design assures invariable coolant flow with variable passages, while LEO-II research engine has separate coolant flow arrangement for cylinder head as well as for cylinder block as show in figure 5.7.b.

Figure 5.7: (a) shows cooling flow arrangement in LEO-I (b) cooling flow arrangement in LEO-II, and in newly designed cylinder head model

a) Cooling Jacket Optimization

Under the consideration of above mentioned coolant flow systems, a new hybrid cooling flow approach is adopted, which has series flow and indiv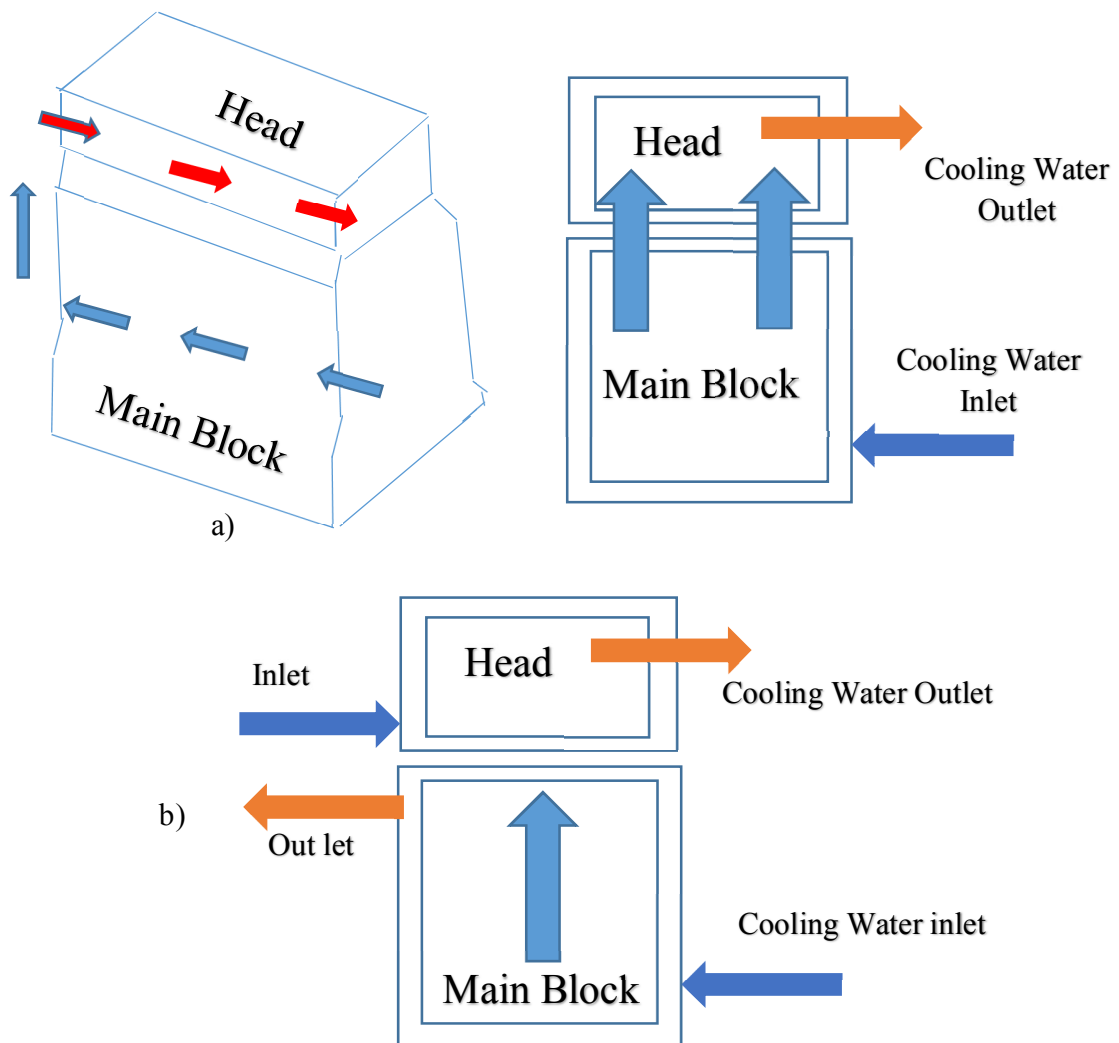idual cooling systems coupled in single design depicted in figure 5.8. As there are no proper recommendations available in literature for designing new cooling jackets, Hoag [24] has presented some guidelines regarding addition of deflectors or restricting the flow areas for proper cooling of critical components already discussed in theoretical review of section 2.4.6. Due to unavailability of proper guidelines in literature, most of the sections of cooling jacket specifically thickness values were used by reviewing previous cut piece section of existing cylinder head.
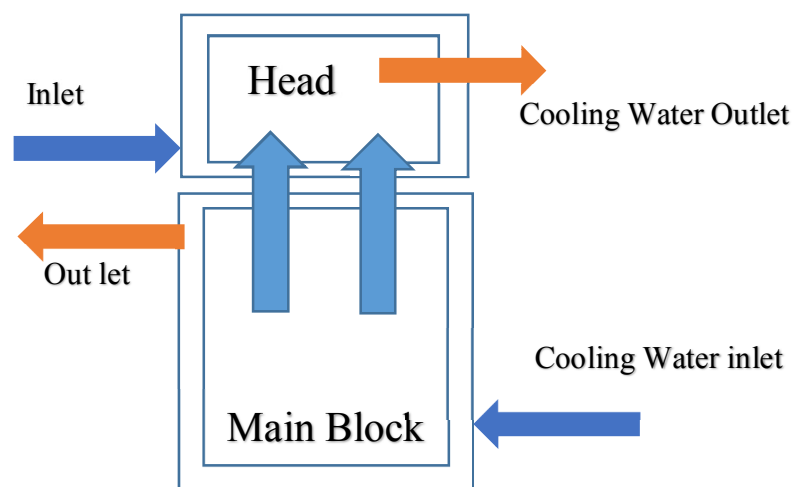
Figure 5.8: Newly designed cooling flow arrangement

A single core-cooling jacket is designed for research engine to ease the casting process shown in figure 5.9, and no sudden contraction areas are made to avoid stagnation points by uniform distribution of flow. The stagnation points could create boiling conditions eventually overheating problems [27]. Multiple factors were considered for designing the new jacket like intake cooling lines positioned from main block towards cylinder head. The outlet is provided at top of jacket to restrict high velocity flow and cavitation bubbles mostly produce due to creation of low-pressure zones. The purpose behind coolant flow from cylinder block to head is to achieve boiling based cooling. It reduces high temperature gradient and thermal stresses within cylinder head by plummeting cooling water volume and increases overall heat transfer coefficient.

Exhaust valve suffer significant heat flux, therefore also require proper cooling at valve guide section. Two coolant bridges are created between intake and exhaust valve seats, and third one in between exhaust-exhaust seats to cool critical areas. The exhaust-exhaust coolant bridge has wider area because of sensitivity to high thermal loads.

Cooling around exhaust valve guides

Injector Sleeve

Coolant from block

Inlet coolant passage

Coolant outlet

Coolant from block

Coolant from block

Smaller thickness for less cooling around intake

Three coolant bridges

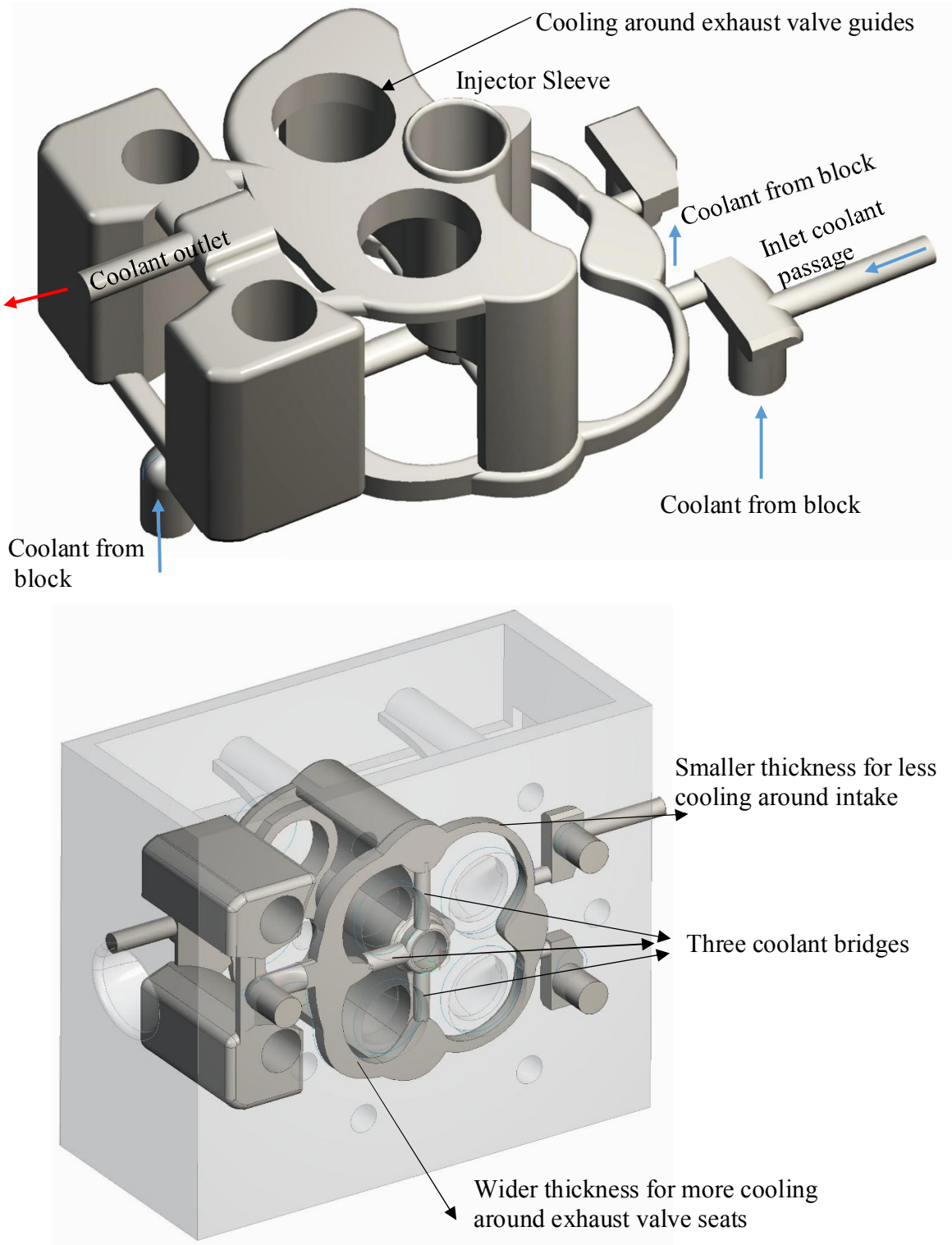Wider thickness for more cooling around exhaust valve seats

Figure 5.9: shows cooling jackets single core model

5.2.5 Direct injection space

HPDI is a novel strategy based on dual fuel strategy for non-premixed combustion of natural gas ignited with source of pilot diesel fuel. The injection pressure of 600 bars for natural gas can be achieved from HPDI system with torque and efficiency level equivalent to diesel engines already discussed in theoretical study. To house dual fuel injector for direct injection of gas in future, the cylinder head would need more space, intended for holding bigger size dual fuel injector. Due to selection of the new intake ports configuration that has altered the location of exhaust ports made some more space that can be utilized for specific purpose of direct fuel injector in new model cylinder head. In the existing model of cylinder head, the available space for diesel injector was about 17 mm, after modified position of ports the available space is around 22 mm with wider space for nozzle tip usually extruded inside combustion chamber and in conformity with appropriate thickness values of valve bridge. Hence, this ample space could be managed for direct injection of gas. But this would require a modular sleeve for multiple injectors, the modular sleeve can hold different types of injectors (diesel or dual fuel injector), which depends on application goals during research activities. The idea is depicted in figure 5.10.
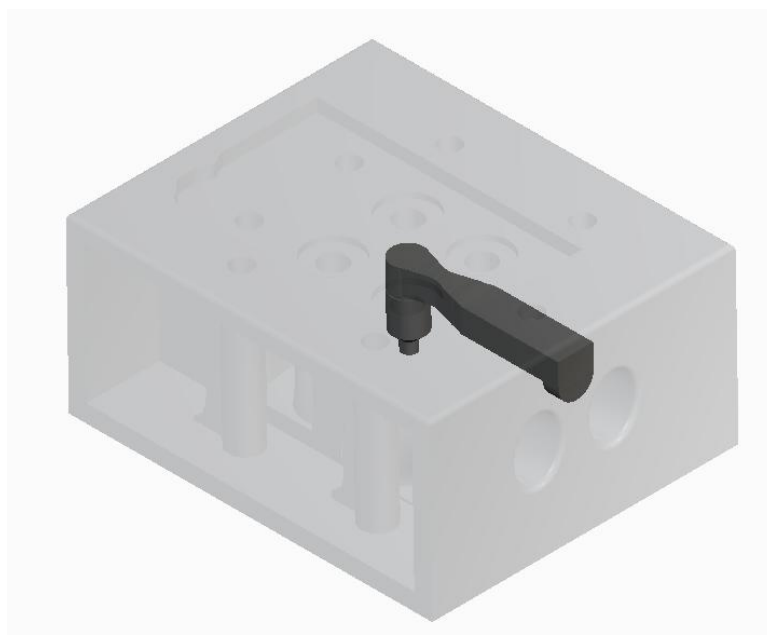

Figure 5.10: Dual fuel injector modular sleeve

6 Additive Manufacturing

The additive manufacturing (3D printing) of new cylinder head was done with nylon-12 as base material to check the suitability of model in relation with defined intake flow parameters like swirl for experimental validation in later stage. Even before going to complete actual casted metallic model involving 3D printed sand cores for cylinder head and cooling jackets, the employed 3D printed design contains two exhaust ports model instead of complicated twin exhaust port (with single outlet) to make 3D printing simplified at first stage, and to save cost.

Two type of processes are adopted: (1) 3D printing of cylinder head with selective laser sintering; a powder based bed fusion process to improve quality level inside intake ports and avoid roughness, which could hinder the air passage and deviate flow regime. The main target was to have dense part with enough stiffness level (2) extrusion-based printing for valve guides.

Steps involved in 3D printing are given below:

1. CAD modeling of completely new cylinder head already explained in previous chapters (4 and 5)
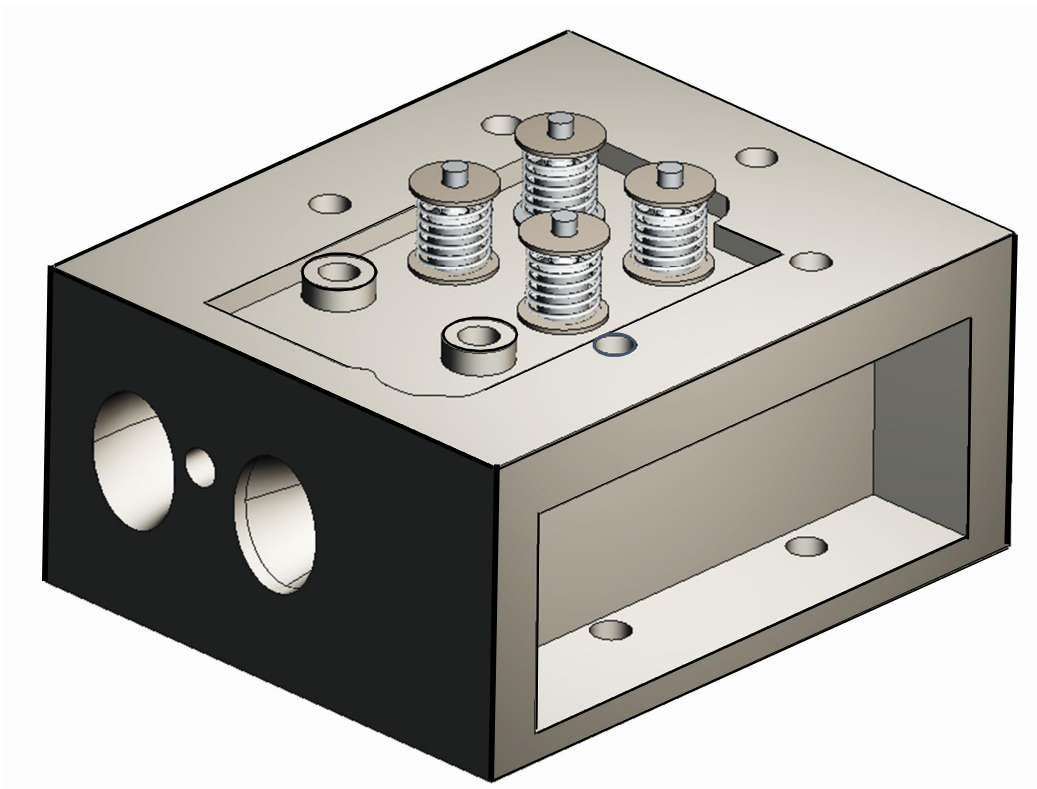

Figure 6.1: Isometric view of completely designed cylinder head with attached springs, washers and valve guides

Figure 6.2: Side view of newly designed cylinder head model

2. Conversion of CAD file to STL file and check the validity of model for printing. The Stereo lithography (STL) is a way of converting CAD file into triplet list of coordinates *x, y,* and *z* or in simplified terms small triangles, and formulates the basis for calculation of the slices. The printed model would be closed to real geometry with fine size of triangles.

3. Moving file to SLS machine for printing the cylinder head model

4. Machine setup for selecting material type and appropriate thickness values of layer from .060-.15mm can be adjusted.

5. SLS exhibits laser to sinter nylon based powered material into solid form structure. The process involves spreading of powdered material on flat platform inside chamber and preheating is done below the melting temperature of material. The next step comprises fusion of material by means of laser and solidification occurs as fuses particles join through mechanical means. Then second layer of powder is spread over previous lowering layer, and this procedure continues until the final shape of product. The benefit of using SLS powder based process for nylon is that spare un-melted powder on bench gives support to structure. The accuracy level of up to 0.2 mm with fine details can be achieved through SLS. SLS usually needs low tolerance during designing phase; the typical tolerances for SLS 3D printed components are ± 0.3 mm or ± 0.05 mm, and shrinkage is not a big problem.

6. Final step involves removal of part and finishing. The cleaning is usually done with compressed air to remove un-sintered powder from the body, which could be gathered and reused. The 3D printed part shown in figure 5.12 has quite good quality due to appropriate usage of thickness values for supported structure during designing process, also because of selection of convenient 3D process for specific nature of job.
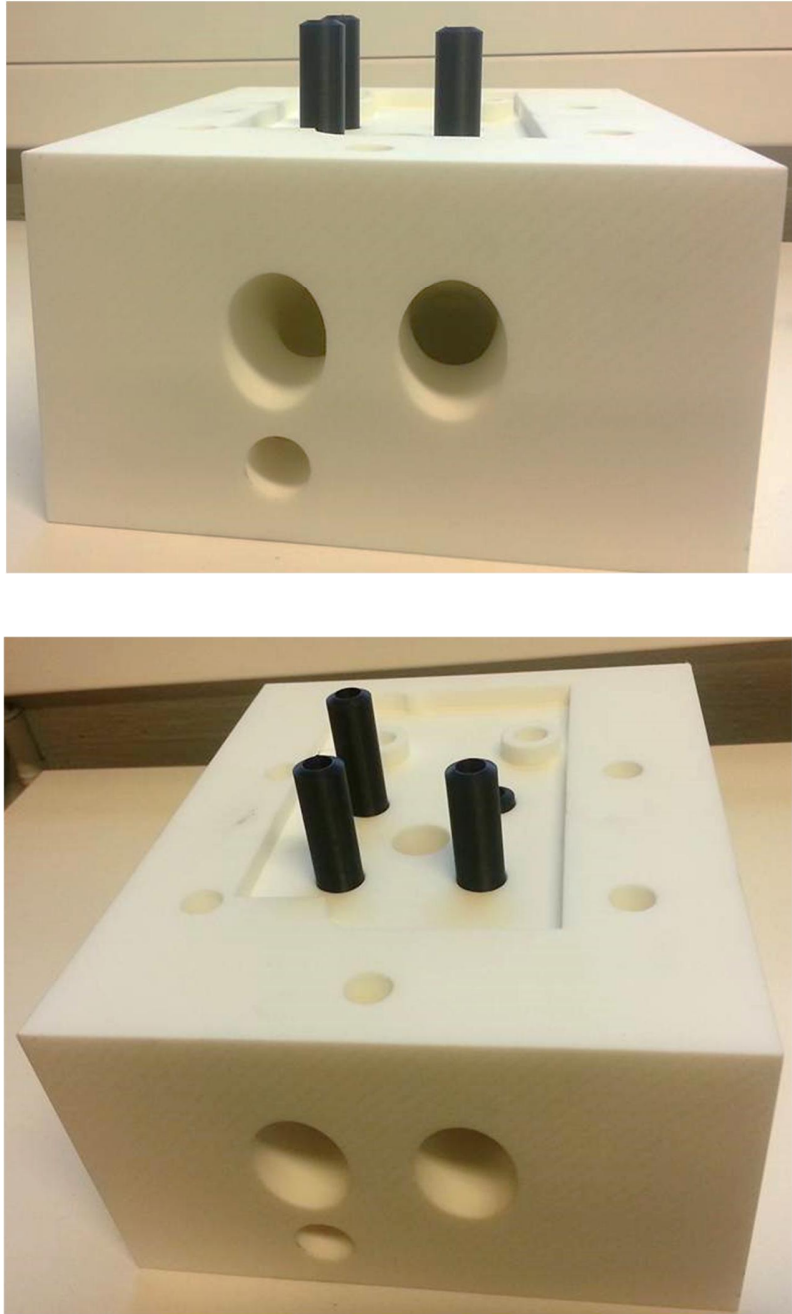
Figure 6.3: 3D printed cylinder head (Mfg. from Materialise) shows intake side with valve guides on top

7 Discussion

The selection of appropriate decisions during designing process have great influence on required cylinder head performance level. These decisions involve some global parameters that effect dimensions of many local components; likewise, the selection of combustion chamber design at global level decision process affects the positon and angle of valves at local level. Therefore, designing of cylinder head is a complicated process in which each minute detail effects global decision making process. Under the constraints of bolts layout, the designing process for intake port was not easy to control turbulence level through minimizing large-scale structures production rate exhibited during steady state CFD analysis. The flow inside cylinder of IC engine is highly confined that involves large separation, rotation and curvature through various interactions between fluid/wall bodies with high spatial and temporal variations. Due to uneven distribution of flow through actual model of tangential port, there was a strong flow separation at lower neck under adverse pressure gradient and high velocity at upper neck. The high velocity forces flow at tangent to cylinder liner and imparted strong angular momentum to generate swirl along cylinder axis. The selected RANS turbulence model (realizable k-ε model) performed well in capturing flow separation under adverse pressure gradient near port lower neck. Nevertheless, with suitable selection of intake ports position at 45° for new cylinder head helped to control formation of large-scale structures through flow-flow interaction, which produced different vortices in between port-valve region and reduces overall angular momentum under the influence of straight port profile to avoid non-perpendicular flow motion as described during the study. The dependence of flow pattern on intake port profile increases as valve lift magnifies, and at lower valve lift flow behavior more depends on valve restriction, which was more signified in case of cylinder head configuration having two directed ports. In the case of helical port, the shape profile imparts significant momentum, which is enough to overcome restriction offers by valve at lower lift. Therefore, even at lower lift in existing model cylinder head the value of swirl ratio was above average.

The most daunting task during entire designing process was to model a single core-cooling jacket with appropriate thickness values selection according to thermal loads distribution under the consideration of avoiding low-pressure zones and stagnant points. By considering thermal loads in mind, during designing process suitable thickness was added around exhaust ports and valve guide to have more efficient cooling around sensitive areas. Moreover, for proper cooling of injector sleeve, the coolant flow can circulate through three interlinked bridges connected with main coolant passage around intake and exhaust ports. The appropriate cooling process is vital to achieve high structural durability, combustion efficiency, and to comply emission regulations.

A new combination of exhaust ports are made in this study according to change in intake ports new position under constrains of many inbuilt features present in existing cylinder head like bots layout. A twin model of exhaust ports with single exit for exhaust gases and two separate exhaust ports model with same throat dimensions as present in existing model are presented in new concept development phase.

During main body designing process, a proper thickness value with CGI as base material for bottom deck is advised to sustain high combustion pressures of up to 220 bars. The value of

valve bridge thickness is 17 mm, which is more than minimum recommended value of 11-12% of cylinder bore to deter cracks under thermal loads. Moreover, due to change in orientation of intake and exhaust ports that has generated more space for injector sleeve; a modular injector design is recommended for future usage of HPDI system.

Selective laser sintering process, an additive manufacturing technique was implemented for custom-made cylinder head design. As cutout technique was adopted during designing procedure and due to proper thickness level, the quality of 3D printed part is very much desirable for experimental testing of flow. As the traditional manufacturing techniques are very much expensive and involves different kind of machining processes to produce one single part with cogitation of substantial tolerances during designing process. Whereas, additive manufacturing technique is highly customized rapid process for low productivity that encompasses less machining work and low tolerances. However, it requires great level of designing knacks when it comes to manufacture cylinder head like part through AM, which exhibits large number of variable thickness levels for various fragments inside main body.

8 Conclusions

8.1 Summary

This study incorporates customized manufacturing technique AM for the development of new cylinder head with no induced intake swirl. The swirl ratio calculation and experimental validation of three cases from existing cylinder head: fully open, closed helical and closed tangential cases confirmed that current model is not suitable for desired flow pattern. At all three cases of the old model, the swirl ratio value was not optimum to be considered for dual fuel oriented combustion research. Nonetheless, during the study, the in-depth analysis of existing cylinder head was performed regarding intake system, bolts pattern and cooling channels. From the inquired examination of existing intake port, a new directed port model was created through CAD modeling after CFD analysis of flow separation near valve-seat region and locating modification points. Therefore, the novelty designed directed port was utilized on existing and newly modeled intake position for probing swirl and flow coefficient. After selection of the most advantageous position for intake ports in terms of swirl ratio, the new exhaust ports were also modeled using same dimensional values specifically at throat section (inlet and outlet) as present in existing model cylinder. The shifted position of intake and exhaust ports has created more space for injector sleeve, which could be utilized for future usage of dual fuel injectors. Thereafter, mainframe of new cylinder head body with calculated thickness values for the bottom deck and valve bridge thickness was modeled with recommended new material for subsequent usage of cylinder head concerning higher combustion pressure. Additionally, a single core-cooling jacket was designed with appropriate consideration of thermal loads distribution from previously conducted theoretical studies.

8.2 Thesis Aims Review

The primary objectives assigned during this thesis work are argued during section 3.1. Let review them again and discuss that the relevant points are accomplished or not.

1. Aim to have no swirl flow in the cylinder of IC engine to study dual fuel combustion phenomenon for research purposes.

   The focus of research work was to accomplish the concerned point during the thesis work, which is achieved by designing new directed port profile/ports location, and discussed in detail during CFD work study.

2. No major modifications relating to bolts layout position for clamping of new cylinder head within main block.

   During designing process of both intake and exhaust ports, a careful consideration relating to seven bolts position for the clamping of cylinder head with main block was made by keeping same main dimensions of intake ports, valves, valve guides, and valve seats.

3. Material optimization.

   The new material CGI is advised during high combustion pressure review study. To sustain that much pressure with new material, a value of bottom deck thickness and valve bridge thickness was also evaluated.

4. Additional space for injector sleeve for pursuit of direct gas injection, which requires more space because of additional sized dual fuel injector.

   Although some additional space is created but this requires more work to be done concerning designing of dual fuel injector sleeve adjustment and clamping.

5. Suitability of CAD model for 3D printing to test model for later check of experimental values for swirl ratio.

   A 3D printed model with almost no interior and exterior defects was successfully manufactured, which validates the adopted designing technique to get acceptable part quality level with selected manufacturing process of AM.

8.3 Recommendations for future work

1. PIV measurements would be required to validate steady-state CFD swirl ratio calculations at selected valve lifts for new cylinder head model.

2. The steady state CFD simulations are considered constructive for initial course of design stage of cylinder head to compare different intake models in terms of flow performance. It does not provide insight of complete intake stroke and flow decay during compression stroke. Therefore, transient simulation work is needed to yield information regarding turbulence intensity, turbulence kinetic energy and flow field's effect during mixing and combustion phase with proper consideration of shape of piston bowl geometry. The complete range of plots can be constructed for mean axial and tangential velocity as a function of crank angle through the entire simulated strokes. The employed turbulence model was based on RANS technique during this study, in later stage, LES approach could be used for more accurate results from simulations.

3. FEA analysis is essential to check the service life, structural durability and integrity of cylinder head under mechanical and thermal loads. This study is indispensable to check validity of recommended material CGI during this research work. The component would also be required to have full load durability test and thermal shock testing under the influence of simulated peak combustion, injection pressure loads and cyclic loads to avoid fatigue failure from brittle cracking. The characterization of fatigue life through appropriate S-N diagram is essential. Although under bolts clamp loads all the components are constrained but the most critical areas are around valve bridge, injector sleeve and appropriate thickness values require around exhaust ports

to avoid thermal cracks. The fatigue assessment is also vital under peak temperature gradients for effective temperature control.

4. During cylinder head developing process, thermal mapping is essential for adequate cooling and to understand heat flux path around cylinder head components exposed to high thermal loads. This process involves different variables like speed, air fuel ratio and loads with respect to heat transfer maps for range of elements implied different temperature gradients inside cylinder head. In the course of cooling jacket designing process the thickness values were considered by reviewing existing cut piece section of cylinder head but it requires complete thermal mapping check for effective thermal load management around valve seat, exhaust valve guides and bottom deck.

5. After flow performance, structural and thermal loads validation studies, the next step could be manufacturing of realistic model as the current 3D printed model was produced with nylon material for flow performance testing. The jet binding process is another 3D printed technique for printing of sand casting cores. The jet binding process can be used for printing two separate sand cores: one for main body comprising of intake and exhaust port, while other for cooling jacket core. The jet binding process usually consists of two materials, sand and liquid binder uses to bind sand particles together layer by layer.

References

[1] S. Cordiner, M. Gambino, S. Iannaccone, V. Rocco, and R. Scarcelli, "Numerical and Experimental Analysis of Combustion and Exhaust Emissions in a Dual-Fuel Diesel/Natural Gas Engine," Energy Fuels, vol. 22, no. 3, pp. 1418–1424, 2008.

[2] N. Dronniou, J. Kashdan, B. Lecointe, K. Sauve, "Optical Investigation of Dual-fuel CNG/Diesel Combustion Strategies to Reduce CO2 Emissions," SAE Int. J. Engines, vol. 7, no. 2, pp. 873-887. DOI: 10.4271/2010-01-0480.

[3] A. McLandress, R. Emerson, P. McDowell, and C. Rutland, "Intake and in cylinder flow Modeling Characterization of Mixing and Comparison with Flow Bench Results," Tech. Rep. 960635, SAE Technical Paper, 1996.

[4] A. Gharehghani, S.M. Mirsalim, and S.A. Jazayeri, "Numerical Investigation of Flow Field and Combustion in Dual Fuel Diesel Engine," Tech. Rep. 2010-01-0480, SAE Paper, 2010.

[5] A. Gharehghani, S. M. Mirsalim, and S. A. Jazayeri, "Numerical and Experimental Investigation of Combustion and Knock in Dual Fuel Gas/Diesel Compression Ignition Engine," Journal of Combustion, vol. 2012 (2012), no. 504590, pp. 10, 2012.

[6] W. H. Kurniawan, S. Abdullah, K. Sopian, Z. M. Nopiah, and A. Shamsudeen, "CFD Investigation of Fluid Flow and Turbulence Flow Field Characteristic in a Four Stroke Automotive Direct Injection Engine," UniMAP Library, 123456789/13620, 2007.

[7] K.Y. Kanga, and J. H. Baekb, "Turbulence Characteristic of Tumble Flow in Four Valve Engine," Experimental Thermal and Fluid Science, vol. 18, no. 3, pp. 231-243, 1998.

[8] D. Karhoff, I. Bücker, J. Dannemann, M. Klaas, and "Experimental Analysis of Three-Dimensional Flow Structures in Two Four-Valve Combustion Engines," Tech. Rep. 2011-24-0044, SAE Technical Paper, 2011.

[9] E. M. Greitzer, C. S. Tan, and M. B. Graf, Internal Flow, Cambridge University Press, 2004.

[10] P. Bergstrand., and I. Denbratt, "The Effects of Leaner Charge and Swirl on Diesel Combustion," Tech. Rep. 2002-01-1633, SAE Technical Paper, 2002.

[11] J. Benajes, S. Molina, J. M. García, and J. M. Riesco, "Effect of Swirl on Combustion and Exhaust Emissions In Heavy-Duty Diesel Engines," SAGE Publications, vol. 218, no. 10, pp. 1141-1148, 2004.

[12] S. Zuelch, K. Banker, R.Deepe, and B. Findeisen, "A New Hardware Assisted Inlet Port Development Process for Diesel Engines Using Doppler Global Velocitimetry," Tech. Rep. 2005-01-0640, SAE Technical Paper, 2005.

[13] E. Mattarelli, M. Borghi, D. Balestrazzi, and S. Fontanesi, "The Influence of Swirl Control Strategies on the Intake Flow in Four Valve HSDI Diesel Engines," Tech. Rep. 2004-01-0112, SAE Technical Paper, 2004.

[14] U.S. Environmental Protection Agency. (n.d.). 40 CFR 86.1342-94, "Calculations; Exhaust Emissions," Retrieved from https://www.law.cornell.edu/cfr/text/40/86.544-90

[15] Semin , and Rosli Abu Bakar, "A Technical Review of Compressed Natural Gas as an Alternative Fuel for Internal Combustion Engines," American Journal of Engineering and Applied Sciences, vol. 1, no. 4, pp. 302-311, 2008.

[16] A. Maghbouli, S. Shafee, R. Khoshbakhti Saray, W. Yang, "A Multi-Dimensional CFD-Chemical Kinetics Approach in Detection and Reduction of Knocking Combustion in Diesel-Natural Gas Dual-Fuel Engines Using Local Heat Release Analysis," SAE Int. J. Engines, vol. 6, no. 2, pp. 777-787. DOI: 10.4271/2013-01-0865.

[17] E. Mattarellia , C. A. Rinaldinia , and V. I. Golovitchev, "CFD 3D Analysis of a Light Duty Fuel (Diesel/Natural Gas) Combustion Engine," Energy Procedia, vol. 45, pp. 929- 937, 2014.

[18] A.Carlucci, D. Laforgia, R. Saracino, and G.Toto, "Study of Combustion Development in Methane-Diesel Dual Fuel Engines, Based on the Analysis of In-Cylinder Luminance," Tech. Rep. 2010-01-1297, SAE Technical Paper, 2010.

[19] A.Gharehghani, S. M. Mirsalim, and S. A. Jazayeri, "Numerical and Experimental Investigation of Combustion and Knock in Dual Fuel Gas/Diesel Compression Ignition Engine," Journal of Combustion, vol. 2012, Article ID 504590, pp. 10, 2012.

[20] V. B. Richard, Natural Gas and Renewable Methane for Powertrains Future Strategies for a Climate-Neutral Mobility, Springer International Publishing, 2016.

[21] J. Sevik, M. Pamminger, T. Wallner, and R. S. Argonne, "Performance, Efficiency and Emissions assessment of Natural Gas Direct Injection compared to Gasoline and Natural Gas port-fuel injection in an Automotive Engine," SAE Int. J. Engines, vol.9, no. 2, pp. 1130-1142. DOI:10.4271/2016-01-0806.

[22]   D. Goudie, M. Dunn, S. Munshi , and E. Lyford-Pike, "Development of a Ignition Heavy Duty Pilot-Ignited Natural Gas Fuelled Engine for Low NOx Emissions," Tech. Rep. 2004-01-2954, SAE Technical Paper, 2004.

[23]   S.Dumitrescu, P. Hill, G. Li, and P.Ouellette, "Effects of Injection Changes on Efficiency and Emissions of a Diesel Engine Fueled by Direct Injection of Natural Gas,'' Tech. Rep. 2000-01-1805, SAE Technical Paper, 2000.

[24]   K. Hoag, and B. Dondlinger, Vehicular Engine Design, Second Edition, Springer International Publishing, 2010.

[25]   E.Andreatta, F. Barbieri, L. Squaiella, and R. Sassake, "Intake Ports Development: Euro IV Diesel Engine Cylinder Head," Tech. Rep. 2008-36-0331, SAE Technical Paper, 2008.

[26]   Z. Lu, T. Wang, X. Li, L. Li, and G. Zhang, "Parametric Design of the Tangential Intake Port in Diesel Engines," Journal of Automobile Engineering, vol. 227, no. 3, pp. 409-421, 2013.

[27]   C. Arcoumanis, and T. Kamimoto, Flow and Combustion in Reciprocating Engines, pp. 340-400, Springer International Publishing, 2009.

[28]   B. R. Dharan, S. Ramdasi, and N. Marathe, "Design / Analysis and Development of Cylinder Head for High Performance 3 Cylinder CRDi Euro-V Diesel Engine for a High Combustion Pressure of 200 Bar," Tech. Rep. 2010-01-1975, SAE Technical Paper, 2010.

[29]   S. Kandreegula, J.Tikoliya ,and H. Nishad, "Integration of Cylinder Head and Intake Manifold for Powertrain Downsizing and Light Weighting using Simulations Tools," Tech. Rep. 2017-01-1723, SAE Technical Paper, 2017.

[30]   T. Hamm, H. J. Ecker, M. Rebbert, M. Grafen "Cylinder Head Concepts for High Peak Firing Pressures," MTZ worldwide, vol. 69, no.6, pp.46–52, 2008.

[31]   P. Mandloi, S. Shrivastava, C. Patil, and S. Kottalgi, "Simulation Driven Design of Engine Cylinder Head," Tech. Rep. 2015-01-1739, SAE Technical Paper, 2015.

[32]   Ossi Kaario, Combustion Simulation, https://people.aalto.fi/new/ossi.kaario.

[33]   A.K. Gupta, D.G. Liley, and N. Syred, Swirl Flows, Abacus Press, Ohio, 1984.

[34]   M. C. Bates, "Parametric Design of the Tangential Intake Port in Diesel Engines," The University of Brighton, Phd Dissertation, 2004.

[35]   N .Gale,"Diesel Engine Cylinder Head Design: The Compromises and the Techniques," Tech. Rep. 900133, SAE Technical Paper, 1990.

[36] K.Y.Kang, and R.D.Reitz "Effect of Intake Valve Alignment on Swirl Generation in DI Diesel Engine," Experimental Thermal And Fluid Science, vol.20, no. 2, pp. 94-103, 1999.

[37] Y. Takenaka, H. Nakajima, and D. Mehri, "Application of Automatic Geometry Creation and Mesh Generation Technique for Port," FISITA World Automotive Congress, 2000.

[38] P. Miles, "The Influence of Swirl on HSDI Diesel Combustion at Moderate Speed and Load," Tech. Rep. 2000-01-1829, SAE Technical Paper, 2000.

[39] J.R. Needham, and S. Whelan, "Meeting the Challenge of Low Emissions and Fuel Economy with the Ricardo Four-Valve High-Speed Direct Injection Engine," Journal of Automobile Engineering, vol. 208, no. pp. 181-190, 1994.

[40] M. Raghu, and P. S. Mehta, "Influence of Intake Port Design on Diesel Engine Air Motion Characteristics," Indian Journal of Engineering and Materials Sciences, vol. 6, pp. 53-58, 1999.

[41] F. Perini, P. C. Miles, and R. D. Reitz "A Comprehensive Modeling Study of in Cylinder Fluid Flows in a High-Swirl, Light-Duty Optical Diesel Engine," Computers and Fluids, vol. 105, pp. 113–124, 2014.

[42] Kawashima, H. Ogawa, and Y. Tsuru, "Research on a Variable Swirl Intake Port for High-Speed 4-Valve DI Diesel Engine," Tech. Rep. 982680, SAE Technical Paper, 1998.

[43] W. Gao,Y. Zhang, D. Ramanujana, K. Ramani, Y. Chen, C. B. Williams, C. C.L. Wang, Y. C. Shin, S. Zhang,and P. D. Zavattieri, "The Status, Challenges, and Future of Additive Manufacturing in Engineering," Computer-Aided Design, vol. 69, pp. 65-89, 2015.

[44] B. P. Conner, G. P. Manogharan, A. N. Martof, L. M. Rodomsky,C. M. Rodomsky, D. C. Jordan, and J. W. Limperos, "Making Sense of 3-D Printing: Creating a Map of Additive Manufacturing Products and Services," Additive Manufacturing, vol. 1-4, pp. 64-76, 2014.

[45] J. Tóth, J.T. Svidró, A. Diószegi, D. Stevenson, "Heat Absorption Capacity and Binder Degradation Characteristics of 3D Printed Cores Investigated by Inverse Fourier Thermal Analysis," International Journal of Metal casting, vol.10,no.3, pp. 306-314,2016.

[46] Y. Li, L. Li, J. Xu, and X.Gong ,"Effects of Combination and Orientation of Intake Ports on Swirl Motion in Four-Valve DI Diesel Engines," Tech. Rep. 2000-01-1823, SAE Technical Paper, 2000.
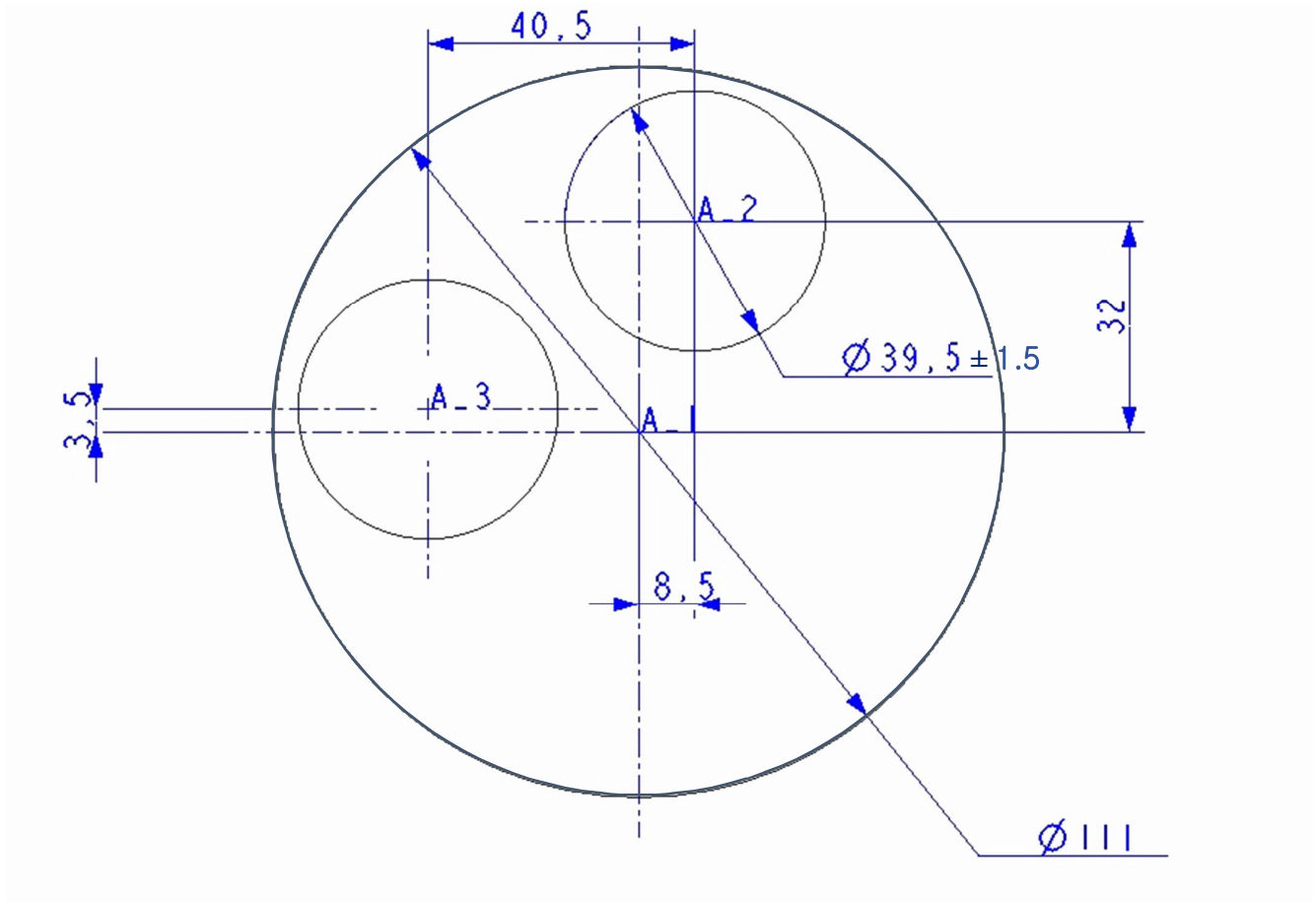
[47]   O. Kaario, E. Lendormy, T.Sarjovaara,and M. Larmi, "In-Cylinder Flow Field of a Diesel Engine," Tech. Rep. 2007-01-4046, SAE Technical Paper, 2007.

[48]   CD-Adapco, Star-CCm+ Documentation, Version 10.04, 2016.

[49]   F. Moukalled L. Mangani, and M. Darwish, "The Finite Volume Method in Computational Fluid Dynamics an Advanced Introduction with OpenFOAM and Matlab," Fluid Mechanics and Its Applications, vol. 133, Springer International Publishing, 2016.

[50]   A. Escue, and J. Cui, "Comparison of Turbulence Models in Simulating Swirling Pipe Flows," Applied Mathematical Modelling, vol.34, no.3, pp. 2840-2849, 2010.

[51]   B. Andersson, R. Andersson, L. Håkansson, M. Mortensen, R. Sudiyo, and B.V. Wachem, Computational Fluid Dynamics for Engineers, Cambridge University Press, 2011.

[52]   Ansys-Fluent, Retrieved from: http://www.afs.enea.it/project/neptunius/docs/fluent/html/th/node 1.htm

[53]   T.H .Shih, W.W. Liou, A. Shabbir, Z.Yang, and J.Zhu, "A New k-ε Eddy-Viscosity Model for High Reynolds Number Turbulent Flows-Model Development and Validation," Computers and Fluids, vol. 24, no. 3, pp. 227–238, 1995.

[54]   S. Dawson and F. Indra, Compacted Graphite Iron – A New Material for Highly Stressed Cylinder Blocks and Cylinder Heads, SinterCast Ltd, London.

[55]   3D Systems Inc. (2014), Selective Laser Sintering (SLS), Retrieved from: http://www.3dsystems.com/quickparts/prototyping-pre-production/selective-laser-sintering-sls. Last accessed 3rd Feb 2014.

[56]   J-P. Kruth, P. Mercelis,J. Vaerenbergh, L. Froyen, and M. Rombouts, "Binding Mechanisms in Selective Laser Sintering and Selective Laser Melting," Rapid Prototyping Journal, vol. 11, no. 1, pp. 26-36, 2005.

[57]   C.C. Kai, and L.K. Fai, Rapid Prototyping: Principles and Applications in Manufacturing, Second Edition, John Wiley & Sons, 2003.

[58]   J. T. Svidró, A. Diószegi, and D. Stevenson, "Heat Absorption Capacity and Binder Degradation Characteristics of 3D Printed Cores Investigated by Inverse Fourier Thermal Analysis," International Journal of Metal casting, vol. 10, no. 3, pp. 306–314, 2016.

[60]   L. J. Clancy, Aerodynamics, Pitman Publishing Limited, London, 1975.

[61]   R. L Simpson, "Turbulent boundary-layer separation," Annual Review of Fluid Mechanics, vol. 21, no. 1, pp. 205-232, 1989.

[62] G. A. Karim, Dual-fuel Diesel Engines, CRC Press, 2015.

[63] H. W. R. Dembinski, "In-cylinder Flow Characterisation of Heavy Duty Diesel Engines Using Combustion Image Velocimetry," Doctoral Thesis, KTH Royal Institute of Technology School of Industrial Engineering and Management Department of Machine Design.

[64] H. Zhao, Advanced Direct Injection Combustion Engine Technologies and Development Diesel Engines, CRC Press, 2010.

[65] P. A. Lakshiminarayanan, and Y.V. Aghav, Modelling Diesel Combustion, Springer 2009.

[66] T. Fuyuto, Y. Hattori, H. Yamashita, and M. Mashida, "Backward Flow of Hot Burned Gas Surrounding High-Pressure Diesel Spray Flame from Multi-hole Nozzle," SAE Int. J. Engines, vol. 9, no. 1, pp. 71-83. DOI: 10.4271/2015-01-1837.

[67] Y. Wakisaka, Y.Hotta, M.Inayoshi, K. Nakakita, I. Sakata and T.Takano, "Emissions Reduction Potential of Extremely High Boost and High EGR Rate for an HSDI Diesel Engine and the Reduction Mechanisms of Exhaust Emissions," SAE Int. J. Fuels Lubr. vol. 1, no 1, pp. 611-623. DO1: 10.4271/2008-01-1189.

[68] A.P. Carlucci, D. Laforgia, R. Saracino, and G.Toto, "Combustion and Emissions Control in Diesel-Methane Dual Fuel Engines: the Effects of Methane Supply Method Combined with Variable In-Cylinder Charge Bulk Motion," Energy Conversion and Management, vol. 52, no. 8-9, pp. 3004-3017, 2011.

[69] P. Olmeda, J Martın, D. Blanco-Cavero, A. Warey, and V. Domenech, "Effect of In-Cylinder Swirl on Engine Efficiency and Heat Rejection in a Light-Duty Diesel Engine, " International Journal of Engine Research, vol. 18,no 1-2, pp. 81-92, 2017.

[70] K.Mori, H. Jyoutaki, K.Kawai, and K.Sakai, "New Quiescent Combustion System for Heavy-Duty Diesel Engines to Overcome Exhaust Emissions and Fuel Consumption Trade-Off," Tech. Rep. 2000-01-1811, SAE Technical Paper, 2000.

[71] J. Rochussen, J. Son, J. Yeo, M. Khosravi, and P.Kirchen, M.et al., " Development of a Research Oriented Cylinder Head with Modular Injector Mounting and Access for Multiple In-Cylinder Diagnostics, " Tech. Rep. 2017-24-0044, SAE Technical Paper, 2017.
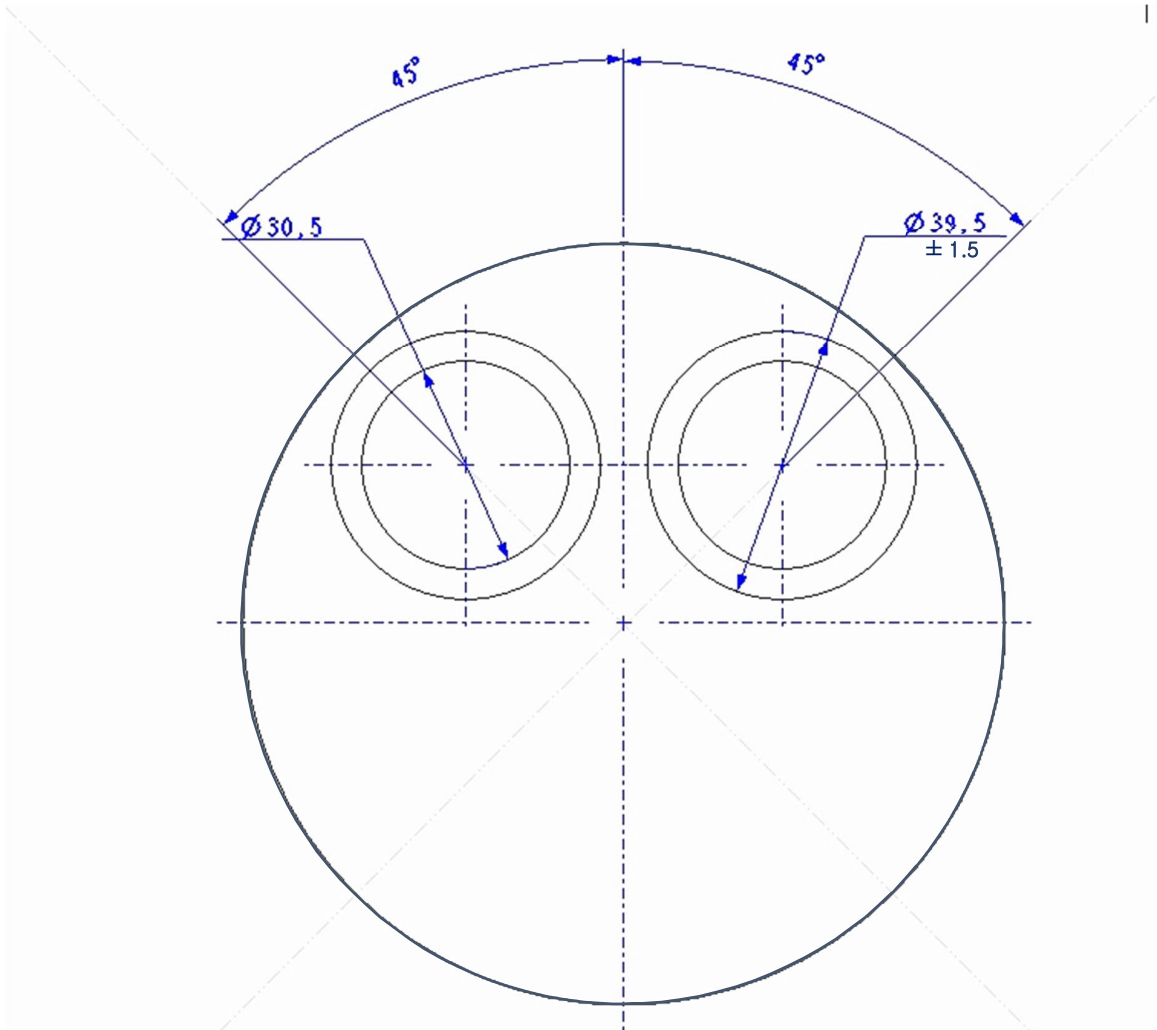
Appendix A

Old Ports Position

Appendix B

New Ports Positions

			Units mm				
Oka Part	Numbe ID-Code	Numilys Description			Standard: Standard		Npt Pcs
General to		Scale 1:1 DRAWING SCALE	Product Ports Position	Customer			
			Rev.			Model name MODEL NAME	
			Design				
		Mass	Check.			Drwaing 2	
		kg	Appr.				

Appendix C

Complete Cylinder Head Drawing